



**UNIVERSITY OF SALERNO**  
**DEPARTMENT OF PHARMACY**



**PhD course in Scienza e Tecnologie per l'Industria Chimica,  
Farmaceutica e Alimentare**

**XI course NS (XXV)  
2009-2012**

*“DESIGN, SYNTHESIS AND BIOLOGICAL  
EVALUATION OF NEW NON-NUCLEOSIDIC  
INHIBITORS OF DNA METHYLTRANSFERASES”*

**Tutor**

Prof. Gianluca Sbardella

**PhD Student**

Monica Viviano

**Coordinators**

Prof. Nunziatina De Tommasi

Prof. Paolo Ciambelli







## INDEX

Chapter 1: Introduction.....	3-27
Chapter 2: Aim of the work.....	31-36
Chapter 3: Chemistry.....	39-67
Chapter 4: Biology.....	71-82
Chapter 5: Docking and binding mode.....	85-90
Chapter 6: Conclusions.....	93
References.....	178-188



## ABSTRACT

The inactivation of tumor suppressor genes, which often results from epigenetic silencing associated with DNA hypermethylation, plays a pivotal role in the development of most forms of human cancer. Moreover, there are several reports demonstrating a strictly link between DNMT1 dysregulation and oncogenesis. Nucleoside analogues effectively inhibit the activity of DNA methyltransferases, but their high cytotoxicity make the development of non-nucleoside inhibitors highly desirable. Procaine and procainamide exhibit a weak DNA demethylating activity and are “repositionable” as non-nucleoside inhibitors. In this thesis, two series of  $\Delta^2$ -isoxazoline constrained analogues of procaine/procainamide are prepared and their inhibitory activity against DNMT1 is tested. Among them, **5b** is far more potent *in vitro* ( $IC_{50} = 150 \mu\text{M}$ ) than other inhibitors and exhibits a dose-dependent antiproliferative effect against HCT116 human colon carcinoma cells. On the basis of competition assays, we assess that **5b** competes with the cofactor and propose it as a novel lead compound for the development of new, longer compounds, obtained by the combination of this SAM-competitive scaffold with “warheads” targeting the nucleotide binding site, as “bisubstrate” inhibitors of DNMT1.

Moreover, starting from a virtual screening approach, the synthesis of the six top scoring compounds, obtained by the analysis of the NCI database, is reported. Among them, NSC140052 results the most powerful compound of this series, becoming the starting point for the synthesis of a small library of new compounds.

Finally, a scalable two-step continuous flow synthesis of nabumetone and related 4-aryl-2-butanones has been developed. As demonstrated for the synthesis of 4-(4-methoxyphenyl)-3-buten-2-one (**52b**), a throughput of 0.35 kg product per hour can easily be obtained using this technique.





## **CHAPTER 1**

### **INTRODUCTION**







## 1.1. Epigenetics

Chromatin structure defines the state in which genetic information in the form of DNA is organized within a cell, influencing the abilities of genes to be activated or silenced. Epigenetics, originally defined by C. H. Waddington<sup>1</sup> as *‘the causal interactions between genes and their products, which bring the phenotype into being’*, involves understanding chromatin structure and its impact on gene function. Nevertheless, the definition of epigenetics has evolved over time as it is implicated in a wide variety of biological processes: the current definition is *‘the study of heritable changes in gene expression that occur independently of changes in the primary DNA sequence’*. Most of these changes are established during differentiation and are stably maintained through multiple cycles of cell division, enabling cells to have distinct identities while containing the same genetic information. This heritability of gene expression patterns is mediated by epigenetic modifications, which include methylation of cytosine bases in DNA or post-translational modifications of histone proteins. Failure of the proper maintenance of heritable epigenetic marks can result in inappropriate activation or inhibition of various signaling pathways and lead to disease states such as cancer.<sup>2,3</sup> These findings have led to a global initiative to understand the role of epigenetics in the initiation and propagation of this disease.<sup>4</sup> The fact that epigenetic aberrations, unlike genetic mutations, are potentially reversible and can be restored to their normal state by epigenetic therapy makes such initiatives promising and therapeutically relevant.<sup>5</sup>

## 1.2. DNA methylation

Epigenetic regulation can be separated into three inter-related layers: DNA methylation, nucleosome positioning and histone modifications.<sup>6</sup> DNA

methylation is probably the most extensively studied epigenetic mark. It plays an important part in genomic imprinting, in DNA repair, in X-chromosome inactivation, and in the silencing of retrotransposons, repetitive elements and tissue-specific genes.

DNA methylation in humans occurs almost exclusively in the context of CpG dinucleotides<sup>7,8</sup> clustered in ~1 kb regions, termed CpG islands.<sup>9</sup> In addition, it also occurs at regions of lower CpG density that lie in close proximity (~2 kb), termed “CpG island shores”.<sup>10,11</sup> Only < 80% of the methylatable CpG population, which represent over 50% of promoters, is methylated. Different CpG sites are methylated in different tissues, creating a pattern of methylation that is gene and tissue specific.<sup>12</sup> This pattern creates a layer of information that confers upon a genome its specific cell type identity.

Moreover, DNA methylation patterns in vertebrates are distinguished by their tight correlation with chromatin structure. Active regions of the chromatin, which enable gene expression, are associated with hypomethylated DNA, whereas hypermethylated DNA is packaged in inactive chromatin.

Therefore, DNA methylation is a highly effective mechanism for silencing of gene expression in vertebrates and plants, either by interfering with the binding of transcription factors,<sup>13,14</sup> or by attracting methylated DNA-binding proteins (MBDs), able to recruit other proteins and histone modifying enzymes, which leads to formation of a closed chromatin configuration and silencing of gene expression. Noteworthy, DNA methylation patterns are altered in the progression of cancer. Both the hypomethylation and hypermethylation of different regions of the genome play roles in contributing to tumorigenesis. During the development of tumors, a genome-wide demethylation occurs and this can promote genomic instability possibly by activating silenced retrotransposons.<sup>15</sup> On the other hand, focal

hypermethylation of CpG islands has been intensively studied in cancer. Nearly all types of cancers have transcriptional inactivation of tumor suppressor genes due to DNA hypermethylation.<sup>6</sup> However, the exact mechanism responsible for the appearance of DNA methylation in a given promoter is not fully understood.

The establishment and maintenance of DNA methylation patterns are governed by catalytically active DNA methyltransferase (DNMT) enzymes.<sup>16</sup>

### ***1.2.1. Chemistry of DNA methylation***

Methylation of DNA occurs immediately after replication by a transfer of a methyl moiety from the donor S-adenosyl-L-methionine (SAM, or AdoMet) in a reaction catalyzed by DNMT. In mammals, DNMTs preferentially methylate position 5 of a cytosine in a 5'-CpG-3' (CpG dinucleotide) context, although non- CpG methylation (CpA, CpT or CpC) has been described.<sup>17</sup>

First, it has been shown that the targeted cytosine is flipped out of the DNA double helix into the catalytic site of the enzymes.<sup>18</sup> The thiolate of the catalytic cysteine in motif IV performs a nucleophilic attack on the 6-position of the cytosine, leading to the formation of the corresponding enamine (Figure 1.1). The tripeptide in motif VI, containing a glutamine residue, allows the subsequent protonation in N3-position. A nucleophilic attack of the enamine on the SAM cofactor is followed by deprotonation of the C5 by a base (depending on the DNMT) in the active site, releasing a molecule of S-Adenosyl-L-Homocysteine (SAH). The methyl group creates a steric clash that favors the  $\beta$ -elimination, allowing the recycling of the enzyme and release of the methylated DNA substrate.<sup>19</sup> The added methyl group now allows the recruitment of regulatory proteins with affinity for methylcytosines.

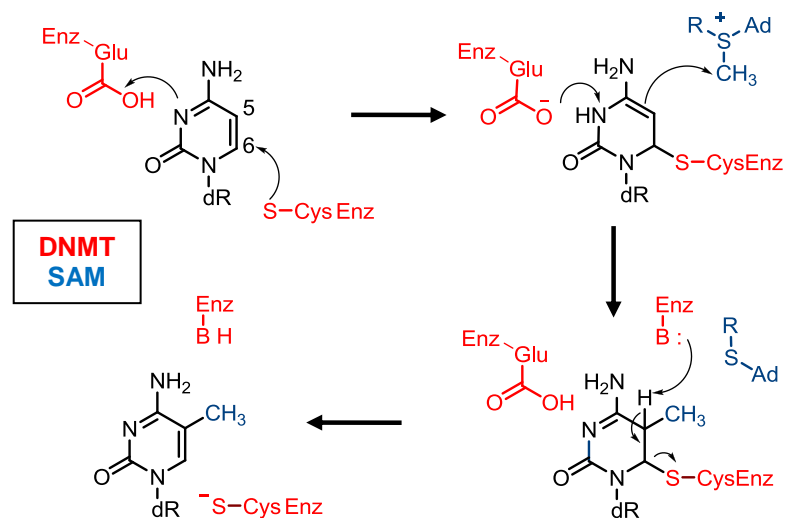


Figure 1.1. Mechanism of reaction catalyzed by cytosine C5 DNA methyltransferases.

### 1.3. DNA Methyltransferases (DNMTs)

In mammals, DNA nucleotide methyltransferases (DNMTs) include four members, in two families that are structurally and functionally distinct. The DNMT3 family establishes the initial CpG methylation pattern,<sup>20</sup> whereas DNMT1 maintains this pattern during chromosome replication and repair.<sup>21</sup> The DNMT3 family includes two active methyltransferases, DNMT3A and DNMT3B, and one regulatory factor, DNMT3-Like protein (DNMT3L).

DNMT1 shows preference for hemimethylated DNA *in vitro*, which is consistent with its role as a maintenance DNMT, whereas DNMT3A and DNMT3B methylate unmethylated and methylated DNA at an equal rate, which is consistent with a *de novo* DNMT role.<sup>22</sup>

DNMT2 appears to provide an example of divergent evolution: it was named based on its high sequence and structural similarity to known DNA MTases, but it actually methylates cytosine 38 in the anticodon loop of tRNA<sup>Asp</sup>.



The catalytically active DNMTs share common features, especially a regulating N-terminal domain and a catalytic C-terminal domain, particularly conserved among different species,<sup>23,24</sup> including ten sequence motifs (I to X), which form the binding site for the cofactor S-Adenosyl-L-Methionine (SAM). Motif IV includes the proline-cysteine dipeptide bearing a catalytic thiolate group. Motif VI contains the glutamine residue allowing the protonation of the 3-position of the cytosine and motif IX maintains the recognition site of the targeted cytosine base (Figure 1.2).<sup>25</sup>

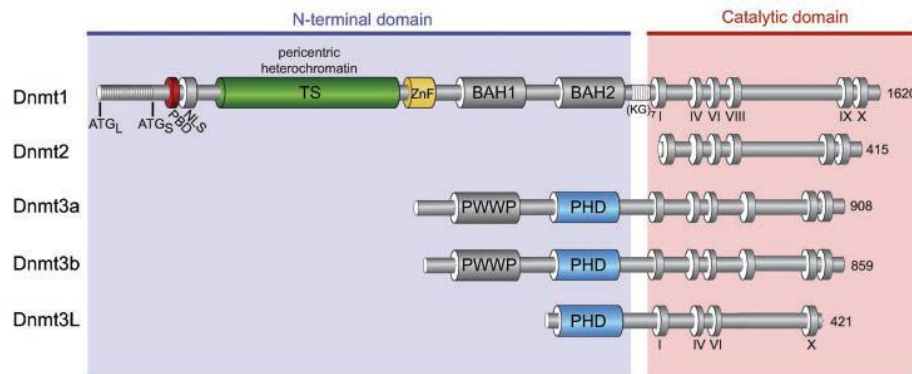


Figure 1.2. Schematic representation of the human DNMT1, DNMT2 and DNMT3s.

On the other hand, the N-terminal part of DNMTs binds to DNA and has several protein recognition domains, guiding the DNMTs to the nucleus, to chromatin and to numerous proteins, hence tightly linking chromatin modulation and DNA methylation.

### 1.3.1. Mammalian DNMTs: characterization and biological role

#### 1.3.1.1. DNMT1

The DNMT1 (Figure 1.3) was the first DNMT to be purified and characterized.<sup>26,27</sup> This enzyme, the most abundant of all the DNMTs in

somatic cells,<sup>28</sup> has 1616 amino acids and can be found as three isoforms in almost every eukaryotes: DNMT1s (somatic cells), DNMT1o (oocyte) and DNMT1p (pachytene).<sup>29</sup> As it has a greater affinity for hemimethylated DNA than unmethylated, it intervenes mainly after DNA replication to methylate the newly synthesized strand.<sup>30,31</sup> Therefore DNMT1 is called “the maintenance methyltransferase”.<sup>32</sup>

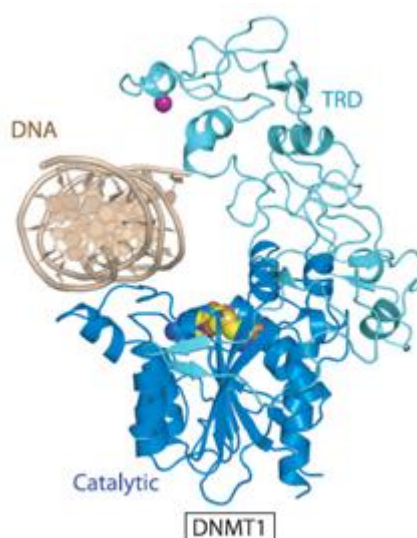


**Figure 1.3.** *The crystal structure of the mDNMT1(650–1602)–DNA 19-nucleotide oligomer complex.* The CXXC, BAH1, and BAH2 domains and CXXC-BAH1 linker of mDNMT1 have been removed for clarity. The bound DNA is in light brown, with the TRD and catalytic core in light and dark blue, respectively.

Disruption of the *Dnmt1* gene in mice can lead to significant demethylation of the genome and strong embryonic lethality. In non-tumoral cells, conditional or total knockout of DNMT1 leads to apoptosis,<sup>33</sup> severe mitotic defects<sup>34</sup> and tumorigenesis through chromosomal instability.<sup>35,36</sup> These results indicate that DNMT1 is essential, both during developmental stages and in somatic cells, to ensure cell proliferation and survival. In cancer cells, disruption of DNMT1 can stop tumor growth and reverse the non-differentiation state, without

enhancing the invasiveness of cells, thus providing a very interesting therapeutic target.<sup>37</sup>

DNMT1 is responsible for the maintenance DNA methylation via two different mechanisms: (i) through its direct interaction with the replication fork and (ii) as an interacting partner of UHRF1 (ubiquitin-like, containing PHD and RING finger domains 1).<sup>38</sup> Indeed, at the beginning of the S phase in somatic cells, DNMT1 is transported to the nucleus, thanks to a nuclear location signal (NLS), and more precisely to the replication foci through a specific sequence located within its N-terminal domain (Targeting Replication Foci: TRF) and its PCNA (Proliferating Cell Nuclear Antigen) binding domain (PBD). It then binds to hemimethylated DNA.<sup>39, 40</sup> The cytosine to be methylated is flipped out into the catalytic pocket and the methyl group of the SAM cofactor is transferred to position 5. Once the first CpG has been entirely methylated, DNMT1 moves along the newly synthesized DNA strand to further methylate.

The second mechanism implies UHRF1, a protein that has a specific affinity for hemimethylated CpG sites and recruits DNMT1 at these sites. Overall, the maintenance of DNA methylation patterns possesses a gross error frequency of circa 5% per CpG site and per cellular division. This leaves to cells some flexibility for subtle but probable important changes in their methylation pattern. This is balanced by DNMT3A and 3B that help DNMT1 in the maintenance of the methylation profile during replication.<sup>41</sup>

DNMT1 has a number of sequence motifs shared with other proteins but of unknown or unconfirmed function. DNMT1 contains two bromo-adjacent homology (BAH) domains, which are also found in origin recognition complex proteins and other proteins involved in chromatin regulation. The BAH motif has been proposed to act as a protein-protein interaction module.

Near the center of the N-terminal domain is a cysteine-rich region that binds zinc ions, present in all confirmed mammalian cytosine methyltransferases, known mammalian proteins affecting cytosine methylation, as well as the methyl-binding domain (MBD) proteins MBD1 and CpG binding protein.<sup>42</sup>

### *1.3.1.2. DNMT2/TRDMT1*



**Figure 1.4.** *Structure of human DNMT2.*

The DNMT2 enzyme (Figure 1.4) was originally assigned as a member of the DNA methyltransferase family on the basis of its very high degree of similarity in sequence and structure to eukaryotic and prokaryotic DNA-(cytosine C5)-methyltransferases. DNMT2 is strongly conserved and can be found in species ranging from *Schizosaccharomyces pombe* to humans, suggesting a very important role in cellular homeostasis.

The former DNMT2 has been recently renamed as TRDMT1 since it does not methylate DNA but rather a cytosine 38 in the anticodon loop of

tRNA<sup>Asp</sup>.<sup>43,44</sup> It has only a very small DNA methyltransferase activity *in vitro* and *in vivo*, suggesting that the N-terminal domain is not absolutely required for this activity, but more for its regulation.<sup>45</sup>

Whereas depletion of DNMT1, DNMT3A, DNMT3B and even DNMT3L genes lead to abnormal phenotypes (male sterility, developmental problems) or even to embryonic death,<sup>46</sup> the depletion of the TRDMT1 gene does not lead to any phenotypic modification. It is, thereby, hypothesized that this enzyme might be particularly useful not during the embryonic development, but rather during species evolution.

#### 1.3.1.3. DNMT3 family

The mammalian genome encodes two functional cytosine methyltransferases of the DNMT3 family, DNMT3A and DNMT3B, which primarily methylate CpG dinucleotides, and a third homologue, DNMT3L, which lacks cytosine methyltransferase activity and functions as a regulatory factor in germ cells.

DNMT3A has been identified as responsible for the imprinting of genes and methylates mainly pericentromeric regions of the DNA, while DNMT3B seems to methylate centromeric regions.<sup>47</sup> Furthermore, mutations on this latter lead, among other defects, to immunodeficiency syndromes and centromeric instabilities.

DNMT3L lacks the catalytic motif and thus shows no methylation activity by itself (Figure 1.2).<sup>48,49</sup> Actually, it is a cofactor of DNMT3A and interacts with histone modifying proteins thus keeping DNA methylation connected to histone modifications. The X-ray crystal structure of the mouse catalytic DNMT3A/3L complex showed the formation of a tetramer: DNMT3L-3A-3A-

3L, suggesting the simultaneous methylation of two CpG sites at one helix turn away from one another (circa 10 bp).<sup>50</sup> In addition, it was shown that the complex oligomerizes on the DNA<sup>51</sup> and that DNMT3A/3B are the only DNMTs to possess the proline-tryptophane-tryptophane-proline (PWWP) sequence, which allows them to directly bind DNA.<sup>52</sup>

Finally, DNMTs can interact with one another. For example, the N-terminal part of DNMT1 can bind to DNMT3A/3B N-terminal part, conferring to DNMT1 a *de novo* methylation activity.<sup>53,54</sup> Similarly, DNMT3 enzymes can act as maintenance methyltransferases, in a DNMT1 deficient background.<sup>55</sup> Therefore the strict separation of maintenance and *de novo* activity between DNMT1 and DNMT3 is controversial and tend to be reconsidered.<sup>56,57</sup>

#### **1.4. DNA methylation and pathologies**

Considering their role in the regulation of gene transcription, DNA methylation (as the other epigenetic marks) is essential for crucial processes such as embryonic development or differentiation and is involved in various pathologies, from neurodegenerative diseases<sup>58</sup> to cancers.<sup>6</sup>

With the increasing accessibility to genome-wide techniques to study DNA methylation, numerous pathologies have been linked to epigenetic disruptions, particularly diseases that are influenced by the environment. Indeed, since DNA methylation is required in the memory process, it has recently been proved to have an important role, not only in Alzheimer's disease,<sup>59</sup> but also in psychiatric diseases (depression, bipolar disorder, schizophrenia).<sup>60</sup>

DNA methylation is clearly involved in auto-immune diseases<sup>61</sup> and even in some genetic disorders (Facioscapulohumeral muscular dystrophy, Crohn

disease, atherosclerosis.).<sup>62,63</sup> Besides, aberrant DNA methylation patterns have been extensively described in numerous cancers.

It has been shown that cancer cells display a global hypomethylation<sup>64</sup> and at the same time a hypermethylation of certain gene promoters.<sup>65</sup> On the one hand, hypomethylation leads to chromosomal instability, since repeated sequences are no longer methylated. On the other hand, hypermethylation leads to silencing of Tumor Suppressor Genes (TSG).

As mentioned above, the reversibility of DNA methylation represents an interesting strategy in oncology. Hence, the use of specific inhibitors of DNMT (DNMTi) might reactivate TSG and induce the reprogramming of cancer cells, leading to their proliferation arrest and ultimately to their death (Figure 1.5).<sup>66</sup>

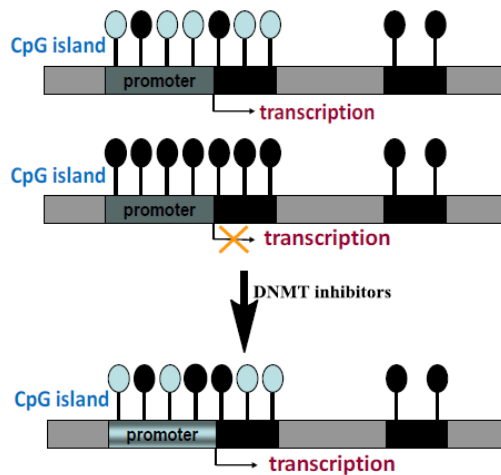


Figure 1.5. Stability and reversibility of epigenetic mutations.

Nevertheless, depleting either one DNMT is sufficient to suppress *in vitro* cell growth. In addition, several studies clearly demonstrated that DNMT1 depletion is sufficient to lead to tumor suppressor genes re-expression and cell

growth arrest in various in vitro cancer cells such as lung, esophagus, stomach, breast, cervix, brain, head and neck.<sup>67,68</sup>

Overall, these data strongly argue in favor of a selective inhibition of DNMT, and in particular of DNMT1, to achieve an antitumor effect.

### **1.5. DNMT inhibitors (DNMTi)**

As discussed above, tumor suppressor genes hypermethylation is often involved in cancers and, because of its reversibility, their demethylation constitutes an interesting therapeutic strategy. Many DNMT inhibitors have been described and are divided into two families: the nucleoside analogues, that have been known and studied for many years, and the non-nucleoside inhibitors, which structure varies according to their inhibitory mechanism.

#### **1.5.1. Nucleoside analogues**

##### **1.5.1.1. First generation molecules: azacitidine, decitabine and zebularine**

Until now, several DNMT1 inhibitors have been identified. They can be divided into different groups. The first one includes cytidine analogs like 5-azacytidine, 5-aza-2'-deoxycytidine and zebularine (Figure 1.6).<sup>69</sup>

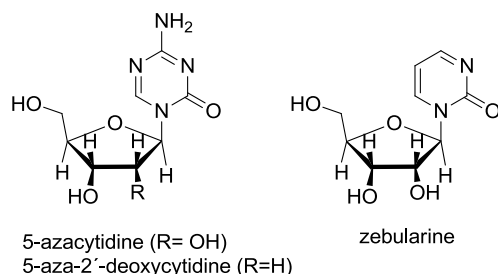


**Figure 1.6. Nucleoside analogues inhibitors of DNMTs.**



The nucleoside analogues 5-azacytidine (5-Aza-CR) and 5-aza-2'-deoxycytidine (5-Aza-CdR), known clinically as azacitidine (Vidaza<sup>®</sup>) and decitabine (Dacogen<sup>®</sup>), respectively, are the two most potent DNMTi. In these molecules, the carbon atom in position 5 is replaced by a nitrogen atom and linked to a ribose or a deoxyribose, respectively (Figure 1.6).

To be active, these compounds need to be integrated into the genome during the S phase (replication) of the cell cycle, allowing a certain specificity towards rapidly proliferating cancer cells (Figure 1.7).

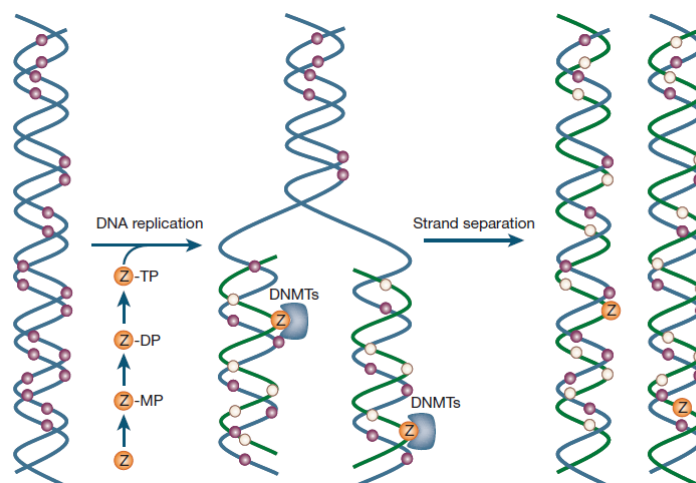


**Figure 1.7. Mechanism of action of nucleoside analogue inhibitors.** Deoxynucleoside analogues are depicted by Z. Pink circles, methylated CpG; cream circles, unmethylated CpG.

Once into the DNA, the cytosine analogues are recognized by the DNMTs and undergo the same reaction as normal cytosines, with the formation of the covalent intermediate between the catalytic cysteine of the enzyme and 6-position of cytosine analogues. However, unlike with cytosine, the  $\beta$ -elimination reaction can no longer occur because of the presence of the nitrogen atom in 5-position, resulting in a covalent irreversible complex. The

enzyme is thereby trapped by the suicide inhibitor, triggering its proteasomal degradation.

At higher doses, these compounds are cytotoxic, therefore they are used at low doses in order to achieve only the demethylation effect with little cytotoxicity. Besides the DNMT inhibition, the ribose analogues are also incorporated into RNA, decreasing the incorporation into DNA and disrupting protein synthesis. This might explain why decitabine is more active than azacitidine, but also why it has also less significant secondary effects, given that the latter can be incorporated not only in dividing cells, but also in quiescent cells.

Together with the HDACi (Histone deacetylase inhibitors), these two compounds are the only “epidrugs” that have been approved, so far, against Myeloid Dysplastic Syndrome (MDS), Acute Myeloid Leukemia (AML) and Chronic Myelomonocytic Leukemia (CMML) for Vidaza<sup>®</sup> by FDA in 2004 and the European Medicines Agency (EMA), and against MDS and AML for Dacogen<sup>®</sup> by FDA in 2006. However, these two DNMT inhibitors are not selective towards the different DNMTs and have strong secondary effects, e.g. renal toxicity and myelotoxicity.<sup>70</sup>

Moreover, 5-Aza-CR and 5-Aza-CdR are readily hydrolyzed in aqueous solution and subject to deamination by cytidine deaminase. The instabilities of these compounds inevitably present a challenge to their clinical applications. To improve the stability and efficacy of 5-Azanucleosides, several other cytidine analogues have been developed. For example, zebularine (a cytidine analogue that lacks an amino group in the 4 position of the pyrimidine ring) can inhibit DNMTs and cytidine deaminase after oral administration.<sup>71</sup> The inefficient metabolic activation of this compound has, however, delayed its clinical use as a single agent.

Compared to the suicide analogues, zebularine is used at higher concentrations to obtain the same demethylation levels in cells but is associated with lower cytotoxicity. Nevertheless, no new information related to a possible clinical development of zebularine has been published recently. Moreover, recent studies have shown that, depending on the used nucleoside analogue (azacitidine, decitabine or zebularine), demethylation patterns of tumor suppressor genes promoters are different, reflecting complex and partially overlapping mechanisms of action.

The use of these drugs raises questions regarding their potential to affect non-cancerous cells epigenetically. However, normal cells divide at a slower rate than malignant cells and incorporate less of these drugs into their DNA resulting in less of an effect on DNA methylation. Also, long-term negative effects of DNA methylation inhibitors in patients have not been found to date.<sup>72</sup>

#### 1.5.1.2. Second generation molecules: pro-drugs

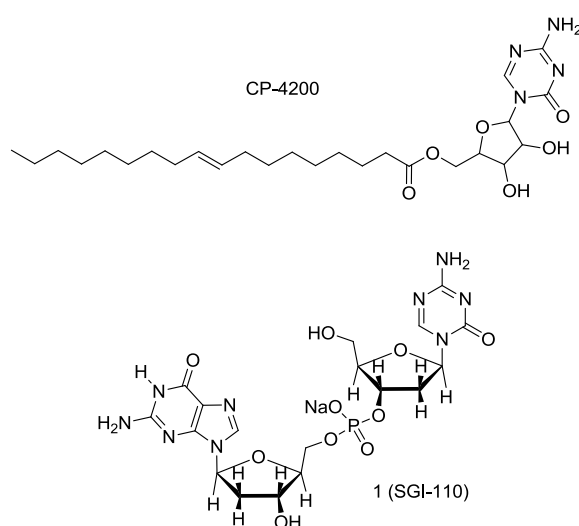


Figure 1.8. Second generation nucleosidic inhibitors of DNMTs.

The success of azacitidine and decitabine as DNMTs inhibitors in human chemotherapy prompted researchers to identify new compounds with a better pharmacokinetic profile. An elaidic acid ester of azacitidine, CP-4200 (Figure 1.8), has been synthesized with the aim of improving the drug cellular uptake. Several cellular assays highlighting the positive effect of CP-4200 on DNA demethylation as well as the dependency on nucleoside transporters have been conducted in comparison with azacitidine. It was demonstrated that CP-4200 acts as a pro-drug of azacitidine, presenting the advantage of a delayed delivery of the chemically instable azacitidine.<sup>73</sup>

SGI-110 (formerly S-110, Figure 1.8) is a second generation DNMT inhibitor that acts as a decitabine pro-drug. SGI-110 is a dinucleotide decitabine-*p*-deoxyguanosine as stable as decitabine in aqueous solution but more resistant to cytidine deaminase. *In vivo*, this enzyme is responsible for the deamination reaction of decitabine into the inactive 5-azadeoxyuridine.<sup>74</sup> SGI-110 is currently in Phase II clinical trials for the treatment of MDS and AML.

These nucleoside-like inhibitors have proved their efficiency in various clinical trials, but their lack of specificity and their strong secondary effects lead to an urgent need for novel more selective DNMT inhibitors.

### ***1.5.2. Non-nucleoside analogues***

A particular interest has recently emerged from non-nucleoside molecules, whose mechanism does not rely on DNA incorporation. Thus, some DNMT inhibitors of various origins and structures have been described during the last years, sharing only a DNA incorporation independent mechanism. Most of

these molecules are compounds that have already demonstrated a biological action against other targets than DNMTs.

Differently from nucleoside analogues, non-nucleoside inhibitors exhibit a wide structural diversity, and can be divided in the following groups.

1.5.2.1. Natural compounds: flavonoids, psammaphin A and curcumin

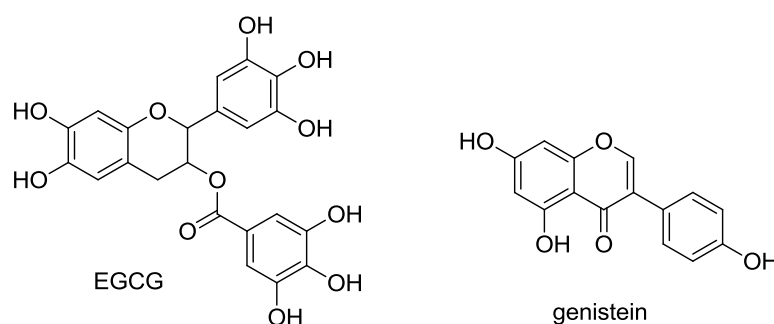


Figure 1.9. Flavonoids as DNMT inhibitors.

Flavonoids (or bioflavonoids) are organic compounds mainly extracted from plants, where they fulfill numerous functions, for example plant pigments or antifungal activity. One of the most studied flavonoid is (-)-epigallocatechin-3-O-gallate (EGCG, Figure 1.9). It is the main polyphenol of the green tea and its preventive anti-cancerous properties have been regularly reported in the literature for many years,<sup>75</sup> along with its numerous targets (protein kinases, highly reactive hydrogen peroxides).

Another well-known molecule of this wide family is genistein (Figure 1.9). It was first extracted from *Genista tinctoria* (Dyer's Broom) in 1889 by Perkin and Newbury, then characterized in 1926 and first synthesized in 1928 by Baker and Robinson.<sup>76</sup> Genistein is the principal isoflavone constituent of

soybean and has been initially considered a phytoestrogenic molecule, then a potential anticancer agent because of its *in vitro* activity against diverse enzymes such as tyrosine kinases, protooncogene HER-2, topoisomerase I or II, protein histidine kinase as well as G2/M block of cell cycle inducer.

Recently, both EGCG and genistein have been characterized as enzymatic and cellular DNMT inhibitors, being able to demethylate RAR $\beta$ , p16<sup>INK4a</sup> and MGMT promoter leading to the re-expression of these tumor suppressor genes.<sup>77</sup> The supposed mechanism of action of flavonoids relies on an indirect inhibition of DNMTs: more precisely, they are substrate of the Catechin-O-Methyltransferase (COMT), a SAM-dependent enzyme, and, as flavonoids become methylated, the SAH concentration increases. Since the intracellular SAM/SAH equilibrium is displaced and considering that SAH is a potent DNMT inhibitor, the DNMTs are no longer able to methylate.

These two flavonoids are now regarded more as chemopreventive drugs than actual treatment drugs, even though their metabolisms drastically decrease their bioavailability, hence lowering their potential activity.

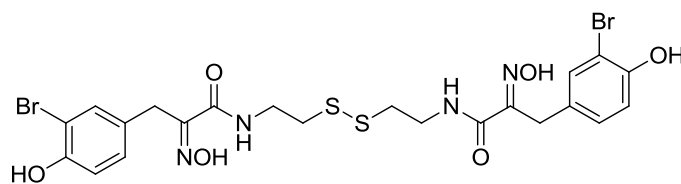


**Figure 1.10.** Structure of *Psammaplin A*.

Psammaplin A (Figure 1.10) is a natural compound extracted for the first time in 1987 from a sponge, the *Psammaplin Aplysilla*. It is a dimer of two

derivatives of 3-bromotyrosine. It possesses both antibacterial and antitumor properties, and was synthesized by Hoshino et al. in 1992.<sup>78</sup>

Psammaplin A was described as inhibitor of about ten different enzymes, such as topoisomerase II, DNA gyrase, leucine aminopeptidase, HDACs or DNMTs.<sup>79</sup>

In a systematic study of several natural derivatives of psammaplin A, it has been shown an activity against DNMT1 and HDACs. Antiproliferative properties of psammaplin A have also been explored on MDA-MB- 435 and A549 cell lines (breast and lung cancer, respectively) with promising results, since it inhibits cell growth at low doses ( $IC_{50} = 2 \text{ mM}$ ). Nevertheless, no DNA demethylation has been highlighted in HCT116 cells,<sup>80</sup> and, in a recent study, psammaplin A exhibited no activity on DNMT1 at 30 and 120 mM.<sup>81</sup>

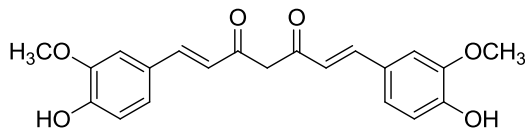


Figure 1.11. Structure of curcumin.

Curcumin (Figure 1.11) and derivatives were selected on the bases of the chemical reactivity of their  $\alpha,\beta$ -unsaturated carbonyl motif towards cysteine thiol functions. Experimental inhibition of the bacterial C5-DNA methyltransferase M. SssI was confirmed for curcumin and derivatives with  $IC_{50}$  around 30 nM.<sup>82</sup> Finally, curcumin at doses higher than 3 mM induced a decrease of global DNA demethylation of leukemia MV4-11 cells.

Despite these results, this molecule and various analogues are known to interact with numerous biological targets *in vitro* and no clear evidence of

pharmacological activities have been demonstrated in *in vivo* models neither in human therapy although the large number of clinical trials.

*1.5.2.2. Inhibitors identified by virtual screening: nanaomycin A and RG108*

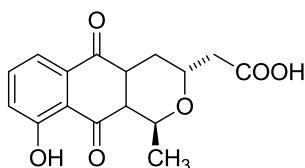


**Figure 1.12. Structure of nanaomycin A.**

Nanaomycin A (Figure 1.12) is a quinone antibiotic isolated in 1975 from a *Streptomyces* strain. Its DNMT1 potential inhibitory properties have been deduced after a virtual *in silico* screening,<sup>83</sup> but exhibited no activity when evaluated on DNMT1 biochemical assay. During further investigations, quite surprisingly, nanaomycin A demonstrated a selective inhibition of DNMT3B. Subsequent cellular characterization was undertaken, namely cytotoxicity evaluations and DNA methylation level examination on three cancer cell lines (A549, HCT116 and HL60, lung, colon and leukemia cell lines, respectively). Molecular docking calculation using a homology model of DNMT3B resulted in a possible model of nanaomycin A into the catalytic domain. However, despite the effects observed on the enzyme and a weak but significant demethylation of the RASSF1A promoter region, the authors concluded that DNMT3B inhibition is not the only mechanism of action of nanaomycin A and may share other cellular targets.<sup>84</sup>



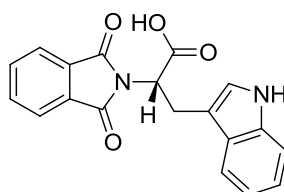


**Figure 1.13.** Structure of the phthalimido-L-tryptophan RG108.

Like nanaomycin A, RG108 (Figure 1.13) is a DNMT inhibitor found by virtual screening on DNMT1.<sup>85</sup> Siedlecki et al.<sup>86</sup> previously established a 3D model of the catalytic domain of DNMT1 by homology with the crystalline structures of bacterial methyltransferases M. HhaI, M. HaeIII and human methyltransferase TRDMT1. They carried out a virtual screening of a small molecules database (NCI database) revealing a simple phthalimido-L-tryptophan skeleton, named RG108, as hit. RG108 inhibits in vitro M. SssI and human DNA methylation in HCT116 and NALM6 (leukemia) cells at 100 mM. Moreover, it has been proved that it can reactivate tumor suppressor genes such as P16<sup>INK4a</sup> and TIMP3, which are repressed by promoters methylation in the cancer cell line HCT116.

Different studies also demonstrated that, at the contrary to other DNMTs inhibitors, RG108 is neither genotoxic, nor cytotoxic, and that it prevents the substrate to enter the catalytic pocket: a carbonyl group of RG108 is positioned at the level of the 6-position of the cytosine, which can prevent the formation of a covalent bond between the cytosine and the thiolate of the catalytic cysteine.

A broad application of RG108 is however limited due to its high hydrophobicity.<sup>87</sup>

1.5.2.3. Drugs used for other indications: SGI-1027, hydralazine, procaine and procainamide

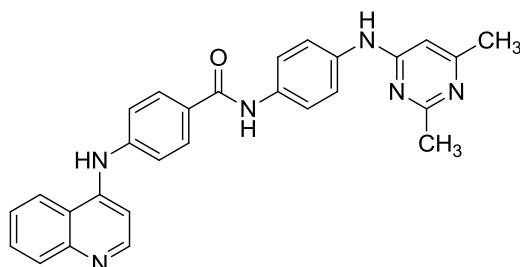
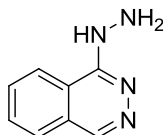


Figure 1.14. Structure of SGI-1027.

SGI-1027 (Figure 1.14) is a lipophilic quinoline inhibiting DNMT1, 3A and 3B that was initially synthesized for its antitumor activities. Indeed, quinolinium salts are known to be reversible but also strong ligands of the DNA minor groove, causing cell death by a still unknown mechanism.<sup>88</sup>

On the contrary, SGI-1027 is a weak base that binds only weakly to AT-rich DNA ( $IC_{50} = 0.51$  mM for the binding to poly(dA-dT)), but has a relatively good stability in physiological media. Its activity was tested *in vitro* on bacterial M. SssI and on mammalian DNMTs.<sup>89</sup>

SGI-1027 is not a competitive inhibitor of DNA but of the cofactor SAM. Besides, it has been observed a rapid proteasomal degradation of DNMT1 after treatment of HCT116 and RKO (colon cancer) by SGI-1027. Even if the degradation seems specific to DNMT1 and suggests a different and not yet known mechanism (sharing the same signal pathway as the nucleoside analogues), all DNMTs are inhibited by SGI-1027 because of the very conserved motifs I and X (involved in the recognition of the SAM cofactor). Finally it demethylates and re-expresses TIMP3 and P16<sup>INK4a</sup> in HCT116.



**Figure 1.15.** Structure of the antihypertensive hydralazine.

Hydralazine (Figure 1.15) is used in the treatment of hypertension and its secondary effects have allowed to discover its DNMT inhibitory action. Despite its frequent use for numerous years, its mechanism remains unknown. Indeed, hydralazine induces the erythematosus lupus in treated patients and this autoimmune disease is associated with a hypomethylation of T cells, confirmed on T cells in culture.<sup>90</sup>

Hydralazine has been tested in phase I on patients who have developed ovary tumors, resulting in demethylation-induced reactivation of tumor suppressor genes in few cases and a mild overall tolerance by patients. Moreover, hydralazine is currently tested in phase III on patients that have developed brain or ovary tumors and also in phase II against chemo-resistant tumors. It is currently in phase II in combination with magnesium valproate, an HDAC inhibitor, and registered in Mexico in the treatment of MDS. Hydralazine is therefore, a promising molecule in anti-cancer treatments, even if its therapeutic scope is restricted to very few cancers. Indeed, its efficiency being limited to a narrow range of cells might turn into an advantage. A specific targeting would circumscribe secondary effects and decrease the risk to induce a global demethylation of the entire DNA, which could lead to a deleterious instability in normal cells.

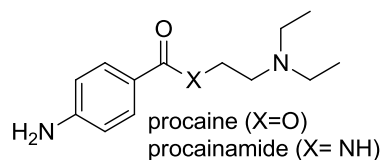


**Figure 1.16.** Structures of procaine and procainamide.

Procainamide and its ester analogue, procaine (Figure 1.16), have been used for the last 30 years as antiarrhythmic and anesthetic agents, respectively. As for hydralazine, its DNMT inhibitory effects were discovered through their secondary effects. In the presence of procainamide, the rate of 5-methylcytosine in Jurkat cells decreased, allowing the re-expression of some genes. The link between procainamide and DNA methylation was first established by demonstrating that procainamide and procaine have an affinity for the CpG-rich regions of DNA, and that are able to suppress growth in these breast cancer cells simultaneously with the occurrence of demethylating events (Figure 1.17).<sup>91</sup>

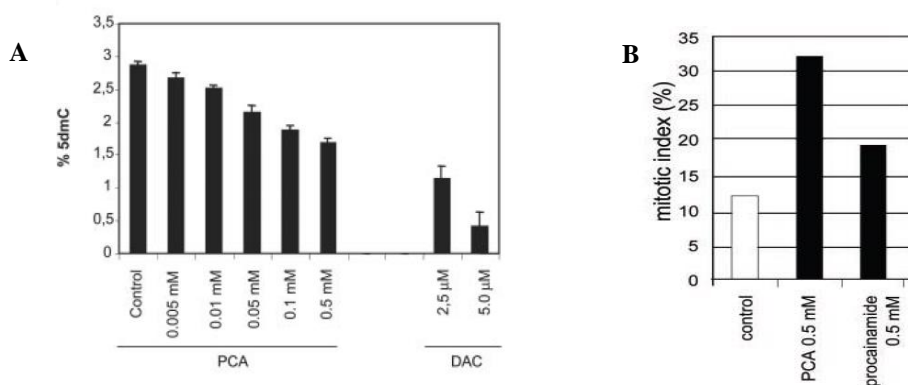


**Figure 1.17.** (A) Measurement of 5-dmC content in MCF-7 cell lines treated with increasing concentrations of procaine (PCA) and decitabine (DAC) as a percentage of the total cytosine pool; (B) Mitotic index, the number of cells in metaphase, anaphase, or telophase with respect to the total number of cells.

Two molecular modeling studies suggested that procainamide binds also to DNMT.<sup>92,93</sup> A systematic *in vitro* and cellular study was carried out on human DNMTs, showing that procainamide inhibits preferentially DNMT1 in the presence of a hemimethylated substrate ( $KI = 7.2 \pm 0.6$  mM) than DNMT3A/3B in the presence of an unmethylated substrate ( $KI > 1000$  mM).<sup>94</sup> This inhibition is competitive compared with the two substrates, SAM and hemimethylated CpG, which implies a decrease of the enzyme affinity for these two factors. The study also highlighted that the inhibition difference between hemimethylated and unmethylated DNA is not due to a difference in affinity of the enzyme for its various substrates. Finally, this studies showed that this inhibition is likely connected to a loss of DNMT1 processivity: by decreasing the affinity of DNMT1 for hemimethylated-DNA, procainamide facilitates the dissociation of the enzyme from the DNA.

So why design new DNMTi? Importantly, DNMTi can be used to address two main issues: 1) the better understanding of DNA methylation in normal and cancer cells, and 2) the specific and efficient targeting of DNA methylation for therapy. In fact, while DNMTs are well-characterized enzymatically, their mechanism of action and their regulation in cells are still not completely elucidated and even less in cancer cells in which aberrant DNA methylation is observed. Small chemicals inhibiting DNA methylation can be useful tools to probe the methylation mechanism both at the enzymatic level and in cells. In parallel, it is also now well established that DNA methylation constitutes a promising therapeutical target in cancer, in particular, but also in other diseases. such as neurological disorders.



## **CHAPTER 2**

### **AIM OF THE WORK**





## 2.1. Aim of the work

As known, the nucleoside-like inhibitors have proved their efficiency in various clinical trials, but their lack of specificity and their strong secondary effects lead to an urgent need for novel non-nucleoside DNMT inhibitors. Being interested in the development of small-molecule modulators of epigenetic targets, we decided to apply two different medicinal chemistry approaches:

1) we prepared a new series of  $\Delta^2$ -isoxazoline derivatives, following on our previous studies that led to the identification of a constrained analogue (**3b**) of procaine as a lead compound for the discovery of new DNMT1 inhibitors;

2) at the same time, we designed and synthesized a small collection of compounds taking advantage of a virtual screening approach.

### 2.1.1. Frozen analogue approach: procaine/procainamide analogues

With respect to the first approach used, we focused our attention on procaine/procainamide as a lead structure for further modification. Originally approved by the FDA as local anesthetic and antiarrhythmic drug, respectively, procaine and procainamide have emerged as potential DNA demethylating agents.<sup>94,95</sup>

It has been reported that procainamide specifically inhibits DNMT1 by reducing the affinity with hemimethylated DNA (substrate) and S-adenosylmethionine (cofactor),<sup>96</sup> thus causing growth arrest<sup>94</sup> and reactivation of tumor suppressor genes in cancer cells.<sup>97</sup> With the aim to increase potency, according to the *frozen analogue approach*, we decided to limit the very high flexibility of procaine/procainamide scaffold by constraining the *N*-alkylamide

moiety into a 4-substituted- or 5-substituted-oxazoline ring (derivatives **1,2** and **3,4**, Figure 2.1).

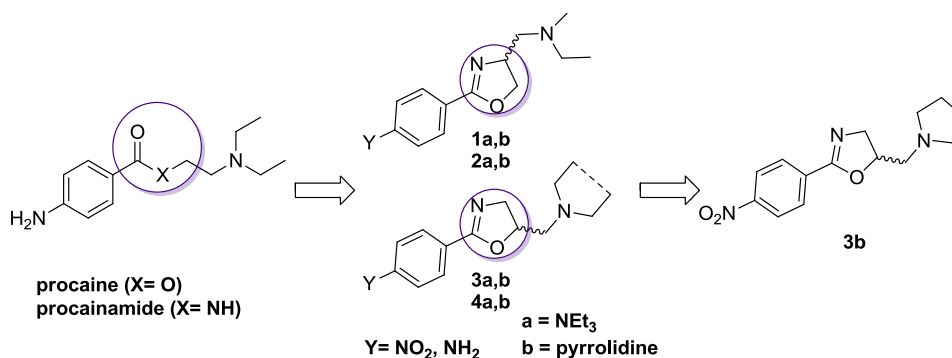


Figure 2.1. Frozen analogue approach of procaine/procainamide.

Among the synthesized compounds, unexpectedly, the nitro derivative **3b** exhibited the highest inhibitory potency against DNMT1 and, when tested for its effects on the genome methylation levels in HL60 human myeloid leukemia cells, it revealed a recognizable demethylation of chromosomal satellite repeats (Figure 2.2).<sup>98</sup>

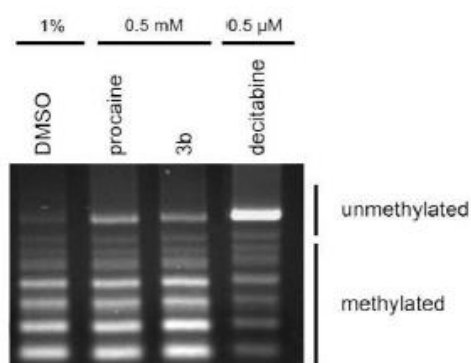


Figure 2.2. Cellular methylation assays. Human myeloid leukemia (HL60) cells were incubated for 72 h with DMSO (1%), procaine (0.5 mM), decitabine (0.5 μM), and test compound **3b** (0.5 mM). COBRA assay of chromosomal satellite repeats (C1S2). DMSO treated cells revealed methylated satellites, but procaine as well as **3b** induced minor demethylation of the repetitive elements. Decitabine treatment was included as positive control and showed the strongest demethylating effect.

To extend structure-activity relationships for this new class of inhibitors, we needed a scaffold more stable and versatile than the oxazoline ring. Therefore, we decided to explore the possibility of replacing it with the  $\Delta^2$ -isoxazoline (C, Figure 2.3) and to introduce a new conformational restriction (D, Figure 2.3).

Once that the biological as well as binding mode investigations of the first two series of compound were completed (Chapter 4 and 5), we realized that they were able to occupy only a portion of the binding site of the enzyme. Therefore, being interested in the development of analogues endowed with improved enzyme binding properties and higher inhibitory potency, we decided to synthesize new, longer compounds, obtained by the combination of the SAM-competitive isoxazoline scaffold with “warheads” targeting the nucleotide binding site, as “bisubstrate” inhibitors of DNMT1. In particular, we designed a small collection of molecules bearing the pyrimidine scaffold, already present in the powerful DNMT1 inhibitor SGI-1027 (Figure 2.3).

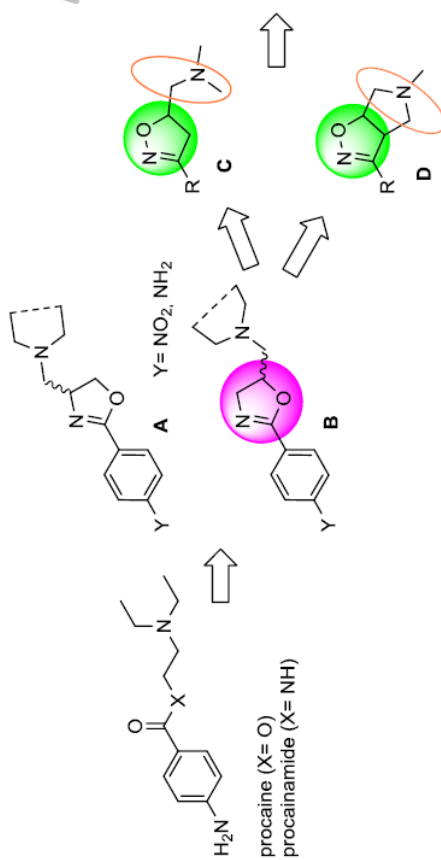
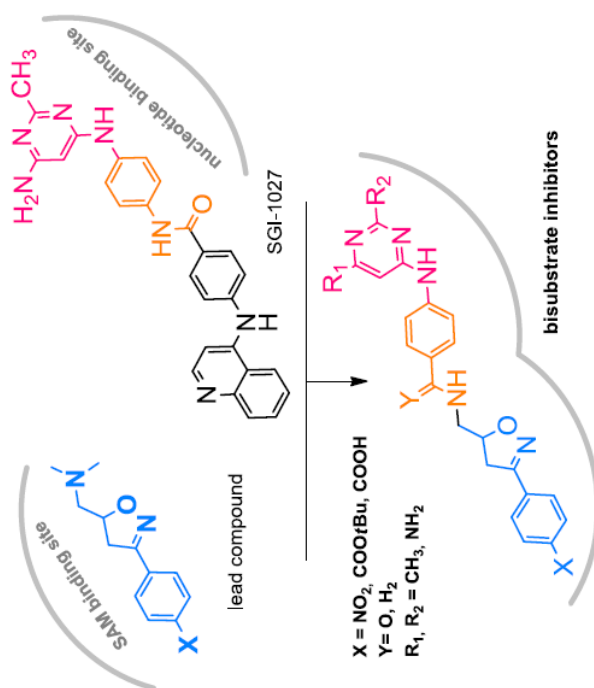


Figure 2.3. Aim of the work.

### 2.1.2. From virtual screening to new DNMT1 inhibitors

At the same time, we paid attention to molecular modeling and virtual screening of compound databases, powerful computational techniques that are increasingly being used in drug discovery projects. These techniques are now commonly applied to understand the binding mode of active compounds and identify new hits.<sup>83,99</sup> In 2011, 260,000 compounds in the Diversity Set available from the National Cancer Institute (NCI) were the starting point to identify additional DNMT1 inhibitors. Six of the top scoring compounds were synthesized by us (Figure 2.4) in order to obtain their DNMT1 inhibitory activity in a biochemical assay.

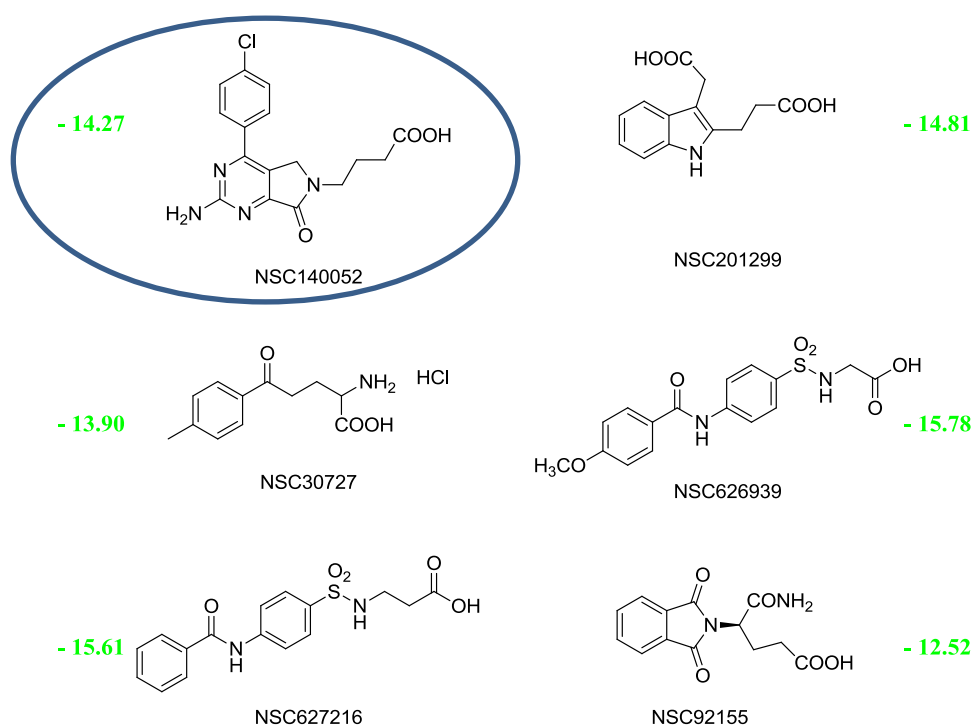
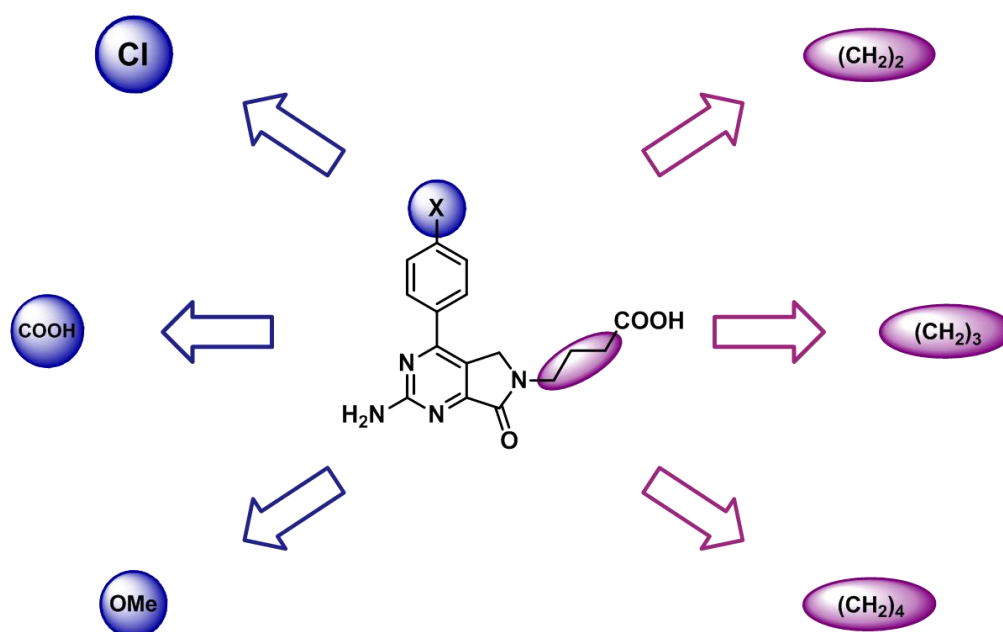


Figure 2.4. Molecules identified by virtual screening and synthesized by our group.

*Chapter 2: Aim of the work*

---

Among them, NSC140052 showed a good and selective inhibitory activity against DNMT1 ( $IC_{50} = 220 \mu\text{M}$ ), so we decided to realize a small library of compounds replacing both the  $-\text{Cl}$  group on the aromatic ring and the length of the aliphatic chain (Figure 2.5).



**Figure 2.5.** *Planned modifications of the hit.*

## **CHAPTER 3**

## **CHEMISTRY**





### 3.1. 1,3-dipolar cycloaddition: an efficient strategy to $\Delta^2$ -isoxazolines

The 1,3-dipolar cycloaddition offers a convenient one-step route for the construction of a variety of complex five-membered heterocycles. 1,3-dipolar cycloadditions of *in situ* generated nitrile oxides with alkenes are well-documented and provide access to  $\Delta^2$ -isoxazolines.<sup>100</sup>

Aldoximes are established precursors of nitrile oxides, and different classes of reagents have been used in the literature for the conversion of aldoximes to nitrile oxides.<sup>101</sup>

The outcome of the reaction is strongly dependent on the nature of the dipolarophile. In fact, with reactive alkenes, it is possible to use a rapid and efficient method, characterized by the *in situ* formation of the nitrile oxide by the corresponding aldoximes after oxidative chlorination, followed by base-induced dehydrochlorination of the intermediate hydroxymoyl chlorides. The so formed nitrile oxide reacts rapidly with the dipolarophile, and the reaction is complete within 15 minutes.

Instead, with sluggish dipolarophiles, the 1,3-dipole must be generated slowly so as to disfavor dimerization of the nitrile oxide to give furoxan (1,2,5-oxadiazol-2-oxide) as an unwanted side product (Figure 3.1).

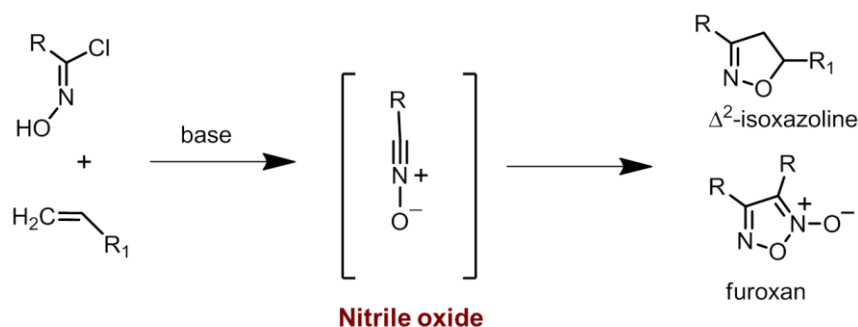


Figure 3.1. 1,3-dipolar cycloaddition.

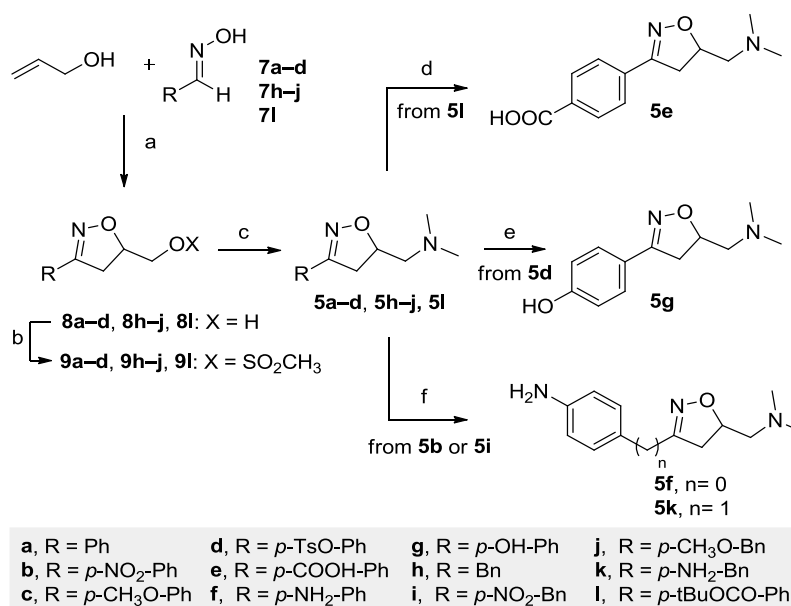
Slow generation of the nitrile oxide can be achieved by addition of an organic base by means of a syringe pump to a solution of the stable precursor hydroximoyl halide and the dipolarophile. Alternatively, an efficient strategy involves the use of a heterogeneous mixture of an organic solvent, e.g., ethyl acetate, and an inorganic base, e.g., NaHCO<sub>3</sub> or KHCO<sub>3</sub>.<sup>102</sup>

Both methods allow the maintenance of a low concentration of the dipole, thus preventing dimerization and promoting its reaction with the dipolarophile. The drawback of the above-described strategy is the slowness of the reaction, which can take up to several days or weeks.

### 3.2. Synthesis of $\Delta^2$ -isoxazolines (**5a-l**)

The key step for the synthesis of  $\Delta^2$ -isoxazolines **5a-l** was the 1,3-dipolar cycloaddition of nitrile oxides to allylic alcohol. Nitrile oxides were formed *in situ* by the corresponding aldoximes **7** after oxidative chlorination with aqueous NaOCl solution (common bleach), followed by base-induced dehydrochlorination of the intermediate hydroxymoyl chlorides (chloroximes). The cycloaddition reaction afforded alcohols **8** in good isolated yields (68-93%) (Scheme 3.1).

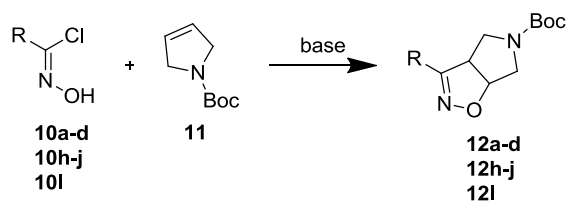
The nucleophilic displacement of the corresponding mesylates **9** with dimethylamine furnished derivatives **5a-d**, **5h-j**, and **5l**. The carboxylic acid derivative **5e** was obtained by deprotecting the t-butyl ester **5l** with trifluoroacetic acid at room temperature. The phenol derivative **5g** was obtained from the corresponding tosylate **5d** after hydrolysis with NaOH. Finally, reduction with zinc powder in acetic acid converted nitro derivatives **5b** and **5i** into the corresponding amino derivatives **5f** and **5k**, respectively.



**Scheme 3.1. Reagents and conditions:** (a) 3% NaOCl, CH<sub>2</sub>Cl<sub>2</sub>, 0 °C to room temperature, 15 min (68-93%); (b) MsCl, TEA, CH<sub>2</sub>Cl<sub>2</sub>, 0 °C to room temperature, 45 min (99%); (c) dimethylamine, THF, 100 °C, sealed tube, 12 h (75-81%); (d) TFA/CH<sub>2</sub>Cl<sub>2</sub> 1:3, room temperature, overnight (99%); (e) 1N NaOH, EtOH, reflux, 1 h (96%); (f) zinc powder, acetic acid, room temperature, 1 h (63-75%)

### 3.3. Synthesis of bicyclic- $\Delta^2$ -isoxazolines (6a-l)

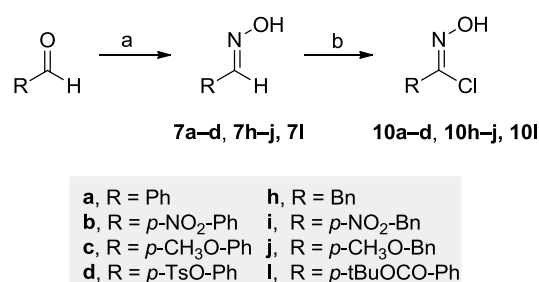
3-Aryl-(or benzyl)-4,5,6,6a-tetrahydro-3aH-pyrrolo[3,4-*d*]-isoxazole derivatives **12** were obtained exploiting the reactivity of different chloroximes with the low-reactive *N*-Boc- $\Delta^3$ -pyrroline **11**<sup>103</sup> (Scheme 3.2)



**Scheme 3.2. General reaction scheme of 1,3-dipolar cycloaddition**

### 3.3.1. Synthesis of the dipoles: the chloroximes

The substituted chloroximes **10** were prepared employing a straightforward two-step strategy: the proper aldehydes were first converted in the corresponding oximes under standard conditions, then derivatives **7** were reacted with NCS in the presence of pyridine to give the corresponding **10a-d**, **10h-j**, and **10l** (Scheme 3.3).



**Scheme 3.3. Reagents and conditions:** (a) NH<sub>2</sub>OH•HCl, Na<sub>2</sub>CO<sub>3</sub>, H<sub>2</sub>O/methanol 1:1, room temperature, 3 h (89-96%); (b) NCS, pyridine, CHCl<sub>3</sub>, 40 °C, 0.5–3h (99%).

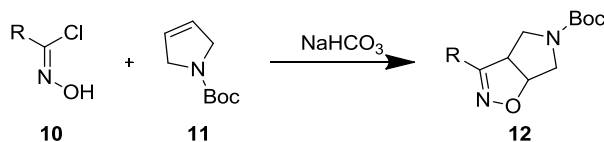
### 3.3.2. Optimizing the 1,3-dipolar cycloaddition

As previously reported with other types of hydroxamoyl halides, *N*-Boc-protected pyrroline **11** has a poor reactivity, and unless the generated dipole is highly reactive (e.g., bromonitrileoxide), the cycloaddition reaction gives low yields.<sup>104</sup> Thus, a slow generation of the dipole is required.

#### 3.3.2.1. Conventional conditions

We initially carried out the reaction under conventional reaction conditions: the nitrile oxide was generated *in situ* by treating chloroximes **10** with excess solid NaHCO<sub>3</sub> in EtOAc, in the presence of alkene **11**, and the reaction was carried out at room temperature. As a result of the partial dimerization of the

dipole, the addition of further aliquots of chloroxime over time was necessary. The cycloaddition reaction proceeded slowly, yielding less than 50% of the desired product after 7 days (Table 1.1). The yield was strongly dependent on the nature of the chloroxime, ranging from 45% (entry c, R=*p*-CH<sub>3</sub>O-Ph) to as low as < 2% (entry e, R=*p*-NO<sub>2</sub>-Bn).

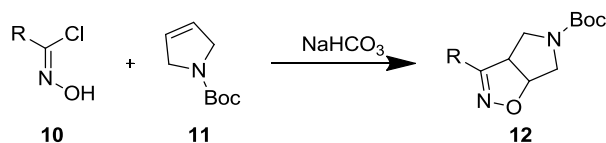


Entry	R	equiv. of 10 <sup>a</sup>	time (days)	solvent <sup>b</sup>	yield <sup>c</sup> (%)
a	Ph	4	7	EtOAc	40
b	<i>p</i> -NO <sub>2</sub> -Ph	4	7	EtOAc	28
c	<i>p</i> -CH <sub>3</sub> O-Ph	4	7	EtOAc	45
d	Bn	4	7	EtOAc	32
e	<i>p</i> -NO <sub>2</sub> -Bn	4	7	EtOAc	< 2
f	<i>p</i> -CH <sub>3</sub> O-Bn	4	7	EtOAc	35

**TABLE 1.1.** Reaction of chloroximes **10** with *N*-Boc- $\Delta^3$ -pyrroline **11** under conventional reaction conditions at room temperature. <sup>a</sup>Added portionwise to the reaction mixture; <sup>b</sup>room temperature; <sup>c</sup>isolated yield.

### 3.3.2.2. Conventional heating and Microwave irradiation

Taking in mind the results obtained, we optimized the reaction conditions using chloroxime **10a** as a model substrate. When the reaction was carried out under conventional heating by refluxing in EtOAc, the yield was comparable to that obtained at room temperature (Table 1.2, entry 1 vs Table 1.1, entry a), but reaction time was reduced from 7 to 3 days and only 2 equiv of **10a** were consumed. The yield can be further improved up to 51% by adding a small percentage of water (1% v/v) to the reaction medium (Table 1.2, entry 2).



entry	equiv of 10a <sup>a</sup>	solvent	time (h)	T (°C)	yield <sup>d</sup> (%)
1	2.0	EtOAc	72	reflux <sup>b</sup>	42
2	2.0	EtOAc + H <sub>2</sub> O (1%)	72	reflux <sup>b</sup>	51
3	1.5	EtOAc	2 x 0.5	80 <sup>c</sup>	35
4	2.0	EtOAc	3 x 0.5	80 <sup>c</sup>	48
5	2.5	EtOAc	4 x 0.5	80 <sup>c</sup>	41
6	3.0	EtOAc	5 x 0.5	80 <sup>c</sup>	34
7	2.0	EtOAc + H <sub>2</sub> O (1%)	3 x 0.5	80 <sup>c</sup>	66
8	2.0	EtOAc + H <sub>2</sub> O (2%)	3 x 0.5	80 <sup>c</sup>	47
9	2.0	EtOAc + H <sub>2</sub> O (1%)	3 x 0.5	90 <sup>c</sup>	56
10	2.0	EtOAc + H <sub>2</sub> O (1%)	3 x 0.5	100 <sup>c</sup>	44

**TABLE 1.2.** Optimization of reaction conditions for the cycloaddition of chloroxime **10a** ( $R=Ph$ ) to *N*-Boc- $\Delta^3$ -pyrroline **11**, under conventional heating or microwave irradiation. <sup>a</sup>Added portionwise to the reaction mixture; <sup>b</sup>conventional heating; <sup>c</sup>microwave irradiation; <sup>d</sup>isolated yield.

The potential usefulness of the microwave-assisted methodology was then investigated, varying the reaction conditions, i.e., the number of equivalents of **10a**, time, temperature, and percentage of added water, with the aim of fine-tuning the best reaction conditions (Table 1.2). The use of solid NaHCO<sub>3</sub> (4 equiv) as a base was kept as a constant in all the experiments. Heating cycles of 30 min each were applied. The first equivalent of chloroxime was added at the beginning of the experiment, and further 0.5 equiv portions were added before every additional heating cycle, since monitoring by TLC showed the presence of unreacted alkene **11**, while chloroxime **10a** was completely consumed. The highest yield was obtained after the addition of 2 equiv of chloroxime and 3 heating cycles (Table 1.2, entry 4).

As observed under conventional heating conditions, the addition of a small percentage of water (1% v/v) to the reaction medium had a positive effect on the reaction outcome (Table 1.2, entry 7 vs 4). Thus, we selected as optimal conditions those reported in entry 7. While operating under these conditions, we extended our procedure to a series of differently substituted chloroximes. The data reported in Table 1.3 demonstrate that this methodology is versatile and can be fruitfully applied to the synthesis of a series of 3-substituted isoxazolines **12**. In fact, all derivatives were obtained in acceptable yields (47-67%).

entry <sup>a</sup>	R	time (h)	yield <sup>b</sup>
1	Ph	3 x 0.5	66
2	<i>p</i> -NO <sub>2</sub> Ph	3 x 0.5	60
3	<i>p</i> -CH <sub>3</sub> OPh	3 x 0.5	67
4	Bn	3 x 0.5	50
5	<i>p</i> -NO <sub>2</sub> Bn	3 x 0.5	47
6	<i>p</i> -CH <sub>3</sub> OBn	3 x 0.5	57

**TABLE 1.3.** Microwave-assisted cycloaddition of chloroximes *10a-c* and *10h-j* to *N*-Boc- $\Delta^3$ -pyrroline *11*. <sup>a</sup>Results obtained using the optimized conditions reported in Table 1.2, entry 7; <sup>b</sup>isolated yield.

Notably, the reaction time was significantly reduced from 7 days (at room temperature) or 3 days (refluxing under conventional heating) to 1.5h, and very importantly, the outcome of the reaction was not anymore dependent on the nature of the chloroxime.

*3.3.2.3. Continuous-flow technique*

The main limitation of the microwave methodology is, however, related to the possibility of scaling up the reaction. In fact, microwave devices commonly available in a research laboratory are designed to fit 0.2-35 mL sealed tubes, allowing performance of the reaction up to a maximum total volume of 25 mL. This entails the need to repeat the reaction several times in order to produce the desired cycloadduct in multigram scale. Moreover, as pointed out above, the procedure, albeit optimized, requires multiple operator interventions to add additional aliquots of chloroxime over time.

Thus, we decided to investigate the feasibility of this type of cycloaddition reaction under continuous-flow conditions.<sup>105,106</sup> For this purpose, we used the R2+/R4 flow system commercially available from Vapourtec (Figure 3.2).



**Figure 3.2.** *R2+/R4 flow chemistry apparatus (Vapourtec).*



Initially, the reaction was performed using a 0.25 M solution of **11** (0.25 mmol) in EtOAc (1 mL) and an equimolar solution of chloroxime **10a** (Table 1.4, entry 1). The solutions were introduced into the flow stream (EtOAc) through two injection loops, mixing was achieved with a simple T-piece, and the combined output was then directed through a glass column containing the base (4 equiv), heated at 90 °C, in which the reaction took place (Figure 3.3).

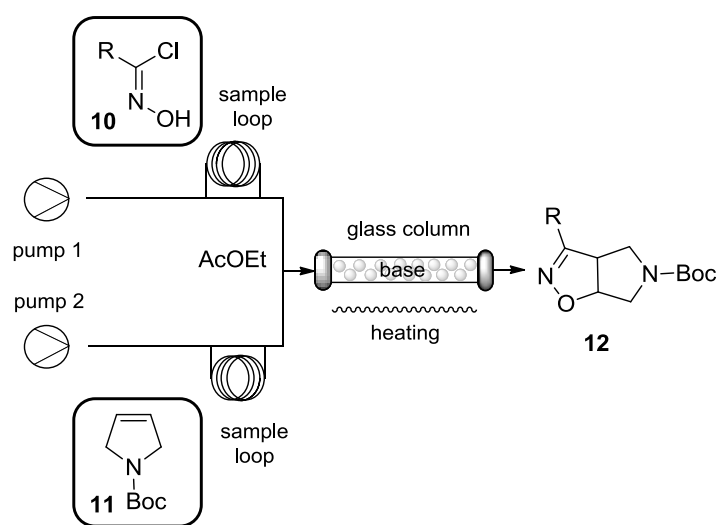
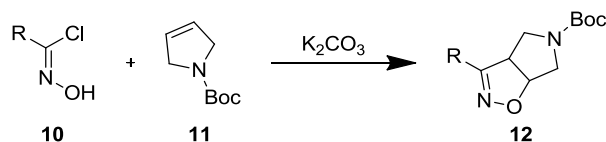


**Figure 3.3.** Schematic representation of the cycloaddition reaction in flow.

First, we chose the appropriate base among a selection of polymer-supported (PS) bases (i.e., PS-sodium carbonate, Amberlyst A-21, PS-DBU), as well as solid  $\text{NaHCO}_3$  and  $\text{K}_2\text{CO}_3$ . All of the PS-bases turned out to be inefficient in the cycloaddition reaction, since the product **12** was isolated in unacceptable yield (<10%). Only solid  $\text{K}_2\text{CO}_3$  gave a good result (50% yield), and so it was selected for the subsequent optimization phase.

The total flow rate was set in a way that the residence time of the reagents in the column was 30 min. The final flow line was then collected and evaporated to give the crude material, which was purified by column chromatography. A positive system pressure was maintained by using an in-line 100 psi back-pressure regulator.



Entry <sup>a</sup>	equiv of 10 <sup>a,b</sup>	<i>T</i> (°C)	residence time (min)	yield <sup>c</sup>
1	1.0	80	30	50
2	1.5	80	30	60
3	2.0	80	30	63
4	1.5	80	10	45
5	1.5	90	10	69
6	4.5	90	10	87
7	1.5	100 <sup>d</sup>	10	45

**TABLE 1.4.** Cycloaddition of chloroxime 10a (*R*=Ph) to *N*-Boc- $\Delta^3$ -pyrroline 11 under continuous-flow conditions <sup>a</sup>Reactions conducted on a 0.25 mmol scale of *N*-Boc- $\Delta^3$ -pyrroline 11 in EtOAc (0.25 M solution), using solid K<sub>2</sub>CO<sub>3</sub> as a base (4.0 equiv). <sup>b</sup>All solutions were prepared in 1mL of EtOAc. <sup>c</sup>Isolated yield. <sup>d</sup>A further increase in the temperature up to 130 °C causes a dramatic reduction of the yield (8%).

As shown in Table 1.4, under continuous-flow conditions it was possible to obtain cycloadduct 12a in good yield (69%, entry 5) in only 10 min using 1.5 equiv of chloroxime 10a. This represents a significant improvement over the above described microwave-assisted methodology, since the reaction time was considerably reduced from 1.5 h to 10 min with a comparable satisfactory

yield (69% vs 66%). However, increasing the temperature to 100 °C was detrimental for the reaction yield (Table 1.4, entry 7 vs 5).

Moreover, using a larger excess of chloroxime **10a** (entry 6), complete conversion of the alkene was observed, and the yield was improved to 87%, but the isolation of the product was hampered by the presence of a large amount of furoxan and other byproducts and required intensive and time-consuming purifications by column chromatography. Therefore, we selected the conditions reported in Table 1.4, entry 5 as the optimal ones and validated our synthetic protocol by applying such optimized conditions to the series of chloroximes **10a-c** and **10h-j**. In all cases (Table 1.5), the cycloadducts were obtained in good yield (60-73%), very short time (10 min), and using as low as 1.5 equiv of chloroxime.<sup>107</sup>

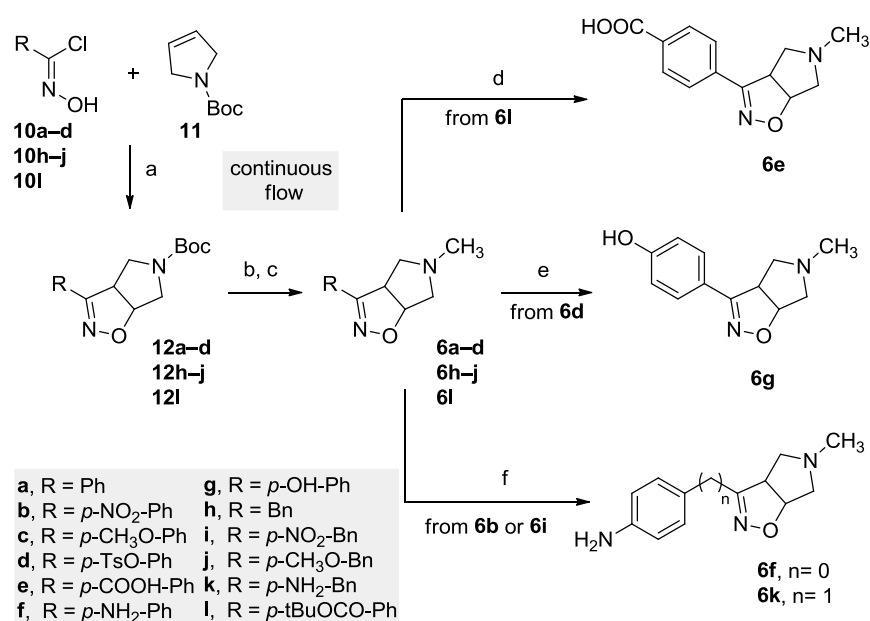
entry <sup>a</sup>	R	time (min)	Yield <sup>b</sup> (%)
1	Ph	10	69
2	<i>p</i> -NO <sub>2</sub> -Ph	10	60
3	<i>p</i> -CH <sub>3</sub> O-Ph	10	73
4	Bn	10	71
5	<i>p</i> -NO <sub>2</sub> -Bn	10	67
6	<i>p</i> -CH <sub>3</sub> O-Bn	10	74

**TABLE 1.5.** Cycloaddition of chloroxime **10a-c** and **10h-j** to *N*-Boc- $\Delta^3$ -pyrroline **11** under continuous-flow conditions <sup>a</sup>Results obtained using the optimized conditions reported in Table 1. 4, entry 5; <sup>b</sup>isolated yields.

Moreover, this process could be easily scaled up by simply letting the instrument run for longer time and using a larger base-containing column, without any intervention from the operator.<sup>108</sup>

## 3.3.3. Synthesis of compounds 6a-l

As previously reported, running the 1,3-dipolar cycloaddition reaction under continuous-flow conditions resulted in a straightforward generation of the *N*-Boc-protected bicyclic- $\Delta^2$ -isoxazolines **12**. Removal of the *N*-Boc group with 4 M HCl solution in dioxane and subsequent methylation with methyl iodide in acetone produced derivatives **6a-d**, **6h-j**, and **6l**. The carboxylic acid derivative **6e** was obtained by deprotecting the *t*-butyl ester **6l** with trifluoroacetic acid at room temperature. Cleavage of the tosylate group of **6d** with NaOH in EtOH afforded derivative **6g**. Finally, reduction with zinc powder in acetic acid converted the nitro-substituted compounds **6b** and **6i** into the corresponding amino derivatives **6f** and **6k**, respectively (Scheme 3.4).



**Scheme 3.4. Reagents and conditions:** (a) R2+/R4 flow reactor, EtOAc, K<sub>2</sub>CO<sub>3</sub>, 80 °C, 10 min (60-73%); (b) 4N HCl, dioxane, room temperature, 1 h (99%); (c) CH<sub>3</sub>I, K<sub>2</sub>CO<sub>3</sub>, acetone, room temperature, 12 h (31-45%); (d) TFA/CH<sub>2</sub>Cl<sub>2</sub> 1:3, room temperature, overnight (99%); (e) 1N NaOH, EtOH, reflux, 1 h (95%); (f) zinc powder, acetic acid, room temperature, 1 h (85-83%).

### 3.4. Synthesis of “bisubstrate” DNMT1 inhibitors

Once that the biological investigation of the first two series of compound was completed (Chapter 4) and being interested in the development of analogues endowed with improved enzyme binding properties and higher inhibitory potency, we decided to synthesize new, longer compounds, obtained by the combination of the SAM-competitive isoxazoline scaffold with “warheads” targeting the nucleotide binding site (i.e. a portion of the well-known DNMT1 inhibitor SGI-1027), as bisubstrate inhibitors of DNMT1 (Figure 3.4).

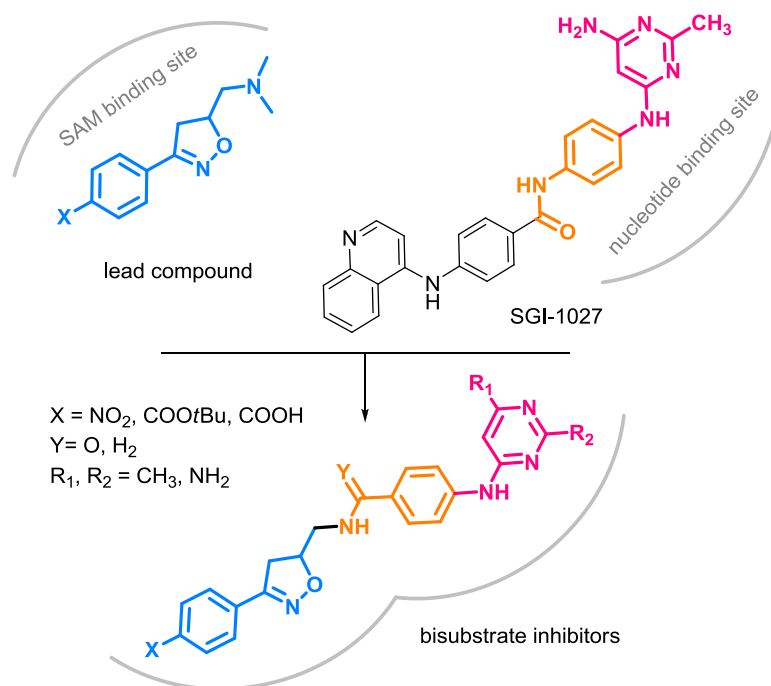
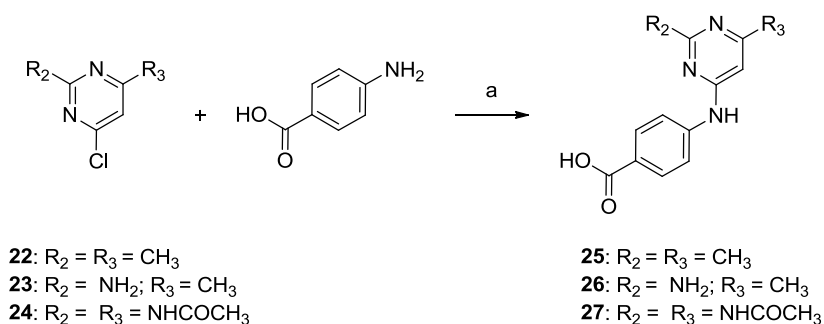


Figure 3.4. Design of novel “bisubstrate” inhibitors of DNMT1.

## 3.4.1. Synthesis of pyrimidinic building blocks

Acids **25-27** were straightforwardly obtained in high yield reacting 4-chloro pyrimidine derivatives **22-24** and *p*-aminobenzoic acid, according the procedure reported in Scheme 3.5.

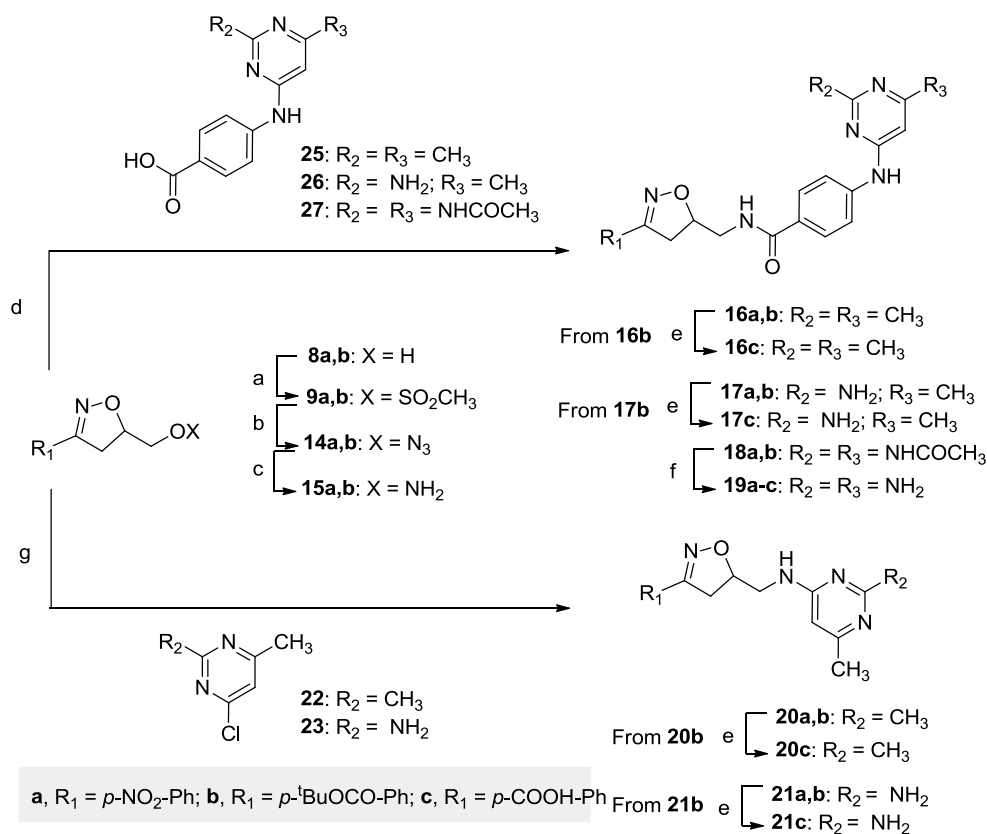


**Scheme 3.5. Reactions and conditions:** (a) MW, 2-propanol, 120 °C, 30 min/1.5 h (90-99%)

## 3.4.2. Synthesis of final compounds (16-21)

The mesylate derivatives **9a-b**, prepared as previously described, were reacted with sodium azide in dimethylformamide to afford azides **14a-b**. These were treated with triphenylphosphine in wet methanol to afford the corresponding amines **15a-b**. Then, derivatives **16a-b**, **17a-b** and **18a-b** were prepared by amide coupling reaction between amines **15a-b** and acids **25-27**, under the standard HBTU/HOBt/DIEA conditions. However, since the amide coupling reaction was slow and gave only low yields (up to 10%) of **19a-b**, we resolved to protect the two amino groups and prepare acetyl derivative **24** (Scheme 3.5). Thus, using this protected derivative, coupling reaction with amines **15a-b** gave in good yield derivatives **18a-b**.

For the synthesis of derivatives of type **20** and **21**, amines **15a-b** were treated under microwave irradiation with the appropriate 4-chloro pyrimidine derivative (**22** or **23**) in 2-propanol.



**Scheme 3.6. Reactions and conditions:** (a)  $\text{MsCl}$ , TEA,  $\text{CH}_2\text{Cl}_2$ ,  $0\text{ }^\circ\text{C}$  to room temperature, 45 min (99%); (b)  $\text{NaN}_3$ , DMF, reflux, 3h (90%); (c)  $\text{PPh}_3$ ,  $\text{MeOH}/\text{H}_2\text{O}$  1:1, room temperature, 30 min (73-82%); (d) HOBt, HBTU, DIEA, THF/DMF 3:1, room temperature, 1-12h (68-80%); (e) DCM/TFA 9:1, room temperature, 30 min (99%); (f) NaOH 1N, EtOH, room temperature to reflux, 2h (43-70%); (g) MW, 2-propanol,  $180\text{ }^\circ\text{C}$ , 30 min (67-80%).

The carboxylic acid derivatives **16c**, **17c**, **20c** and **21c** were obtained by deprotecting the *t*-butyl esters **16b**, **17b**, **20b** and **21b**, respectively, with trifluoroacetic acid at room temperature. Finally, treating derivative **18a** in methanol with 1N aqueous solution of NaOH, deprotected compound **19a** was obtained. When these reaction conditions were applied on derivative **18b**, formation of both *t*-butyl ester **19b** and the corresponding acid **19c** was observed (Scheme 3.6).

### 3.5. Virtual screening: a new approach for the discovery of DNMT1 inhibitors

Until now, most compounds associated with DNA methylation inhibition have been identified fortuitously, and even fewer have been validated as directly targeting DNMTs *in vitro* or *in vivo*. Limited studies have been reported thus far to explore systematically the DNMT inhibition properties of large compound databases. Experimental characterization of hundreds or thousands of small molecules as demethylating agents would be a daunting task in terms of cost and time. To accelerate systematic screening, computational techniques, including virtual screening, are increasingly being used to identify active compounds.<sup>86</sup>

In 2011, in collaboration with Prof. Jose Medina-Franco (Torrey Pines Institute for Molecular Studies, Florida, United States), 260,000 compounds in the Diversity Set available from the National Cancer Institute (NCI; <http://dtp.nci.nih.gov/>) were the starting point to identify additional DNMT1 inhibitors. Six of the top scoring compounds (Figure 3.5) were synthesized by us in order to obtain their DNMT1 inhibitory activity in a biochemical assay.

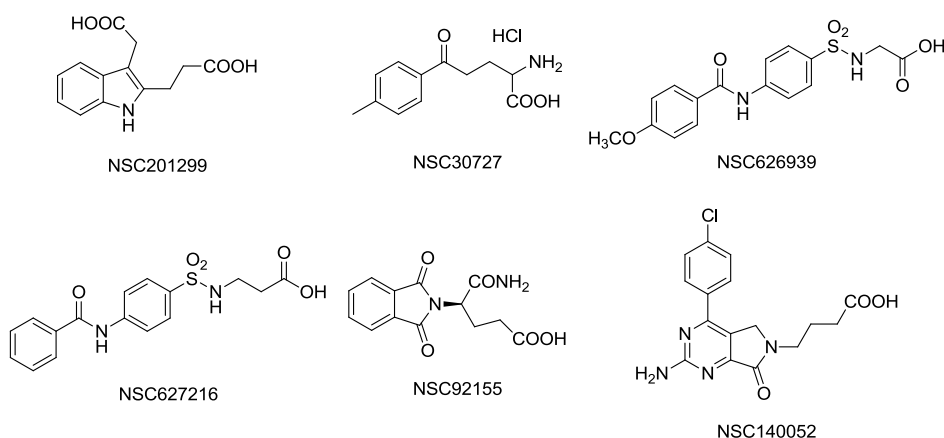
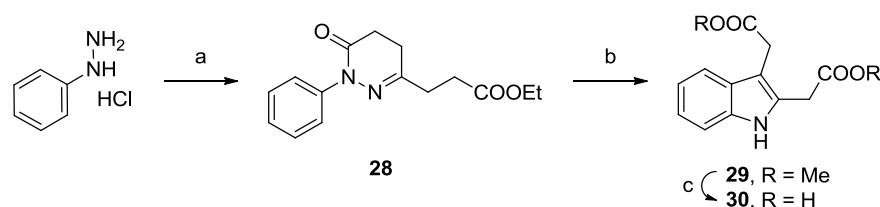


Figure 3.5. The six top scoring compounds identified from NCI database.



## 3.5.1. Synthesis of NSC201299 (30)

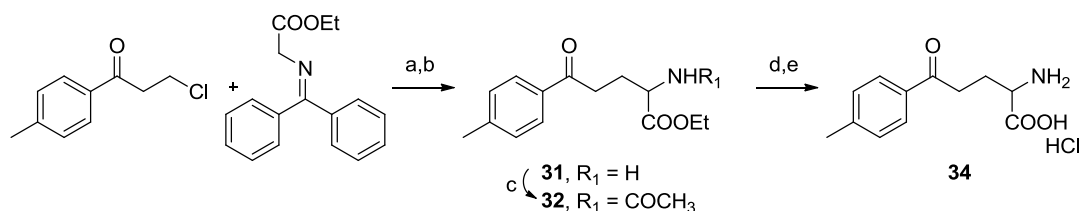
For the preparation of derivative **29**, the well-known Fischer indole synthesis<sup>109</sup> starting from the symmetrical diethyl 4-oxopimelate was chosen. In order to obtain the indolic scaffold, a two-step procedure, taking advantage of the smooth formation of pyridazinone **28**, followed by treatment with saturated HCl/MeOH solution at reflux, proved to be efficient (73% overall yield).<sup>110</sup> Finally, subsequent hydrolysis of **29** gave the corresponding acid **30** (Scheme 3.7).



**Scheme 3.7. Reactions and conditions:** (a) diethyl-4-oxopimelate, toluene, reflux, 48h (90%); (b) HCl/MeOH, reflux, 24h (80%); (c) NaOH 1N, MeOH, room temperature, 3h (99%).

## 3.5.2. Synthesis of NSC30727 (34)

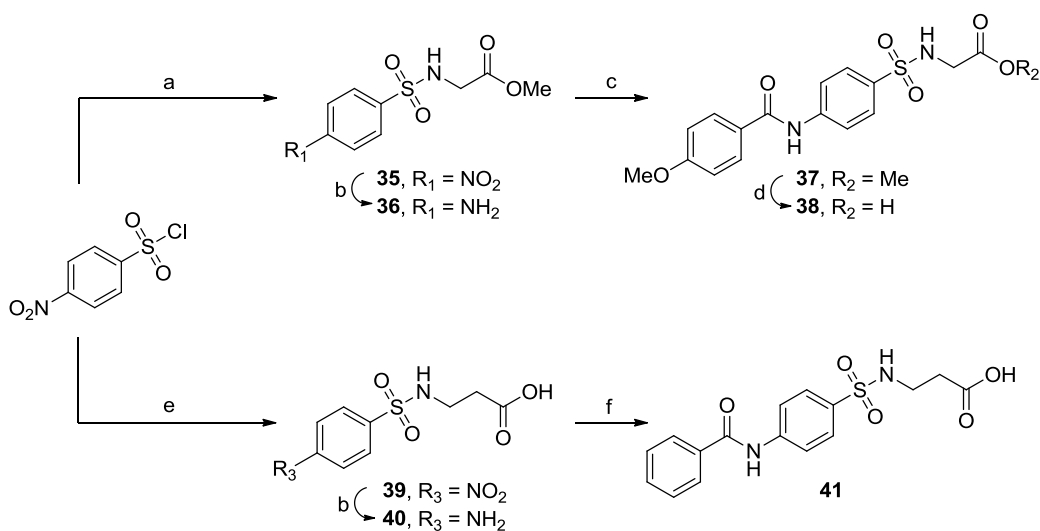
The 2-amino-5-oxo-5-(*p*-tolyl)pentanoic acid **34** was obtained exploiting a five-step procedure, as depicted in Scheme 3.8. The first step was a nucleophilic substitution, followed by protection and deprotection of the amino and carboxylic moieties.



**Scheme 3.8. Reactions and conditions:** (a) DIPEA, DMPU, BuLi, THF dry, -78 °C, 2h; (b) HCl 2N, Et<sub>2</sub>O, room temperature, 1h (60%); (c) Acetic anhydride, CH<sub>2</sub>Cl<sub>2</sub>, room temperature, 4h (99%); (d) Amb. 900 OH, EtOH/H<sub>2</sub>O, room temperature, 3h; (e) HCl 1N, room temperature, 30 min (99%).

## 3.5.3. Synthesis of NSC626939 (38) and NSC627216 (41)

The sulfonamides **35** and **39** were obtained by reaction between 4-nitrobenzene-1-sulfonyl chloride and secondary amines. The nitro group was promptly reduced to the key intermediates **36** and **40** by heterogeneous catalytic (palladium/activated carbon) hydrogenation. The reaction of this compounds with 4-methoxybenzoyl chloride in dry THF, or with benzoyl chloride in THF/H<sub>2</sub>O gave the corresponding derivatives **37** and **41**. The subsequent hydrolysis of **37** with aqueous lithium hydroxide in methanol furnished the corresponding acid **36** (Scheme 3.9).

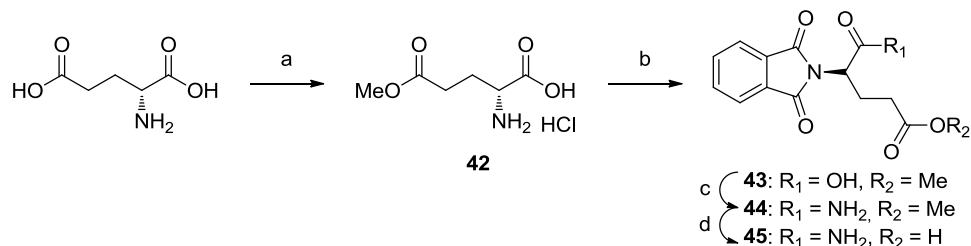


**Scheme 3.9. Reactions and conditions:** (a) Gly-OMe HCl, TEA, dry CH<sub>2</sub>Cl<sub>2</sub>, room temperature, 1.5h (57%); (b) H<sub>2</sub>, Pd/C, EtOH, room temperature, 2h (99%); (c) 4-methoxybenzoyl chloride, TEA, dry THF, room temperature, 12h (77%); (d) LiOH, H<sub>2</sub>O/MeOH, room temperature, 2.5h (90%); (e) β-Ala, NaOH 1N, room temperature, 3h (37%); (f) benzoyl chloride, NaHCO<sub>3</sub>, THF/H<sub>2</sub>O, reflux, 48h (70%).

## 3.5.4. Synthesis of NSC97155 (45)

Compound **43** was synthesized by treating *N*-ethoxycarbonylphthalimide with the glutamine derivative **42**, in the presence of sodium carbonate.<sup>111</sup> The

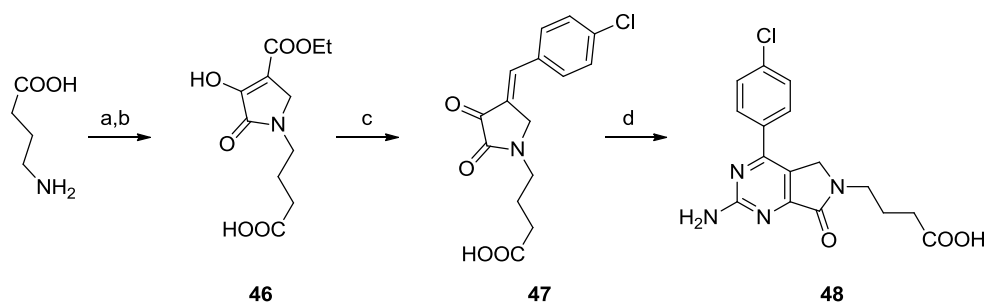
subsequent amidation and hydrolysis gave the final compound **45** in short time and high yields, as shown in Scheme 3.10.



**Scheme 3.10. Reactions and conditions:** (a)  $\text{SOCl}_2$ , MeOH, room temperature, 30 min (99%); (b) *N*-ethoxycarbonylphthalimide,  $\text{Na}_2\text{CO}_3$ ,  $\text{H}_2\text{O}$ , from 0 °C to room temperature, 1h (99%); (c) isobutyl chloroformate, NMM,  $\text{NH}_3$ , THF, room temperature, 1.5h (51%); (d) HCl 2N, dioxane, room temperature, overnight (99%).

### 3.5.5. Synthesis of NSC140052 (**48**)

The first step in the synthesis of pyrrolo[3,4-*d*]-pyrimidine **48** was carried out by the addition of the sodium salt of  $\gamma$ -aminobutyric acid to ethyl acrylate in absolute ethanol. Condensation of this intermediate with ethyl oxalate in the presence of sodium ethoxide gave derivative **46** in moderate yield. Finally, the benzilidene derivative **47**, obtained by acid-catalyzed condensation of **46** with 4-chlorobenzaldehyde, was subjected to addition of guanidine in order to achieve the desired compound **48** (Scheme 3.11).<sup>112</sup>

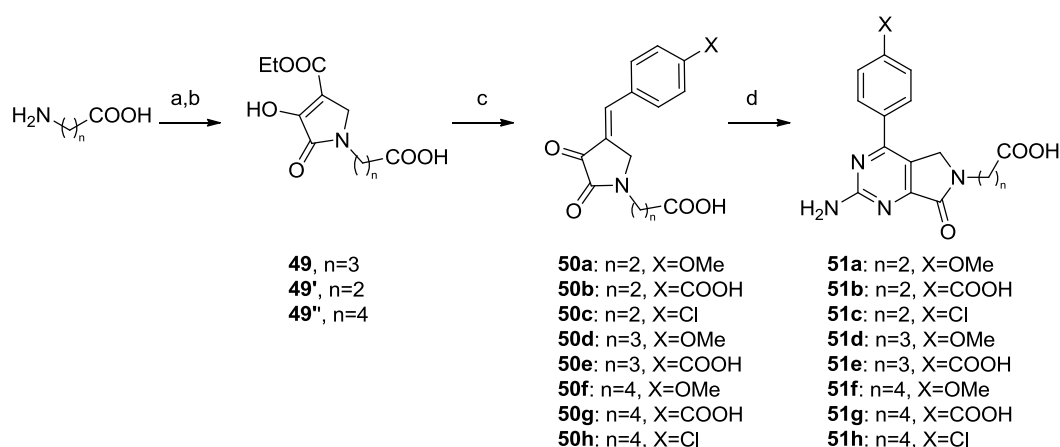


**Scheme 3.11. Reactions and conditions:** (a) NaOEt, ethyl acrylate, EtOH, from 0 °C to room temperature, 12h; (b) NaOEt, diethyl oxalate, 80 °C, 3h (52%); (c) 4-chlorobenzaldehyde, HCOOH, HCl 6N, 100 °C, 2.5h (40%); (d) NaOEt, guanidine, EtOH, room temperature, 72h (30%).

### 3.6. From NSC140052 to novel pyrrolo[3,4-*d*]-pyrimidines: new DNMT1 inhibitors (51a-h)

As emerged from the biological assays (Chapter 4), in the series of derivatives found *via* virtual screening, NSC140052 resulted the most powerful compound, showing a good inhibitory activity against DNMT1 ( $IC_{50} = 220 \mu\text{M}$ ).

Being interested in the synthesis of new small molecule derivatives of this new *hit*, and taking advantage of its synthetic procedure previously described, we developed a small library of compounds characterized by several functional groups on the aromatic ring (-OCH<sub>3</sub>, -COOH, -Cl) and different length of the side chain (from 2 to 4 carbon atoms) as shown in Scheme 3.12.



**Scheme 3.12. Reactions and conditions:** (a) NaOEt, ethyl acrylate, EtOH, from 0 °C to room temperature, 12h; (b) NaOEt, diethyl oxalate, 80 °C, 3h (52-66%); (c) Aldehydes, HCOOH, HCl 6N, 100 °C, 2.5h (40-86%); (d) NaOEt, guanidine, EtOH, room temperature, 72h (30-40%).

### 3.7. Six months abroad: Microwave and Continuous-flow chemistry in the lab of Prof. C. O. Kappe

Once that the potency of microwave and flow techniques was validated in the field of 1,3-dipolar cycloaddition, and with the aim to improve my knowledge in this fields, I've been for six months at the Karl-Franzens-Universität, Graz, Austria, in the laboratory of Prof. C. O. Kappe.

#### 3.7.1. Background & Aim of the work

High-temperature chemistry offers many distinct benefits, as demonstrated by the recent success of microwave-assisted organic synthesis.<sup>113</sup> The short reaction times experienced in microwave chemistry protocols form an ideal basis for continuous flow processing, where short residence times are essential in order to achieve a high throughput.

Starting from this background, we planned and realized an extension of this concept, demonstrating that conditions optimized using batch microwave system on a milliliter scale can be translated to a laboratory-scale microreactor setting, and can be further adapted to a mesofluidic flow regime that allows a L/h throughput, therefore more closely resembling pilot-plant/production-scale capabilities (Figure 3.6).

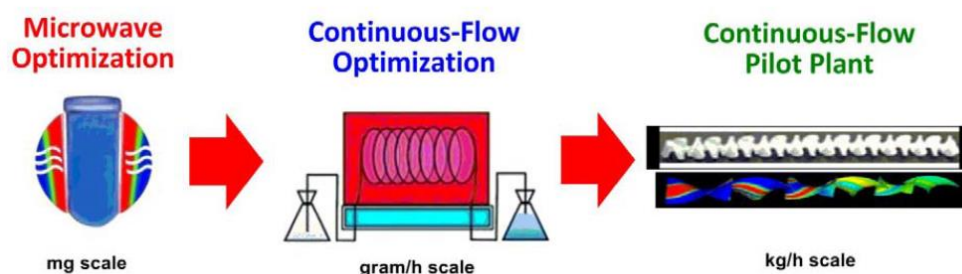
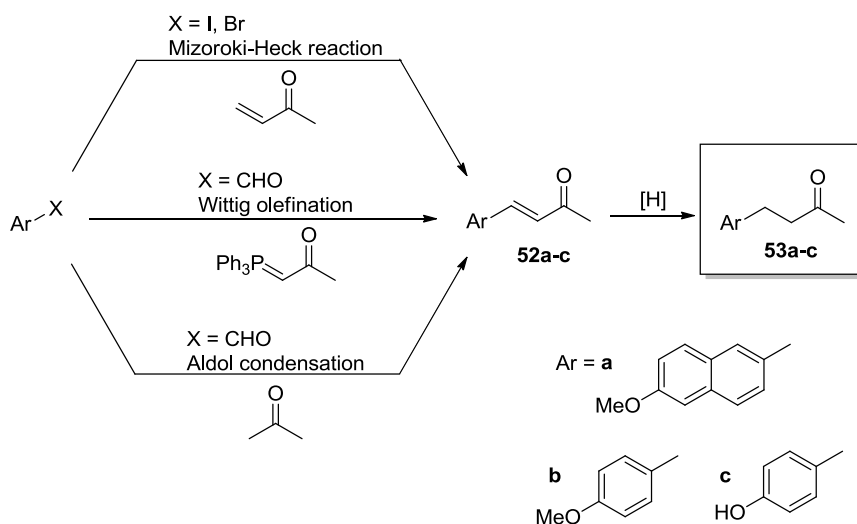


Figure 3.6. Aim of the work.

As model systems, we evaluated different continuous flow strategies for the generation of the anti-inflammatory drug nabumetone [4-(6-methoxy-2-naphthalenyl)-2-butanone] and related 4-aryl-2-butanones using a combination of two process-intensified flow reaction steps. The synthetic routes were first optimized on small scale using controlled microwave batch technology and then translated to continuous flow processes. Ultimately, a custom built large-scale mesofluidic flow setup capable of processing 2.7 L/h was designed to significantly expand the scale of the process.<sup>114</sup>

### 3.7.2. Planned synthesis of derivatives 53a-c

Some of the most efficient general published methods for synthesizing 4-aryl-2-butanones **53a-c** are summarized in Scheme 3.13. All three protocols (Mizoroki-Heck, Wittig, and aldol reactions) involve the initial preparation of the corresponding 4-aryl-3-buten-2-ones **52a-c** which is then followed by selective hydrogenation of the C=C double bond to 4-aryl-2-butanones **53a-c**.

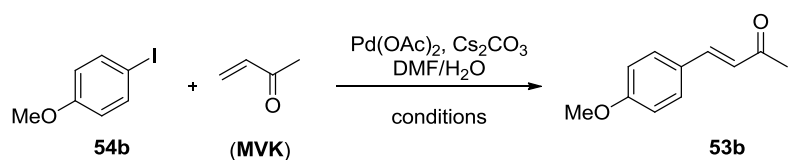


Scheme 3.13. Different synthetic strategies to 4-aryl-butanones **53a-c**

With the aim of developing process-intensified methods for the rapid synthesis of the key intermediates **52a-c** in a flow format, we have initially optimized the above transformations under microwave batch conditions and then adapted for use in a flow reactor. The final hydrogenation was achieved in a commercially available flow hydrogenation device (H-Cube).

### 3.7.3. Mizoroki-Heck reaction

The starting point for our studies involved the adaptation of the Mizoroki-Heck reaction of methyl vinyl ketone (MVK) with 4-iodoanisole (**54b**) into a high-speed microwave protocol leading to **52b** (Table 1.6).<sup>115</sup>



Entry <sup>a</sup>	Conditions	Pd(OAc) <sub>2</sub> [mol%]	MVK [equiv]	T [°C]/ t [min]	Flow rate [mL/min]	Conv [%] <sup>b</sup>	Product purity [%] <sup>c</sup>
1	MW	1	1.1	160/20	-	> 99	60
2	MW	1	1.5	160/20	-	> 99	72 (74) <sup>d</sup>
3	MW	0.5	1.5	160/20	-	> 99	70
4	MW	0.2	1.5	160/20	-	> 99	74 (76) <sup>d</sup>
5	MW	0.1	1.5	160/20	-	84	57
6	MW	0.2	1.5	180/10	-	> 99	69 (66) <sup>d</sup>
7	flow	0.2	1.5	180/10	1.6	> 99	73 (67) <sup>d</sup>

**TABLE 1.6. Optimization of the Mizoroki–Heck reaction of 4-iodoanisole (**54b**) and methyl vinyl ketone (MVK) under microwave batch and continuous flow conditions.** <sup>a</sup> General conditions: 0.4 mmol **54b**, Cs<sub>2</sub>CO<sub>3</sub> (1.1 equiv), DMF/H<sub>2</sub>O 3:1 (3 mL); single-mode microwave irradiation (IR temp monitoring). Flow experiments (60 bars pressure) were performed using a ThalesNano X-Cube Flash instrument equipped with a 16 mL stainless steel coil. <sup>b</sup> Conversions refer to HPLC peak area integration at 230 nm. <sup>c</sup> Product purity refers to relative peak area (%) ratios of crude HPLC traces. <sup>d</sup> Isolated yield after flash chromatography.

In our hands, the Mizoroki-Heck coupling proceeded well under controlled microwave conditions. Special attention was paid to the selection of a proper base for this transformation ( $\text{Cs}_2\text{CO}_3$ ), keeping the general requirement for homogeneous reaction conditions for subsequent translation to a continuous flow process in mind. After different experiments, we were able to identify the optimal set of conditions which worked best in a small-scale microwave batch environment (Table 1.6, entry 6), and that could be applied to the flow-chemistry apparatus.

Continuous-flow experimentation was performed in a high-temperature, high-pressure microtubular flow unit that can be used for processing homogeneous reaction mixtures (X-Cube Flash, Thales Nanotechnology Inc.). Although the successful results (67% isolated yield), due to the comparatively low selectivity achieved in this Mizoroki-Heck coupling and the required product purification of the crude reaction mixture, and in consideration of the high costs of catalyst and starting materials (aryl-iodides) it was decided not to further pursue this avenue on scale.

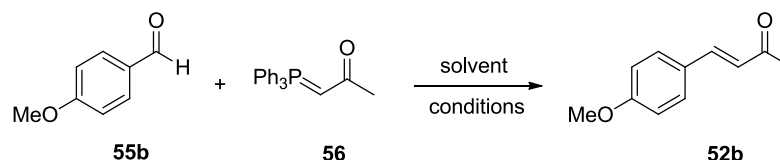
#### **3.7.4. Wittig reaction**

As a second synthetic strategy to access the key intermediates **52a-c**, the Wittig olefination of aldehydes **55a-c** in the presence of (acetylmethylene)triphenylphosphorane (**56**) was investigated (Scheme 3.13). In our hands, employing aldehyde **55b** and phosphorane **56** in MeCN or DMF at temperatures of 190-210 °C, high conversions were achieved under microwave conditions within 10-20 min (Table 1.7).

Although MeCN behaved well as solvent, truly homogeneous reaction conditions were only obtained in DMF up to concentrations of 0.1 M.



Therefore, the conditions reported in Table 1.7, entry 6 were selected as optimal conditions for both batch and continuous flow processing and was also applied to the synthesis of **52a** and **52c**, providing the desired products in high yield (97% and 98% respectively).



Entry <sup>a</sup>	Conditions	<b>55b</b> [equiv]	Temp [°C]/time[min]	Solvent	Conversion [%] <sup>b</sup>
<b>1</b>	MW	1.5	190/20	MeCN	94
<b>2</b>	MW	1.5	200/20	MeCN	98
<b>3</b>	MW	1.7	200/20	MeCN	100 (94) <sup>c</sup>
<b>4<sup>d</sup></b>	MW	1.7	200/20	DMF	97
<b>5<sup>d</sup></b>	MW	1.7	210/20	DMF	99 (95) <sup>c</sup>
<b>6<sup>d</sup></b>	MW	1.7	210/10	DMF	99 (96) <sup>c</sup>
<b>7<sup>e</sup></b>	flow	1.7	210/10	DMF	99 (97)

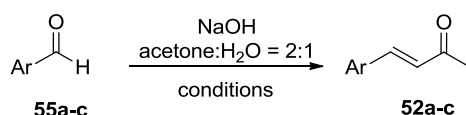
**TABLE 1.7. Reaction optimization for the Wittig reaction of *p*-anisaldehyde (**55b**) and (acetylmethylene)triphenylphosphorane (**56**) under microwave batch and continuous flow conditions.** <sup>a</sup>General conditions: 0.4 mmol **55b**, 1.5-1.7 equiv **56**, 3 mL of solvent, single-mode microwave irradiation, IR temperature control. <sup>b</sup>HPLC peak area integration at 230 nm. <sup>c</sup>Isolated yields using flash chromatography. <sup>d</sup>Homogeneous reaction conditions. <sup>e</sup>Flow experiments were performed in a Uniqsis FlowSyn™ instrument using a 10 mL stainless steel coil (**55b**, 0.1 M).

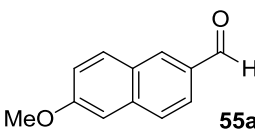
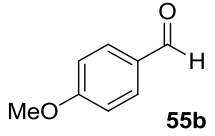
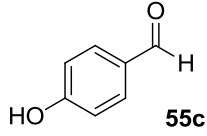
Nevertheless, from the standpoint of process chemistry, the use of an expensive organophosphorous reagent (atom economy), and the generation of stoichiometric amounts of triphenylphosphine oxide byproduct are clearly not suitable for a production route.

## 3.7.5. Aldol reaction

In view of our interest to develop economic and efficient synthetic strategies for the preparation of **53a-c** on an industrial scale, we focused our attention on the aldol route (Scheme 3.13), which apart from the readily available aryl aldehyde precursors **55a-c** only requires acetone and an inorganic base as starting materials.<sup>116, 117</sup>

Employing *p*-anisaldehyde, full conversion was achieved using 0.06 equiv of NaOH (10% aqueous solution) at 120 °C within one minute (Table 1.8).



Substrate <sup>a</sup>	Condition	Temp [°C] /time [s]	Flow rate [mL/min]	Conversion [%] <sup>b</sup>	Yield [%] <sup>c</sup>
 <b>55a</b>	batch (0.8 M)	70/450	-	> 99	97
	flow (0.1 M) <sup>d</sup>	70/450	1.34	> 99	94
 <b>55b</b>	batch (0.7 M)	120/60	-	> 99	94
	flow (0.7 M) <sup>e</sup>	120/60	5	> 99	90
 <b>55c</b>	batch (0.6 M) <sup>d</sup>	70/450	-	80	69
	flow (0.6 M) <sup>d,f</sup>	70/450	1.34	85	78

**TABLE 1.8.** Reaction optimization for the aldol reaction of acetone with aldehydes **55a-c** under microwave batch and continuous flow conditions. <sup>a</sup> General reaction conditions: **55a-c** (0.1-0.8 M), NaOH (0.06 equiv), acetone/water 2:1. Batch experiments were carried out using a single-mode instrument (IR temperature sensor). Flow experimentation was performed in a Uniqsis FlowSyn™ device. <sup>b</sup> HPLC peak area integration at 230 nm. <sup>c</sup> Isolated yield after flash chromatography. <sup>d</sup> 10 mL stainless steel coil. <sup>e</sup> 5 mL stainless steel coil. <sup>f</sup> 2 equiv of NaOH, acetone/water 1:1.

Applying these conditions to the flow reactor system, we initially performed the aldol reaction using a 5-mL stainless steel reaction coil, a 5 mL/min flow rate (1 min residence time), and 120 °C temperature. As the aldol condensation proceeds also very slowly at room temperature, freshly prepared reaction mixtures were used. For the synthesis of **52a** and **52c** a 10-mL stainless steel coil in combination with a 1.34 mL/min flow rate was utilized to ensure the required residence time of 450 s at 70 °C. In the case of naphthylaldehyde **55a** the concentration had to be lowered to 0.1 M because of solubility issues. Nevertheless, full conversion and a high isolated yield of the corresponding aldol condensation product **52a** was obtained (94%).

### 3.7.6. Large-scale flow aldol condensation

In order to demonstrate the scalability of the flow reaction conditions obtained in a laboratory-scale microreactor using steel coils of 5-10 mL internal volume to larger scales more similar to those used in a pilot or production setting we have additionally performed the aldol condensation of *p*-anisaldehyde and acetone shown in Table 1.8 in a mesofluidic flow setup, in collaboration with Microinnova Engineering (Graz, Austria) (Figure 3.7).

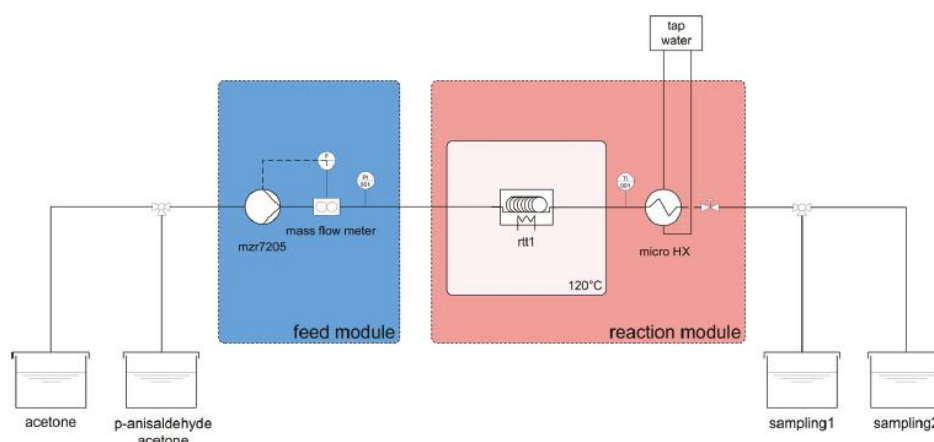


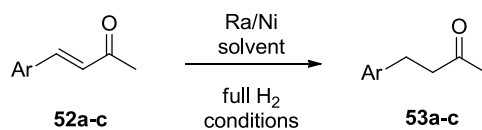
**Figure 3.7.** Schematic representation of the mesofluidic flow setup.

The feed module consists of a microannular gear pump, a Coriflow mass flow meter and a piezosensitive pressure sensor. On the other hand, the reaction module consists of a Teflon residence time tubing (~1 m length), situated in a silicon oil bath, with 8 mm inner diameter and filled with Teflon mixing elements, in addition to a micro heat-exchanger and a pressure maintaining valve. The overall flow rate in the experiments was 2.4 kg/h, which corresponds to a product flow of 0.35 kg/h. In 104 min, 4.65 L reaction mixture were processed at 120 °C: starting from 0.54 kg of aldehyde, we recovered 0.67 kg of product, without further purifications!

### ***3.7.7. The final step: continuous flow hydrogenation***

For the selective reduction of the double bond in 4-aryl-3-buten-2-ones, we have investigated a continuous-flow hydrogenation protocol employing a fixed-bed catalyst (H-Cube, Thales Nanotechnology Inc.).<sup>118</sup> The flow hydrogenation of model substrate **52b** was initially optimized using Ra/Ni cartridge, as it provided high selectivity for the double-bond hydrogenation at room temperature.

Having established the optimum flow hydrogenation conditions for the model substrate, we were interested in investigating the synthesis of the other compounds. Although our initial flow experiments involved EtOH as the solvent, the comparatively low solubility of **52b** and **52c** led us to utilize DMF and, as a consequence, to change the reaction conditions (Table 1.9).



Substrate <sup>a</sup>	Solvent	Conc [M]	Flow rate [mL/min]	Temp [°C]	Conv [%] <sup>b</sup>	Yield [%] <sup>c</sup>
<b>52a</b>	DMF	0.5	1	100	> 99	90
<b>52b</b>	EtOH	0.5	1.5	25	> 99	94
<b>52c</b>	DMF	0.7	1	35	> 99	91

**Table 1.9.** *Optimized reaction conditions for the flow hydrogenation of 4-aryl-3-buten-2-ones 5a-c.*<sup>a</sup> H-Cube, Full-H<sub>2</sub> mode at atmospheric pressure, substrate in EtOH or DMF, 30 × 4 mm i.d. catalyst cartridge, ~150 mg catalyst. <sup>b</sup> Determined by GC/MS (peak area %). <sup>c</sup> Isolated product yield after flash chromatography.

In summary, using the synthesis of 4-aryl-2-butanones **53a-c** as model transformations, we have demonstrated that small scale microwave batch processing is a useful tool to optimize reaction conditions for achieving high product yields and selectivities in the shortest possible reaction times. The resulting time-temperature histories were easily translated to conventionally heated high-temperature continuous flow reactors using 1000  $\mu\text{m}$  stainless steel coils. Because of the high surface-to-volume ratio in these type of microreactors, rapid heat transfer to and from the reaction mixture can be attained, therefore closely mimicking the situation of a small scale microwave experiment. Using appropriate static mixers in connection with a mesofluidic tubular reactor, the conditions obtained from laboratory scale instruments can be directly scaled by a factor of  $\sim 10$  without reoptimization of conditions. As demonstrated for the synthesis of 4-(4-methoxyphenyl)-3-buten-2-one (**52b**), a throughput of 0.35 kg product per hour can easily be obtained using this technique.



## **CHAPTER 4**

## **BIOLOGY**





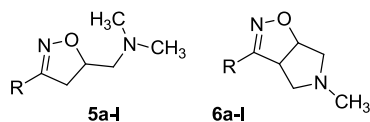
#### 4.1. Biological evaluation of $\Delta^2$ -isoxazoline derivatives

All the biological assays have been performed by Prof. Frank Lyko, Prof. Dirk Kuck (Division of Epigenetics, German Cancer Research Center, Heidelberg, Germany) and Reaction Biology Corp. ("RBC", Malvern, Pennsylvania, USA).

##### 4.1.1 Inhibitory activities against DNMT1

To date, there is no standardized biochemical assay available that delivers reliable data of the enzymatic activity of DNMTs. Recently, Kuck et al.<sup>83</sup> established a biochemical *in vitro* methylation assay using recombinant DNMT1, isolated and purified from Sf9 insect cells (derived from *Spodoptera frugiperda*). Tritium labeled S-adenosylmethionine (SAM) was used as methyl group donor, and the incorporation of radioactivity was quantitated by a scintillation counter.

In accordance with previous reported data by our research group,<sup>98</sup> a preliminary screening of the activity of compounds **5a-1** and **6a-1** at the single concentration of 2 mM was performed, using procaine, RG108, and S-adenosylhomocysteine (SAH) as reference compounds (2 mM DMSO solution). Procaine (as well as procainamide) was reported to inhibit DNMT activity at high drug concentrations. In addition, the assay sensitivity required comparably high concentrations (500 nM) of enzyme and, consequently, high concentrations of test compounds (Table 4.1).



Compd	R	Mean (%) <sup>a</sup>	SD <sup>b</sup>
ctrl	-	100.3	1.78
<b>5a</b>	Ph	NA <sup>c</sup>	-
<b>5b</b>	<i>p</i> -NO <sub>2</sub> -Ph	0.3	0.02
<b>5c</b>	<i>p</i> -CH <sub>3</sub> O-	3.3	0.02
<b>5d</b>	<i>p</i> -TsO-Ph	90.6	0.09
<b>5e</b>	<i>p</i> -COOH-	23.0	0.21
<b>5f</b>	<i>p</i> -NH <sub>2</sub> -Ph	20.2	0.28
<b>5g</b>	<i>p</i> -OH-Ph	88.0	0.37
<b>5h</b>	Bn	17.1	0.08
<b>5i</b>	<i>p</i> -NO <sub>2</sub> -	14.8	0.16
<b>5j</b>	<i>p</i> -CH <sub>3</sub> O-	NA <sup>c</sup>	-
<b>5k</b>	<i>p</i> -NH <sub>2</sub> -	28.3	0.39
<b>6a</b>	Ph	NA <sup>c</sup>	-
<b>6b</b>	<i>p</i> -NO <sub>2</sub> -Ph	34.9	0.30
<b>6c</b>	<i>p</i> -CH <sub>3</sub> O-	95.6	0.39
<b>6d</b>	<i>p</i> -TsO-Ph	18.6	0.06
<b>6e</b>	<i>p</i> -COOH-	NA <sup>c</sup>	-
<b>6f</b>	<i>p</i> -NH <sub>2</sub> -Ph	5.1	0.06
<b>6g</b>	<i>p</i> -OH-Ph	NA <sup>c</sup>	-
<b>6h</b>	Bn	84.0	0.07
<b>6i</b>	<i>p</i> -NO <sub>2</sub> -	3.8	0.07
<b>6j</b>	<i>p</i> -CH <sub>3</sub> O-	1.7	0.02
<b>6k</b>	<i>p</i> -NH <sub>2</sub> -	3.3	0.05
procaine <sup>d</sup>	-	NA <sup>c</sup>	-
RG108 <sup>d</sup>	-	NA <sup>c</sup>	-
SAH <sup>d</sup>	-	0.5	0.01

**TABLE 4.1. Biochemical DNMT assay of compounds 5a-k and 6a-k against hDNMT1.** <sup>a</sup>The relative enzymatic activity (in percent) is shown as the mean value of three measurements. <sup>b</sup>Standard deviation values are indicated in percentage points. <sup>c</sup>Not active. <sup>d</sup>Procaine, RG108, and SAH were used as reference compounds. All compounds were tested in a concentration of 2 mM against 500 nM of DNMT1. Compounds with an inhibition greater than 20% were scored as positive.

Even if accurate structure-activity relationships could not be derived from this assay, a few empirical considerations could be drawn pointing at the identification of potential inhibitors and to rule out inactive compounds.

It is noticeable that while both procaine and RG108 were inactive in this assay, a number of tested compounds show a clear-cut inhibition of the enzyme activity (Table 4.1), particularly when a nitro- or an amino- group is present as a substituent of the benzene ring (compounds **5b**, **5f**, **5i**, **5k** and **6b**, **6f**, **6i**, **6k**). Indeed, at the tested concentration, these compounds reduced the activity of DNMT1 at a very low level (0.3% in the case of **5b**, Table 4.1), a particularly significant outcome for non-nucleosidic inhibitors.

Similarly to what we previously reported for their oxazolino analogues,<sup>1</sup> nitro-substituted isoxazolines derivatives seem to be more active than their amino- counterparts (nearly 70-fold in the case of compounds **5b** and **5f**, Table 4.1), but this become less evident (nearly 2-fold) when the phenyl ring linked to the heterocycles is replaced by a benzyl moiety (compare the inhibition elicited by compounds **5b** and **5f** with those elicited by **5i** and **5k**, respectively). It is noteworthy that quite an opposite trend is observed in the case of bicyclic derivatives **6**. In fact, the nitrophenyl-substituted pyrrolidinoisoxazoline **6b** is 6-fold less active than its aminophenyl-counterpart (Table 4.1), whereas the activities of the benzylic analogues **6j** and **6k** are comparable. In a similar way, the introduction of the methoxy group produced active derivatives only in the case of phenyl-substituted isoxazolines (compound **5c**) and benzyl-substituted pyrrolidinoisoxazolines (compound **6j**), whereas the corresponding benzyl- and phenyl- analogues (compounds **5j** and **6c**, respectively) were inactive.

Following the above considerations, we then selected derivatives **5b**, **5f**, **5i**, **6f**, **6i**, and **6j** among the most active compounds and carried out dose-response

assay to generate curves from which the corresponding  $IC_{50}$  values were obtained (Figure 4.1).

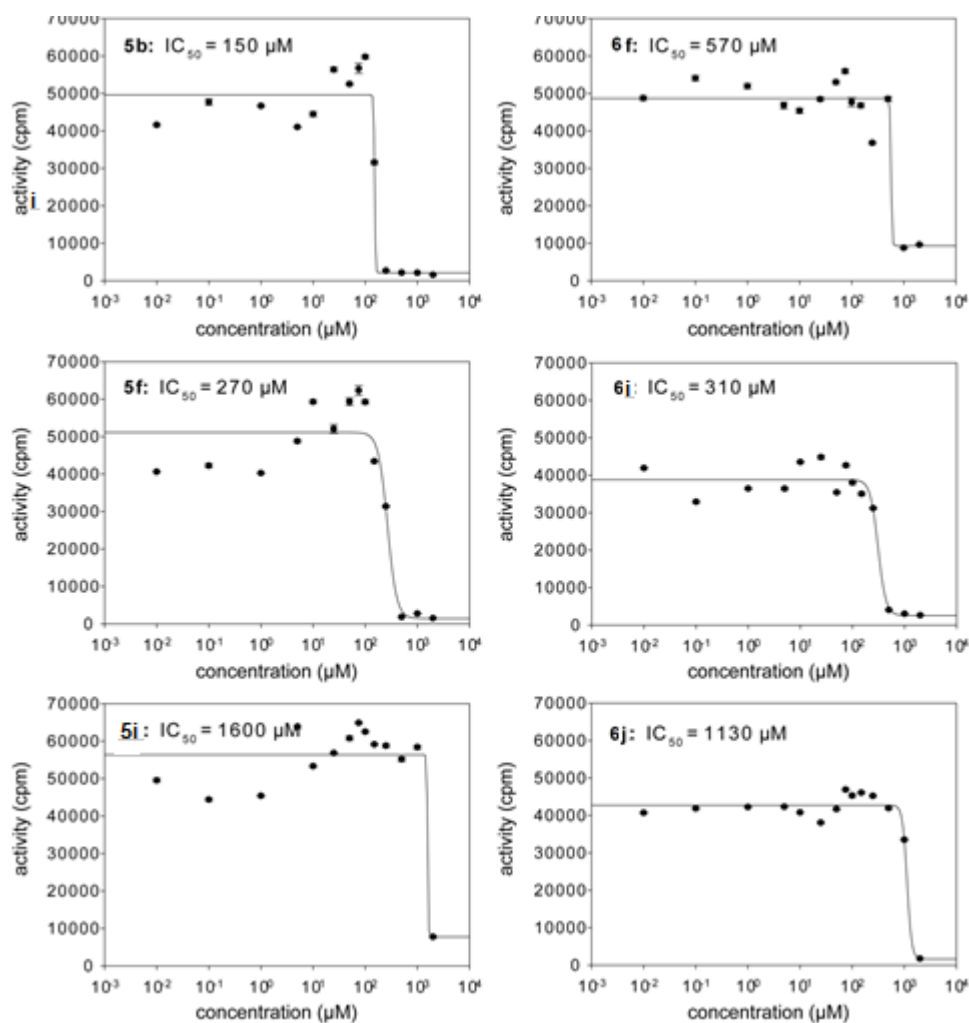


**Figure 4.1.** Dose–response plots for selected compounds 5b, 5f, 5i, 6f, 6i, and 6j against DNMT1. The  $IC_{50}$  concentrations of selected compounds were determined by biochemical DNMT assays under identical conditions (500 nM enzyme, 0.7  $\mu\text{M}$  AdoMet, 400 nM hemimethylated oligo). Each data point represents the mean  $\pm$  SD of three measurements, and the data were analyzed by SigmaPlot version 12.0.

In agreement with results in Table 4.1, the nitrophenyl isoxazoline **5b** showed the highest inhibition of DNMT1 with an  $IC_{50}$  value of 150  $\mu$ M, whereas its amino- counterpart **5f** as well as the aminophenyl- and the nitrobenzyl-substituted pyrrolidinoisoxazolines **6f** and **6j** were 2- to 4-fold less potent ( $IC_{50}$  values of 270, 570, and 310  $\mu$ M, respectively). Both the nitrobenzyl isoxazolines **5j** and the methoxybenzyl pyrrolidinoisoxazoline **6k** were consistently less active ( $IC_{50}$  values of 1600 and 1130  $\mu$ M, respectively). SAH was used as a nonspecific positive control and confirmed its efficient inhibition of DNMT1 ( $IC_{50}$  of 4  $\mu$ M, dose-response curve not shown).

#### 4.1.2. Competition assays

As derivative **5b** emerged as the most promising candidate for further development, we decided to gain a better understanding of the kinetic mechanism(s) for the observed inhibition of DNMT1. Because mutational analyses are long-lasting and may affect the enzyme conformation, we applied a simple method reported by Lai and Wu for assessing the mode of inhibition.<sup>119</sup> According to this method, the mode of inhibition can be evaluated by holding the inhibitor constant at its  $IC_{50}$  concentration and varying the substrates. The behavior of the curves obtained under these conditions will point to the mode of inhibition. For DNMTs, these substrates are the methyl group donor SAM and the DNA (represented by a short oligo) and each of them binds to its distinct binding site in the catalytic domain of DNMT1.

Therefore, the concentration of **5b** was kept constant at 150  $\mu$ M ( $IC_{50}$  value, Figure 4.1), and either the SAM or the oligo substrate was varied.

It can be seen that increasing the SAM concentration can nearly completely relieve the enzyme inhibition, whereas this is not affected by increasing the oligo substrate (Figure 4.2).

According to the model,<sup>119</sup> this is consistent with an inhibitor that is competitive with respect to SAM and noncompetitive with respect to the oligo.

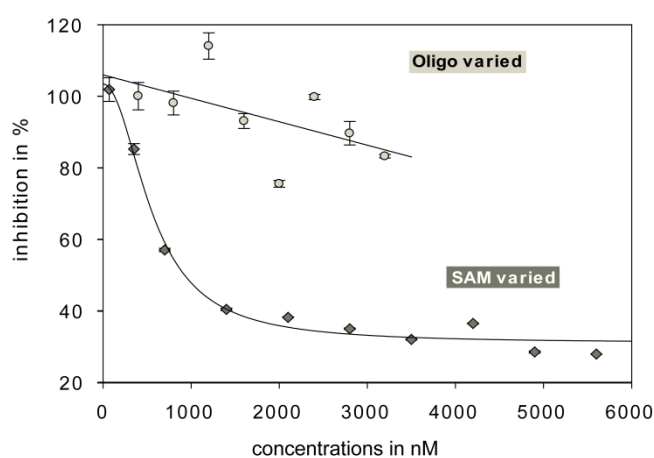


**Figure 4.2** *Derivative 5b competes with the SAM binding site.* The catalytic domain of DNMT1 has two binding sites, one for the oligo substrate and one for the SAM substrate. A modified biochemical DNMT activity assay was established to determine the mode of action of **5b**. Competition experiments were performed by increasing the concentration of the oligo substrate (oligo varied) or, alternatively, the SAM substrate (SAM varied). The assay was performed under standard conditions; please note that DNMT1 concentration was always kept constant (500 nM) as well as the inhibitor (**5b**) concentration (150  $\mu$ M). The initial enzymatic activity under standard conditions in presence of the inhibitor was defined as 100% inhibition before increasing substrate concentrations to look for competition events. According to the model of Lai and Wu (see text), **5b** competes with SAM for the cofactor binding site but not for the oligo-binding site.

Of note, these experiments represent one of the first efforts to elucidate experimentally the binding site of a non-nucleoside inhibitor of DNMT1.

### 4.1.3. Inhibition of cell proliferation

Finally, we explored the effect of compound **5b** on the proliferation of HCT116 human colon carcinoma cell line. To this end, cells were incubated for 72h with increasing concentrations (300, 500, and 750  $\mu\text{M}$ ) of **5b** in comparison to azacytidine (1  $\mu\text{M}$ ) or DMSO alone for control. The proliferation was assessed by counting viable cells after trypan blue staining. As shown in Figure 4.3, in these conditions compound **5b** induces a strong and dose-dependent antiproliferative effect, with a  $\text{GI}_{50}$  value (the concentration of the compound that inhibits cell growth by 50%) of 360  $\mu\text{M}$ .

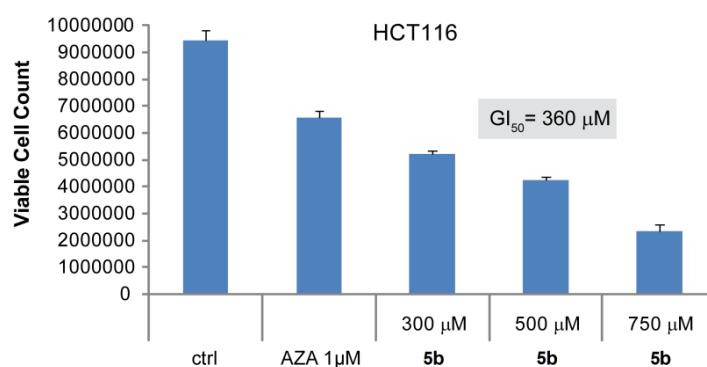


**Figure 4.3.** Derivative **5b** induces a strong antiproliferative effect after 72h in HCT116 human colon carcinoma cells compared to DMSO treated cells. Azacytidine was included as a positive control. Ctrl are DMSO treated cells.  $\text{GI}_{50}$  value was determined by SigmaPlot 12.0 (Systat Software Inc., San Jose, CA).

### 4.1.4. Illumina Infinium<sup>®</sup> methylation assay

In order to systematically characterize the demethylation responses after **5b** treatment in HCT116 human cancer cell lines, a new methylation assay was used. In fact, in the last years, huge progress has been made in the development of array- or sequencing-based technologies for DNA methylation analysis. In particular, the Illumina Infinium<sup>®</sup> Human Methylation 450K

BeadChip (Illumina Inc., CA, USA) allows the simultaneous quantitative monitoring of more than 480,000 CpG positions, offering the highest resolution for understanding methylation changes.<sup>120</sup> Upon treatment with bisulfite, unmethylated cytosine bases are converted to uracil, while methylated cytosine bases remain unchanged. The assay interrogates these chemically differentiated loci using two site-specific probes, one designed for the methylated locus (M bead type) and another for the unmethylated locus (U bead type). Single-base extension of the probes incorporates a labeled di-deoxy nucleoside triphosphate (ddNTP), which is subsequently stained with a fluorescence reagent. The level of methylation for the interrogated locus can be determined by calculating the ratio of the fluorescent signals from the methylated vs unmethylated sites.

As shown in Figure 4.4., compound **5b** is able to induce a reliable decrease in methylation of specific loci in HCT116 human colon carcinoma cells. On the basis of these findings, we proposed **5b** as a novel lead compound for the development of non-nucleoside DNMT inhibitors.

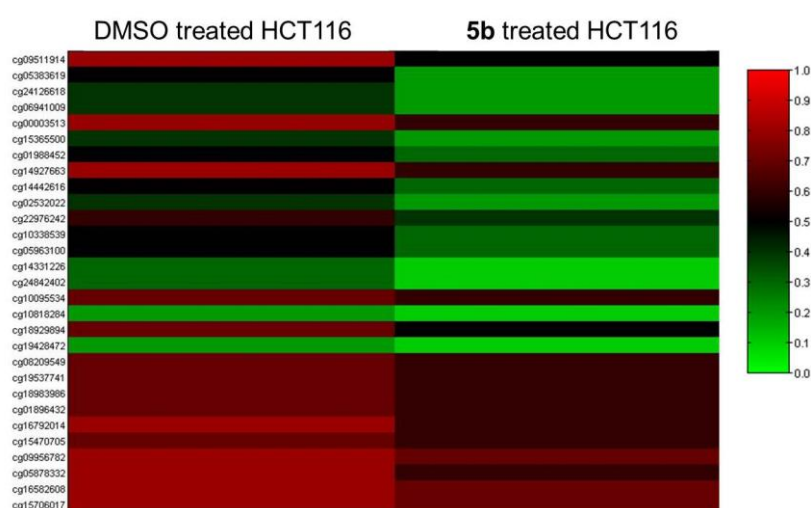
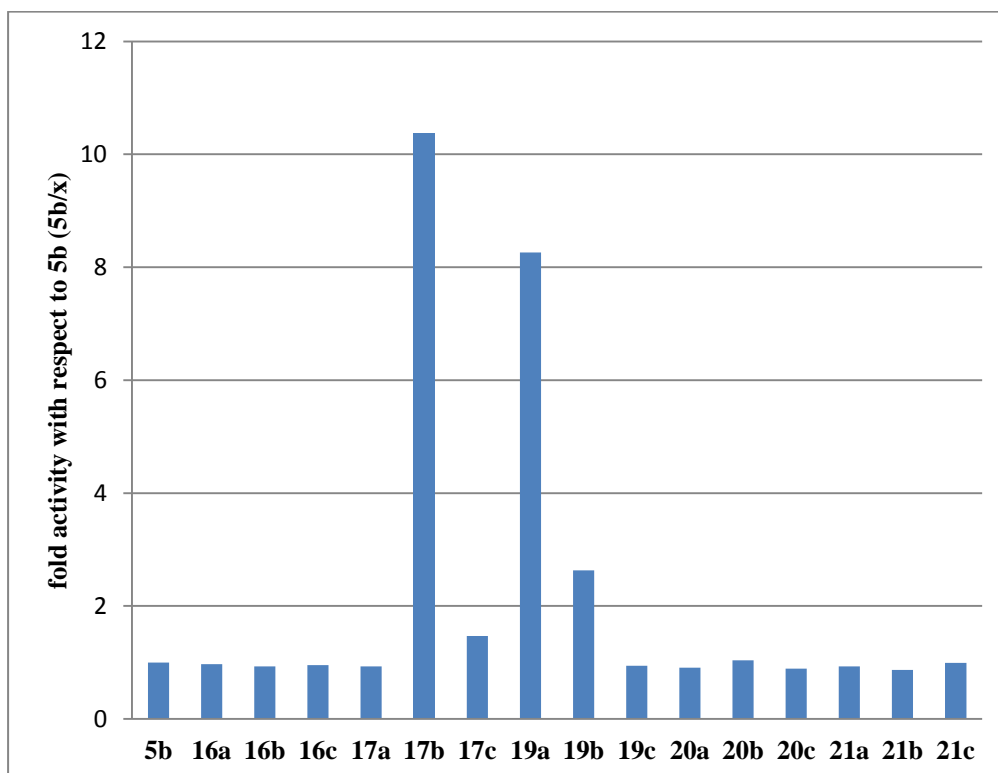


Figure 4.4. Illumina Infinium<sup>®</sup> 450K analysis heatmap of demethylated loci.



## 4.2. Biological evaluation of “bisubstrate” inhibitors

As derivative **5b** competes with SAM for the binding site, a proper derivatization of this scaffold could lead to longer “bisubstrate” inhibitors, able to occupy both DNA and SAM binding pockets. Docking studies as well as biological assays are ongoing to evaluate the potency of these new compounds in inhibiting the activity of DNMT1. Preliminary data show that some of them are 2 to 10 fold more effective than the lead compound in inhibiting the target (Figure 4.5).



**Figure 4.5.** Comparison of the new molecules with the lead compound at 100  $\mu\text{M}$ . Human DNMT1 with N-terminal GST tag, expressed in baculovirus expression system, 0.005 mg/ml Poly(dI-dC), 1  $\mu\text{M}$   $^3\text{H}$ -SAM.

### 4.3. Biological evaluation of NCI lead-like set

Taking advantage of a docking-based virtual screening approach with a validated homology model of DNMT1, six compounds of the NCI lead-like set were prepared and their inhibitory activity against DNMT1 was tested.

Applying the same procedure developed for the isoxazoline derivatives, a preliminary screening of the activity of NSC compounds at the single concentration of 2 mM was performed.

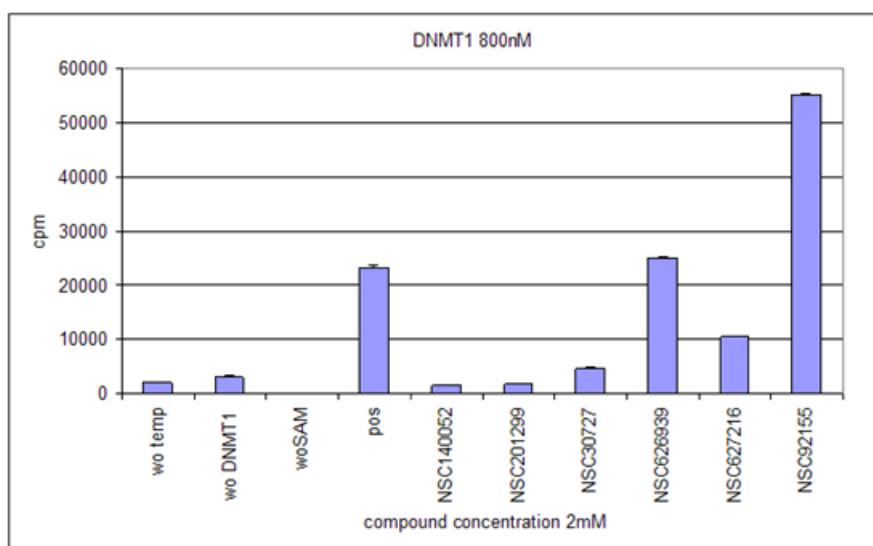
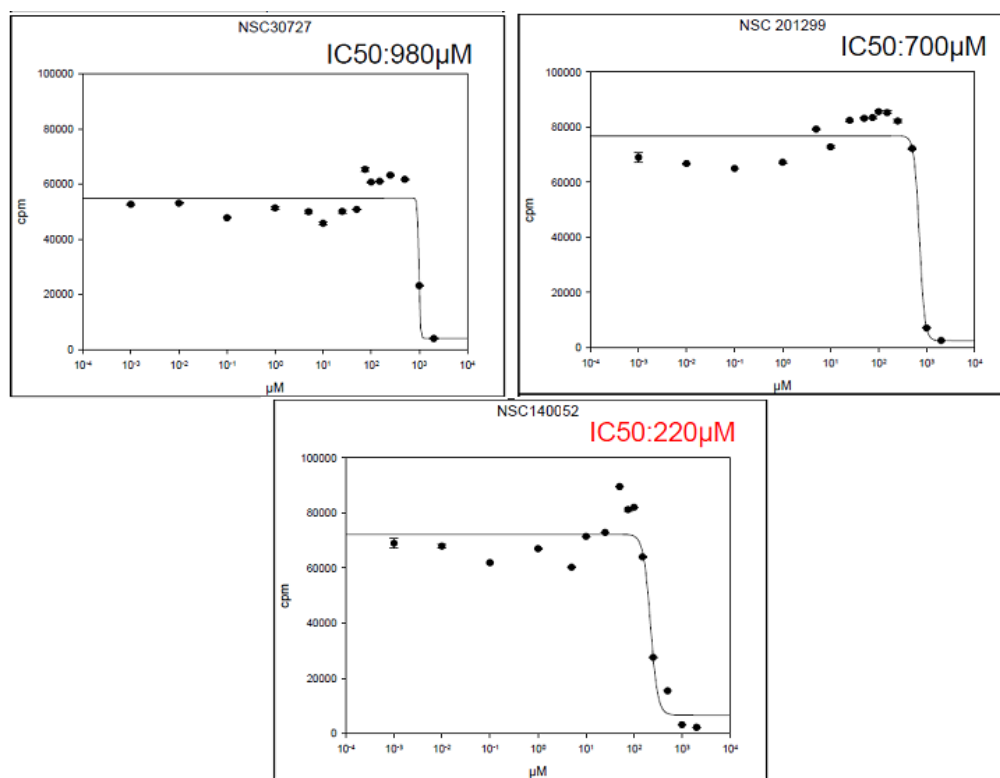


Figure 4.6. Biochemical DNMT assay of NSC compounds against hDNMT1.

As shown in Figure 4.6, some derivatives emerged as the most promising candidates for further biological investigations. In fact, following the above considerations, we selected **NSC140052**, **NSC201299** and **NSC30727** among the most active compounds and carried out dose-response assay to generate curves from which the corresponding  $IC_{50}$  values were obtained (Figure 4.7).



**Figure 4.7.** Dose–response plots for selected compounds against DNMT1. The IC<sub>50</sub> concentrations of selected compounds were determined by biochemical DNMT assays under identical conditions (500 nM enzyme, 0.7 μM AdoMet, 400 nM hemimethylated oligo). Each data point represents the mean ± SD of three measurements, and the data were analyzed by SigmaPlot version 12.0.

In agreement with results in Figure 4.6, the pyrrolo[3,4-*d*]-pyrimidine **NSC140052** showed the highest inhibition of DNMT1 with an IC<sub>50</sub> value of 220 μM, whereas the 2-amino-5-oxo-5-(*p*-tolyl)pentanoic acid **NSC30727** as well as the indole derivative **NSC201299** were less potent (IC<sub>50</sub> values of 980, and 700 μM, respectively). Starting from this findings, we proposed it as a *hit* for the development of novel DNMT1 inhibitors.

#### 4.4. Biological evaluation of analogues of NSC140052

As derivative **NSC140052** resulted the most powerful compound of the series, we developed a small library of compounds characterized by several modifications of the *hit*. Docking studies as well as biological assays are ongoing to evaluate the potency of these new compounds in inhibiting the activity of DNMT1. Preliminary data show that the new derivatives with an acid group on the aromatic ring are 2 to 27 fold more active than the lead in inhibiting DNMT1 (Figure 4.8).

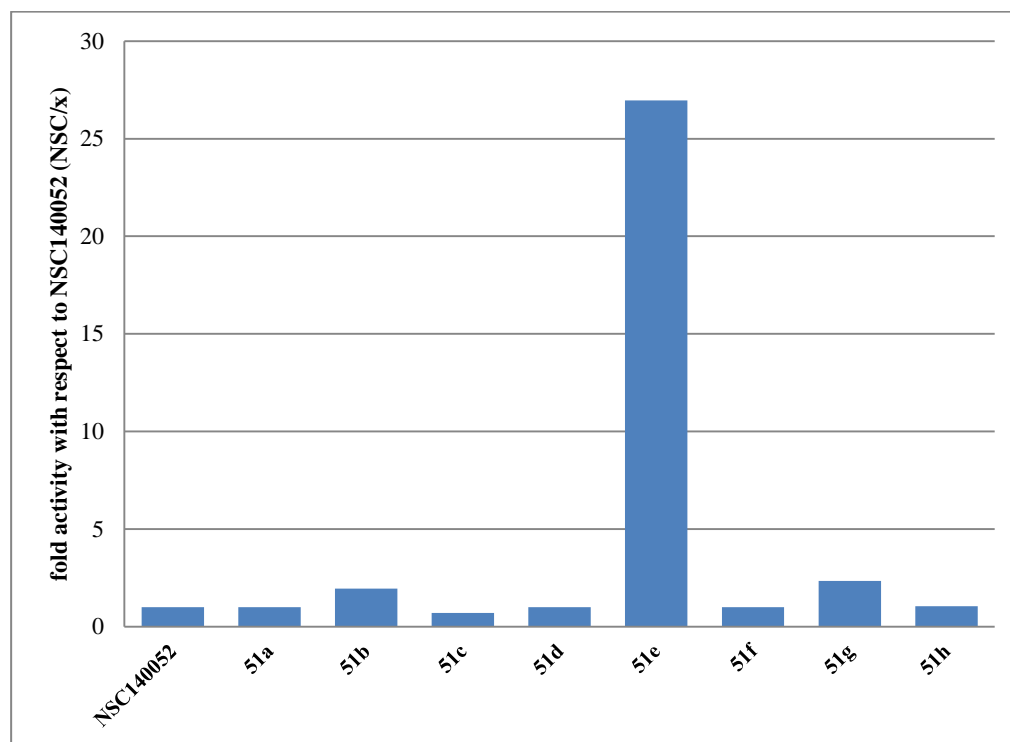


**Figure 4.8.** Comparison of derivatives 51a-h with the lead compound at 1 mM. Human DNMT1 with N-terminal GST tag, expressed in baculovirus expression system, 0.005 mg/ml Poly(dI-dC), 1  $\mu\text{M}$   $^3\text{H}$ -SAM).

## **CHAPTER 5**

### **DOCKING AND BINDING MODE**



### **5.1. Docking and binding mode of $\Delta^2$ -isoxazoline derivatives**

On the basis of the results of the competition assay discussed above, the binding mode of **5b** into the binding pocket of the cofactor of human DNMT1 was analyzed using molecular modeling studies.

Molecular docking and other computational approaches are increasingly being used to explore the ligand-binding interactions of DNMT inhibitors.<sup>121</sup> Until now, molecular modeling studies have been conducted using validated homology models of the methyltransferase domain of DNMT1.<sup>86, 93</sup> However, a crystallographic structure of human DNMT1 has been recently published<sup>122</sup> which contains the methyltransferase domain bound to DNA-containing unmethylated CpG sites.

On the basis of the experimental results of the competition assays, the binding of **5b** into the binding site of the cofactor was further explored using molecular docking. Briefly, the R and S configurations of **5b** in neutral and protonated forms (at the amino group) were flexibly docked into the crystallographic structure of the methyltransferase domain of human DNMT1 using Glide Extra Precision (XP), version 5.7.<sup>123</sup>

The calculated docking scores of the R and S configurations of **5b** in protonated form were -4.0 and -3.5 kcal/mol, respectively. The docking score of the neutral form of each configuration was -3.0 kcal/mol. These results suggest that **5b** binds to the cofactor binding site in the protonated form. The docking scores of **5b** were higher, i.e. less favorable, than the calculated docking score for SAH, which was -7.6 kcal/mol. The docking scores are in agreement with the results of the experimental DNMT1 inhibition assays, which shows that SAH is a more potent inhibitor than **5b**.

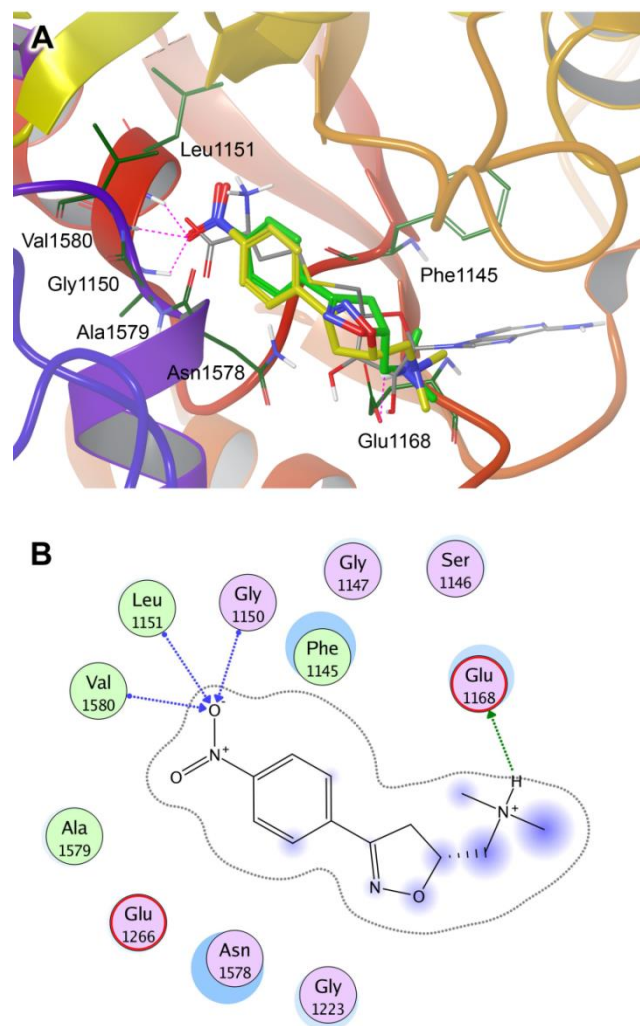


**Figure 5.1.** (A) Comparison of the binding modes of the R (green) and S (yellow) configurations of **5b** predicted by *Glide*. Crystallographic SAH (gray) is shown as reference. Hydrogen bonds for R-**5b** are displayed as magenta dashes. Selected amino acids residues within 4.5 Å of **5b** are shown. Nonpolar hydrogen atoms are omitted for clarity. (B) Two dimensional interaction map displaying amino acid residues within 4.5 Å of R-**5b**. The ligand proximity contour is depicted with a dotted line. The ligand solvent exposure is represented with blue circles; larger and darker circles on ligand atoms indicate more solvent exposure. The receptor solvent exposure differences, in the presence and absence of the ligand, are represented by the size and intensity of the turquoise discs surrounding the residues; larger and darker discs indicate residues highly exposed to solvent in the active site when the ligand is absent. Figure created with the Ligand Interactions application of MOE.



Figure 5.1A shows a tridimensional binding model of the protonated R and S configurations (carbon atoms in green and yellow, respectively). The structure of co-crystallized SAH is shown as a reference (carbon atoms in gray). Together with the comparable docking energies calculated for the two configurations (see above), this hints that both enantiomers have similar enzymatic inhibitory activity.

A two-dimensional representation of the binding mode of R-**5b** is shown in Figure 5.1B. According to the derived docking model, **5b** occupies the binding site of the cofactor which is created by residues from the motifs I-III and X of the methyltransferase domain.<sup>124</sup> Compound **5b** binds in the region where the L-homocysteine and ribose moieties of SAH bind. The  $\Delta^2$ -isoxazoline ring makes contacts with the side chain of Asn1578 and the backbone of Phe1145. The phenyl rings makes hydrophobic interactions mainly with Gly1147, Gly1223, Ala1579, and the backbone atoms of Ser1146 and Asn1578. The positively charged amino group forms a hydrogen bond with the side chain of Glu1168, which is located in motif II. Of note, two oxygen atoms (O2' and O3') of the ribose ring of SAH also form hydrogen bond interactions with the side chain of Glu1168. The nitro group of **5b** occupies a region similar to the carboxylate group of SAH making similar interactions with the binding pocket. Hydrogen bonds between the oxygen atoms of the nitro group of **5b** and the backbone NH of Gly1150 (motif I), Leu1151, and Val1580 (motif X) were also predicted by Glide (Figure 5.1).<sup>18</sup>

Docking and binding mode studies for the new, longer  $\Delta^2$ -isoxazoline are ongoing to evaluate the potency of these compounds in inhibiting the activity of DNMT1.

## **5.2. Docking and binding mode of NSC derivatives**

With the aim to identify novel DNMT1 small molecule inhibitors with chemical scaffolds different from the currently known inhibitors, we performed, in collaboration with Prof. Jose Medina-Franco (Torrey Pines Institute for Molecular Studies, Port St. Lucie, FL, USA), a multistep structure-based virtual screening of more than 260,000 compounds obtained from the NCI Open Database.<sup>125</sup>

In order to focus the virtual screening on compounds that could be promising for further development, we selected a subset of lead-like compounds.<sup>126</sup> This selection was made based on properties and functional groups using the FILTER program<sup>127</sup> that reduced the initial NCI Database to a subset of 65,375 compounds.

Since no crystallographic structure of the catalytic site of human DNMT1 was available at the time of this study, we used an established homology model<sup>86</sup> in all steps of the virtual screening. This model has been successfully used for previous virtual screening<sup>128</sup> and modeling studies.

After selecting lead-like compounds, we employed a fast docking protocol to further filter the NCI lead-like set.<sup>83</sup> The prepared set was docked into the DNMT1 active site using the GLIDE Extra Precision (XP) docking module.

A total of 6 consensus compounds with favorable docking scores were identified out and the chemical structures are shown in Table 5.1. The compounds selected from the virtual screening with DNMT1 were tested experimentally in order to assess biochemical selectivity (Chapter 4).

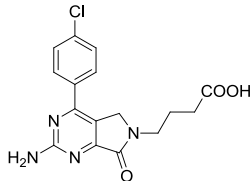
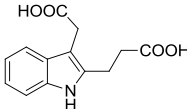
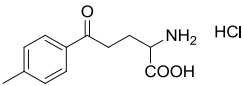
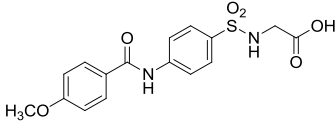
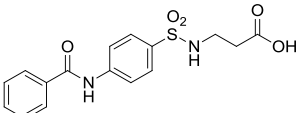
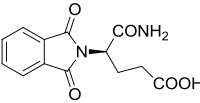
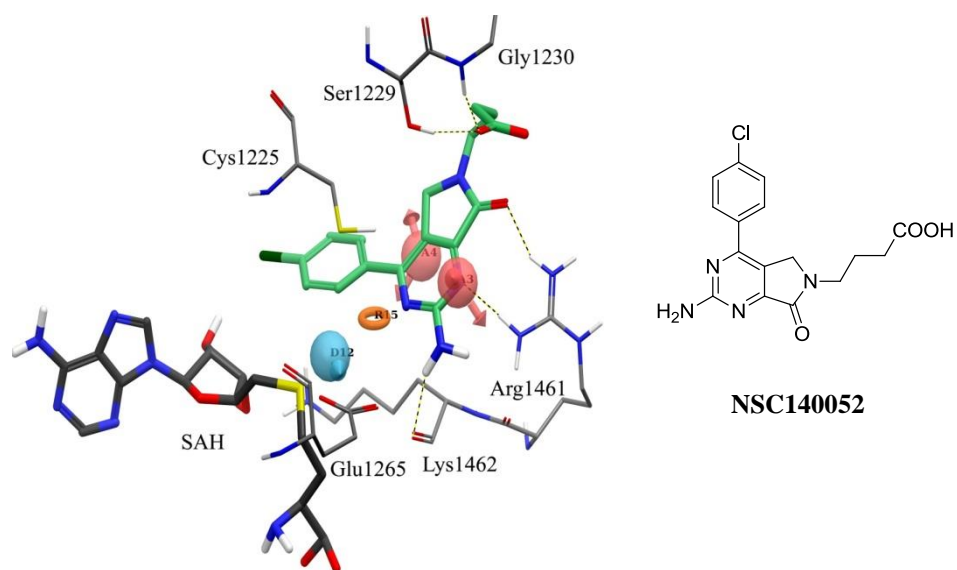
Derivatives	Name	Glide XP Docking energies (kcal/mol)
	NSC140052	-14.27
	NSC201299	-14.81
	NSC30727	-13.90
	NSC626939	-15.78
	NSC627216	-15.61
	NSC92155	-12.52

TABLE 5.1. Calculated docking scores of 6 hits tested experimentally.

Taking advantage of the biological results previously reported, the binding mode of the most active compound was realized. As shown in Figure 5.2, the 2-amino-pyrimidine of NSC140052 forms H-bond with Lys1462, and carboxylate forms strong H-bond with Ser 1229 and Gly1230. It demonstrates a binding mode similar to 5-azacytidine.



**Figure 5.2.** Binding mode of NSC140052 predicted by Glide. Hydrogen bonds are displayed as yellow dashes. Selected amino acids residues within 4.5 Å of NSC140052 are shown.

Docking and binding mode studies for the new, pyrrolo[3,4-*d*]-pyrimidines are ongoing to evaluate the potency of these compounds in inhibiting the activity of DNMT1.

## **CHAPTER 6**

## **CONCLUSIONS**



## Conclusion

Being responsible of DNA methylation, DNA methyltransferases are recognized as valuable epigenetic targets for the development of anti-cancer therapies. Nucleoside inhibitors exert their effects by incorporation into DNA inducing substantial DNA demethylation and reactivation of hypermethylated genes. Yet, they also carry considerable concerns about toxicity. Because of these problems, the search and the development of non-nucleoside compounds, which can effectively inhibit DNA methylation without being incorporated into DNA, is being actively pursued. Being interested in the development of small-molecule modulators of epigenetic targets, we focused our attention on:

- Procaine/procainamide as a lead structure for further modification: we prepared constrained analogues with an oxazoline ring, then replaced with the more stable  $\Delta^2$ -isoxazoline. On the basis of the experimental evidence of the enzymatic as well as competition assays, we proposed **5b** as a lead compound for the synthesis of new, longer analogues as “bisubstrate” inhibitors. Indeed, further studies were performed to develop analogues endowed with improved enzyme binding properties and higher inhibitory potency (from 2 to 10 fold more active than the lead).

- Compounds obtained from a docking-based virtual screening approach: starting from 260,000 molecules, six of them were synthesized and tested as DNMT1 inhibitors. Among them, NSC140052 became the starting point for the synthesis of new pyrrolo-pyrimidines. Docking studies as well as biological assays are ongoing to evaluate the potency of these new compounds in inhibiting the activity of DNMT1. However, preliminary data show that some of them are 2 to 27 fold more active than the lead in inhibiting the target.





## **CHAPTER 7**

### **EXPERIMENTAL SECTION**



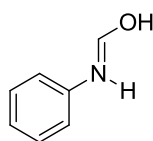
All chemicals were purchased from Sigma Aldrich (Milan, Italy) or from Alfa Aesar GmbH (Karlsruhe, Germany) and were of the highest purity. All solvents were reagent grade and, when necessary, were purified and dried by standard methods. All reactions requiring anhydrous conditions were conducted under a positive atmosphere of nitrogen in oven-dried glassware. Standard syringe techniques were used for anhydrous addition of liquids. Reactions were routinely monitored by TLC performed on aluminum-backed silica gel plates (Merck DC, Alufolien Kieselgel 60 F254) with spots visualized by UV light ( $\lambda = 254, 365$  nm) or using a  $\text{KMnO}_4$  alkaline solution. Solvents were removed using a rotary evaporator operating at a reduced pressure of  $\sim 10$  Torr. Organic solutions were dried over anhydrous  $\text{Na}_2\text{SO}_4$ . Chromatographic separations were performed on silica gel (silica gel 60, 0.015-0.040 mm; Merck DC) columns. Melting points were determined on a Stuart SMP30 melting point apparatus in open capillary tubes and are uncorrected.  $^1\text{H}$  NMR spectra were recorded at 300MHz on a Bruker Avance 300 spectrometer. Chemical shifts are reported in  $\delta$  (ppm) relative to the internal reference tetramethylsilane (TMS). When compounds were tested as salts, NMR data refer to the free base. Mass spectra were recorded on a Finnigan LCQ DECA ThermoQuest (San Jose, USA) mass spectrometer in electrospray positive and negative ionization modes (ESI-MS). Purity of tested compounds was established by combustion analysis, confirming a purity  $\geq 95\%$ .

## 7.1. $\Delta^2$ -isoxazoline derivatives

### General procedure for the synthesis of oximes (7)

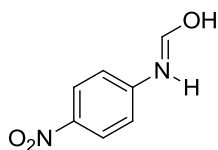
To a suspension of the proper aldehyde (30.0 mmol) and hydroxylamine hydrochloride (2.29 g, 33.0 mmol) in a 1:1 mixture of H<sub>2</sub>O/MeOH (40 mL), an aqueous solution of Na<sub>2</sub>CO<sub>3</sub> (1.59 g, 15.0 mmol, 20 mL) was slowly added. The resulting mixture was stirred at room temperature for 3h, and then methanol was evaporated. The aqueous phase was extracted with Et<sub>2</sub>O (3 x 30 mL). The combined organic phases were washed with brine (30 mL), dried (Na<sub>2</sub>SO<sub>4</sub>), filtered, and concentrated in vacuo to give the title compounds **7**, which were used in the next step without further purification.

#### 7a: Benzaldehyde oxime<sup>129</sup>

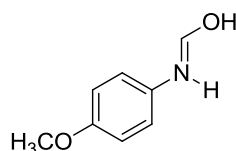


Pale yellow oil, 96% yield. <sup>1</sup>H NMR (300 MHz, CDCl<sub>3</sub>):  $\delta$  9.15 (br s, 1H), 8.20 (s, 1H), 7.63–7.54 (m, 2H), 7.45–7.35 (m, 3H). ESI-MS  $m/z$ : 122 (M+H)<sup>+</sup>.

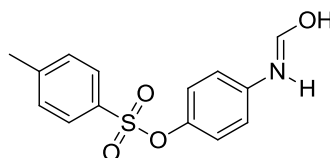
#### 7b: 4-nitrobenzaldehyde oxime<sup>130</sup>



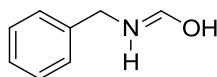
Yellow solid, 95% yield. <sup>1</sup>H NMR (300 MHz, CDCl<sub>3</sub>):  $\delta$  8.25 (d, J = 8.7 Hz, 2H), 8.20 (s, 1H), 7.98 (s, 1H), 7.75 (d, J = 8.7 Hz, 2H). ESI-MS  $m/z$ : 167 (M+H)<sup>+</sup>.

**7c: 4-methoxybenzaldehyde oxime**<sup>131</sup>

White solid, 94% yield. <sup>1</sup>H NMR (300 MHz, CDCl<sub>3</sub>): δ 8.10 (s, 1H), 8.05 (br s, 1H), 7.52 (d, J = 8.8 Hz, 2H), 6.91 (d, J = 8.8 Hz, 2H), 3.84 (s, 3H). ESI-MS *m/z*: 152 (M+H)<sup>+</sup>.

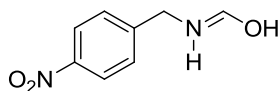
**7d: (4-[[4-(4-methylphenyl)sulfonyl]oxy]-benzaldehyde oxime**

White solid, 99% yield. <sup>1</sup>H NMR (300 MHz, CDCl<sub>3</sub>): δ 8.08 (s, 1H), 7.71 (d, J = 8.4 Hz, 2H), 7.50 (d, J = 8.7 Hz, 2H), 7.43 (s, 1H), 7.31 (d, J = 8.4 Hz, 2H), 7.01 (d, J = 8.7 Hz, 2H), 2.45 (s, 3H). ESI-MS *m/z*: 292 (M+H)<sup>+</sup>.

**7h: 2-phenylacetaldehyde oxime**<sup>132,133</sup>

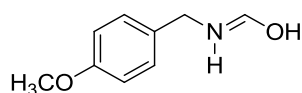
Pale yellow solid, 91% yield. 55:45 mixture of geometric isomers **a** and **b**. <sup>1</sup>H NMR (300 MHz, CDCl<sub>3</sub>): δ 8.41 (br s, 1H, isomer **a**), 7.88 (br s, 1H, isomer **b**), 7.57 (t, J = 6.3, 1H, isomer **b**), 7.45–7.15 (m, 5H, isomer **a** and 5H isomer **b**), 6.93 (t, J = 5.3 Hz, 1H, isomer **a**), 3.75 (d, J = 5.3 Hz, 2H, isomer **a**), 3.57 (d, J = 6.2, 2H, isomer **b**). ESI-MS *m/z*: 136 (M+H)<sup>+</sup>.

**7i: (*p*-nitrophenyl)-acetaldehyde oxime**



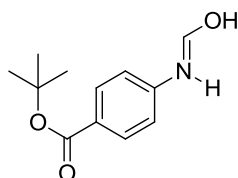
Yellow solid, 87% yield. 60:40 mixture of geometric isomers **a** and **b**.  $^1\text{H}$  NMR (300 MHz,  $\text{CDCl}_3$ ):  $\delta$  8.19 (m, 2H, isomer **a** and 2H, isomer **b**) 7.92 (br s, 1H, isomer **a**), 7.55 (t,  $J = 6.1$ , 1H, isomer **b**), 7.48 (br s, 1H, isomer **b**), 7.42–7.38 (m, 2H, isomer **a** and 2H, isomer **b**), 6.90 (t,  $J = 5.5$  Hz, 1H, isomer **a**), 3.84 (d,  $J = 5.5$  Hz, 2H, isomer **a**), 3.65 (d,  $J = 6.1$ , 2H, isomer **b**). ESI-MS  $m/z$ : 181 ( $\text{M}+\text{H}$ ) $^+$ .

**7j: (*p*-methoxyphenyl)acetaldehyde oxime**



White solid, 90% yield. 55:45 mixture of geometric isomers **a** and **b**.  $^1\text{H}$  NMR (300 MHz,  $\text{CDCl}_3$ ):  $\delta$  7.65 (br s, 1H, isomer **a**), 7.51 (t,  $J = 6.2$ , 1H, isomer **b**), 7.23 (br s, 1H, isomer **b**), 7.20–7.09 (m, 2H, isomer **a** and 2H, isomer **b**) 6.93–6.78 (m, 3H, isomer **a** and 2H, isomer **b**), 3.82 (s, 3H, isomer **a** and 3H, isomer **b**), 3.68 (d,  $J = 5.4$ , 2H, isomer **a**), 3.49 (d,  $J = 6.2$ , 2H, isomer **b**). ESI-MS  $m/z$ : 166 ( $\text{M}+\text{H}$ ) $^+$ .

**7l: 4-(*tert*-Butoxycarbonyl)benzaldehyde oxime**



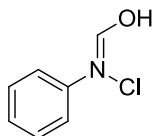
4-(*tert*-Butoxycarbonyl)benzaldehyde was prepared according to a described procedure<sup>134</sup> and the corresponding oxime **7l** was prepared according to the general procedure reported above. White solid, 70% yield.  $^1\text{H}$  NMR (300 MHz,

$\text{CDCl}_3$ ):  $\delta$  9.23 (br s, 1H), 8.18 (s, 1H), 8.00 (d,  $J = 8.5$  Hz, 2H), 7.62 (d,  $J = 8.5$  Hz, 2H), 1.60 (s, 9H). ESI-MS  $m/z$ : 166 ( $\text{M}+\text{H}-t\text{Bu}$ )<sup>+</sup>.

### General procedure for the synthesis of chlorooximes (10)

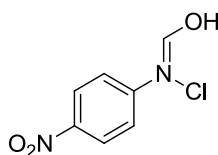
To a solution of the proper aldoxime (2.75 mmol) in  $\text{CHCl}_3$  (10 mL), pyridine was added (20.0  $\mu\text{L}$ , 0.27 mmol). The reaction mixture was heated at 40 °C, and *N*-chlorosuccinimide (0.40 g, 3.03 mmol) was added portionwise. After the reaction was complete (0.5-3h, monitored by TLC), the mixture was diluted with  $\text{CH}_2\text{Cl}_2$  (30 mL) and washed with brine (3 x 10 mL). The organic phase was dried ( $\text{Na}_2\text{SO}_4$ ), filtered, and concentrated in vacuo to give the title compounds **10**, which were used in the cycloaddition step without further purification.

### 10a: *N*-hydroxybenzenecarboximidoyl chloride<sup>101</sup>



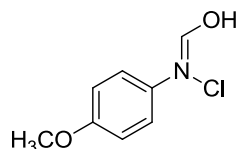
Pale yellow amorphous solid, 98% yield. <sup>1</sup>H NMR (300 MHz,  $\text{CDCl}_3$ ):  $\delta$  8.62 (br s, 1H), 7.90–7.78 (m, 2H), 7.48–7.36 (m, 3H).

### 10b: *N*-hydroxy-4-nitro-benzenecarboximidoyl chloride<sup>135</sup>



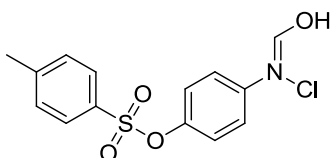
Pale yellow solid, 97% yield. <sup>1</sup>H NMR (300 MHz,  $\text{CDCl}_3$ ):  $\delta$  8.31 (br s, 1H), 8.27 (d,  $J = 9.0$  Hz, 2H), 8.04 (d,  $J = 9.0$  Hz, 2H).

**10c: N-hydroxy-4-methoxy-benzenecarboximidoyl chloride**<sup>136</sup>



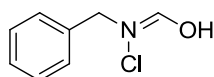
Yellow solid, 97% yield. <sup>1</sup>H NMR (300 MHz, CDCl<sub>3</sub>): δ 7.78 (d, J = 8.4 Hz, 2H), 7.70 (br s, 1H), 6.92 (d, J = 8.4 Hz, 2H), 3.85 (s, 3H).

**10d: N-hydroxy-4-[[[(4-methylphenyl)sulfonyl]oxy]-benzenecarboximidoyl chloride**



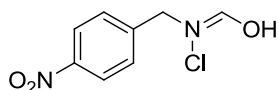
White solid, 99% yield. <sup>1</sup>H NMR (300 MHz, CDCl<sub>3</sub>): δ 7.97 (s, 1H), 7.78 (d, J = 8.4 Hz, 2H), 7.72 (d, J = 7.8 Hz, 2H), 7.32 (d, J = 7.8 Hz, 2H), 7.03 (d, J = 8.4 Hz, 2H), 2.45 (s, 3H).

**10h: N-hydroxy-2-phenylacetimidoyl chloride**<sup>137</sup>



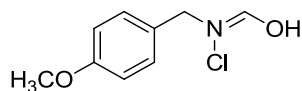
Yellow solid, 95% yield. <sup>1</sup>H NMR (300 MHz, CDCl<sub>3</sub>): δ 8.15 (br s, 1H), 7.45–7.13 (m, 5H), 3.81 (s, 2H).

**10i: N-hydroxy-2-(4-nitrophenyl)acetimidoyl chloride**<sup>10</sup>

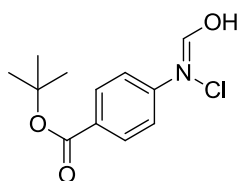


Pale yellow solid, 96% yield. <sup>1</sup>H NMR (300 MHz, CDCl<sub>3</sub>): δ 8.21 (d, J = 8.4 Hz, 2H), 8.12 (s, 1H), 7.45 (d, J = 8.4 Hz, 2H), 3.91 (s, 2H).



**10j: *N*-hydroxy-2-(4-methoxyphenyl)acetimidoyl chloride**<sup>138</sup>

Pale yellow solid, 96% yield. <sup>1</sup>H NMR (300 MHz, CDCl<sub>3</sub>): δ 9.29 (br s, 1H), 7.17 (d, J = 8.4 Hz, 2H), 6.87 (d, J = 8.4 Hz, 2H), 3.78 (s, 3H), 3.72 (s, 2H).

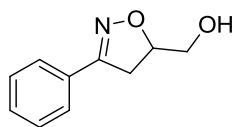
**10l: *N*-hydroxy-2-(4-*tert*-butoxycarbonylphenyl)acetimidoyl chloride**

White solid, 80% yield. <sup>1</sup>H NMR (300 MHz, CDCl<sub>3</sub>): δ 8.10 (s, 1H), 8.05 (d, J = 8.8 Hz, 2H), 7.89 (d, J = 8.8 Hz, 2H), 1.60 (s, 9 H).

**General procedure for the synthesis of 3-substituted-5-hydroxymethyl-****4,5-dihydroisoxazoles (8)**

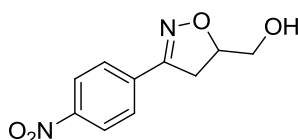
To a vigorously stirred solution of the proper aldoxime (7.00 mmol) and allylic alcohol (0.81 mg, 0.95 mL, 14.0 mmol) in CH<sub>2</sub>Cl<sub>2</sub> (50 mL) at 0 °C, a solution of common bleach (3% aqueous solution of NaOCl, 35 mL, 14.0 mmol) was added dropwise, keeping the temperature below 5 °C. The resulting biphasic mixture was vigorously stirred at room temperature for 15 min. The aqueous phase was separated and extracted with CH<sub>2</sub>Cl<sub>2</sub> (3 x 20 mL). The combined organic phases were washed with brine (25 mL), dried (Na<sub>2</sub>SO<sub>4</sub>), filtered, and concentrated in vacuo. The residue was purified by silica gel chromatography (EtOAc/hexane) to give the title compounds **8**, which were recrystallized from the appropriate solvent.

**8a: 5-hydroxymethyl-3-phenyl-4,5-dihydroisoxazole**



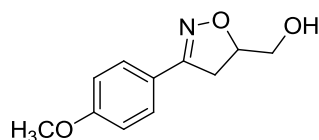
White solid, 87% yield; mp (EtOAc/hexane) 83–84 °C.  $^1\text{H}$  NMR (300 MHz,  $\text{CDCl}_3$ ):  $\delta$  7.72–7.60 (m, 2H), 7.45–7.35 (m, 3H), 4.94–4.81 (m, 1H), 3.88 (ddd,  $J = 12.1, 6.3, 3.3$  Hz, 1H), 3.68 (ddd,  $J = 12.1, 6.3, 4.7$  Hz, 1H), 3.39 (dd,  $J = 16.5, 10.4$  Hz, 1H), 3.29 (dd,  $J = 16.5, 8.0$  Hz, 1H), 2.09 (t,  $J = 6.3$  Hz, 1H). ESI-MS  $m/z$ : 178 ( $\text{M}+\text{H}$ ) $^+$ .

**8b: 5-hydroxymethyl-3-(4-nitrophenyl)-4,5-dihydroisoxazole**



Pale-yellow solid, 82%; mp (MeOH) 141–143 °C.  $^1\text{H}$  NMR (300 MHz,  $\text{CDCl}_3$ ):  $\delta$  8.30 (d,  $J = 8.4$  Hz, 2H), 7.84 (d,  $J = 8.4$  Hz, 2H), 5.02–4.92 (m, 1H), 3.96 (ddd,  $J = 12.1, 4.4, 3.6$  Hz, 1H), 3.72 (ddd,  $J = 12.1, 7.7, 4.4$  Hz, 1H), 3.42 (dd,  $J = 16.5, 10.5$ , 1H), 3.36 (dd,  $J = 16.5, 8.5$  Hz, 1H), 1.92–1.84 (m, 1H). ESI-MS  $m/z$ : 223 ( $\text{M}+\text{H}$ ) $^+$ .

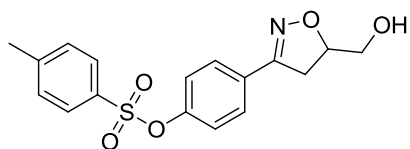
**8c: 5-hydroxymethyl-3-(4-methoxyphenyl)-4,5-dihydroisoxazole**



White solid, 83% yield; mp (EtOAc) 144–146 °C.  $^1\text{H}$  NMR (300 MHz,  $\text{CDCl}_3$ ):  $\delta$  7.60 (d,  $J = 8.7$  Hz, 2H), 6.92 (d,  $J = 8.7$  Hz, 2H), 4.89–4.79 (m, 1H), 3.89–3.82 (m, 4H), 3.68 (dd,  $J = 12.0, 3.7$  Hz, 1H), 3.37 (dd,  $J = 16.8$ ,

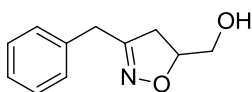
10.7 Hz, 1H), 3.25 (dd,  $J = 16.8, 7.7$  Hz, 1H), 1.80 (br s, 1H). ESI-MS  $m/z$ : 208 (M+H)<sup>+</sup>.

**8d: 5-hydroxymethyl-3-(4-(tosyloxy)phenyl)-4,5-dihydroisoxazole**



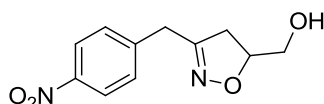
White solid, 83% yield; mp (i-PrOH) 85–87 °C. <sup>1</sup>H NMR (300 MHz, CDCl<sub>3</sub>):  $\delta$  7.68 (d,  $J = 8.0$  Hz, 2H), 7.56 (d,  $J = 8.0$  Hz, 2H), 7.30 (d,  $J = 8.0$  Hz, 2H), 7.00 (d,  $J = 8.0$  Hz, 2H), 4.90–4.79 (m, 1H), 3.84 (dd,  $J = 12.4, 3.3$  Hz, 1H), 3.65 (dd,  $J = 12.4, 4.4$  Hz, 1H), 3.32 (dd,  $J = 16.8, 11.0$  Hz, 1H), 3.22 (dd,  $J = 16.8, 7.7$  Hz, 1H), 2.43 (s, 3H), 2.18 (br s, 1H). ESI-MS  $m/z$ : 348 (M+H)<sup>+</sup>.

**8h: 3-benzyl-5-hydroxymethyl-4,5-dihydroisoxazole**



Pale-yellow oil, 80% yield. <sup>1</sup>H NMR (300 MHz, CDCl<sub>3</sub>):  $\delta$  7.40–7.15 (m, 5H), 4.70–4.58 (m, 1H), 3.71 (dd,  $J = 12.1, 3.3$  Hz, 1H), 3.67 (s, 2H), 3.51 (dd,  $J = 12.1, 5.0$  Hz, 1H), 2.85 (dd,  $J = 17.1, 10.5$  Hz, 1H), 2.71 (dd,  $J = 17.1, 7.7$  Hz, 1H), 2.10 (br s, 1H). ESI-MS  $m/z$ : 192 (M+H)<sup>+</sup>.

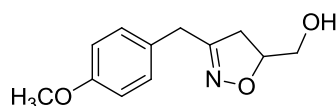
**8i: 5-hydroxymethyl-3-(4-nitrobenzyl)-4,5-dihydroisoxazole**



Yellow solid, 93% yield; mp (EtOAc/hexane) 69–71 °C. <sup>1</sup>H NMR (300 MHz, CDCl<sub>3</sub>):  $\delta$  8.20 (d,  $J = 8.5$  Hz, 2H), 7.42 (d,  $J = 8.5$  Hz, 2H), 4.74–4.66 (m, 1H),

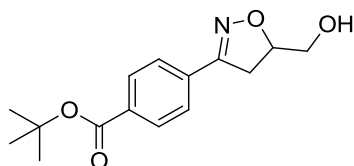
3.89–3.70 (m, 3H), 3.53 (dd,  $J = 12.2, 4.1$  Hz, 1H), 2.89 (dd,  $J = 17.6, 10.7$  Hz, 1H), 2.79 (dd,  $J = 17.6, 7.5$  Hz, 1H), 1.92 (br s, 1H). ESI-MS  $m/z$ : 237 (M+H)<sup>+</sup>.

**8j: 5-hydroxymethyl-3-(4-methoxybenzyl)-4,5-dihydroisoxazole**



White solid, 78% yield; mp (isopropyl ether) 70–71 °C. <sup>1</sup>H NMR (300 MHz, CDCl<sub>3</sub>):  $\delta$  7.11 (d,  $J = 8.5$  Hz, 2H), 6.82 (d,  $J = 8.5$  Hz, 2H), 4.66–4.54 (m, 1H), 3.76 (s, 3H), 3.66 (dd,  $J = 12.3, 3.2$  Hz, 1H), 3.58 (s, 2H), 3.48 (dd,  $J = 12.3, 4.6$  Hz, 1H), 2.82 (dd,  $J = 17.3, 11.0$  Hz, 1H), 2.68 (dd,  $J = 17.3, 7.8$  Hz, 1H), 2.58 (br s, 1H). ESI-MS  $m/z$ : 222 (M+H)<sup>+</sup>.

**8l: 3-(4-tert-butyloxycarbonylphenyl)-5-hydroxymethyl-4,5-dihydroisoxazole**



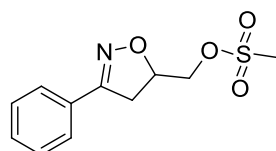
White solid, 68% yield; mp (i-PrOH) 89–91 °C. <sup>1</sup>H NMR (300 MHz, CDCl<sub>3</sub>):  $\delta$  7.99 (d,  $J = 8.8$  Hz, 2H), 7.69 (d,  $J = 8.8$  Hz, 2H), 4.96–4.84 (m, 1H), 3.90 (dd,  $J = 12.4, 3.0$  Hz, 1H), 3.70 (dd,  $J = 12.4, 4.1$  Hz, 1H), 3.40 (dd,  $J = 16.8, 10.7$  Hz, 1H), 3.30 (dd,  $J = 16.8, 8.2$  Hz, 1H), 2.20 (br s, 1H), 1.60 (s, 9H). ESI-MS  $m/z$ : 278 (M+H)<sup>+</sup>.

**General procedure for the synthesis of (3-substituted-4,5-dihydroisoxazol-5-yl)methyl methanesulfonates (9)**

To a solution of the proper (3-substituted-4,5-dihydroisoxazol-5-yl)methanol **8** (1.66 mmol) and triethylamine (0.28 mL, 2.00 mmol) in dry CH<sub>2</sub>Cl<sub>2</sub> (20 mL),

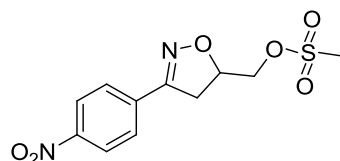
methanesulfonyl chloride (0.16 mL, 2.00 mmol) was added at 0 °C. The resulting mixture was stirred at room temperature for 45 min, and then the solvent was evaporated. The residue was taken up with water (20 mL) and extracted with CH<sub>2</sub>Cl<sub>2</sub> (3 x 20 mL). The combined organic phases were washed with 1N HCl (2 x 10 mL), NaHCO<sub>3</sub>, saturated aqueous solution (2 x 10 mL), and brine (10 mL), dried (Na<sub>2</sub>SO<sub>4</sub>), filtered, and concentrated in vacuo. Mesylates **9** were obtained in quantitative yields and used without further purification in the subsequent reaction. Recrystallization from the suitable solvent gave an analytical sample.

**9a: 5-hydroxymethyl-3-phenyl-4,5-dihydroisoxazole methanesulfonate**



White solid; mp (i-PrOH) 109–111 °C. <sup>1</sup>H NMR (300 MHz, CDCl<sub>3</sub>): δ 7.70–7.60 (m, 2H), 7.42–7.38 (m, 3H), 5.06–4.96 (m, 1H), 4.39 (dd, J = 11.3, 3.9 Hz, 1H), 4.27 (dd, J = 11.3, 5.0 Hz, 1H), 3.45 (dd, J = 17.0, 11.0 Hz, 1H), 3.30 (dd, J = 17.0, 7.2 Hz, 1H), 3.09 (s, 3H). ESI-MS *m/z*: 256 (M+H)<sup>+</sup>.

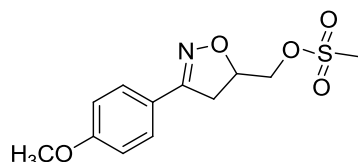
**9b: 5-hydroxymethyl-3-(4-nitrophenyl)-4,5-dihydroisoxazole methanesulfonate**



White solid; mp: (MeOH/H<sub>2</sub>O) 171–173 °C. <sup>1</sup>H NMR (300 MHz, CDCl<sub>3</sub>): δ 8.29 (d, J = 8.8 Hz, 2H), 7.84 (d, J = 8.8 Hz, 2H), 5.19–5.06 (m, 1H), 4.45 (dd, J = 11.3, 4.1 Hz, 1H), 4.39 (dd, J = 11.3, 4.7 Hz, 1H), 3.54 (dd, J = 16.8, 11.0

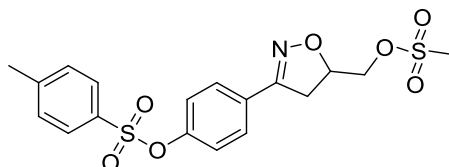
Hz, 1H), 3.36 (dd,  $J = 16.8, 7.2$  Hz, 1H), 3.09 (s, 3H). ESI-MS  $m/z$ : 301 (M+H)<sup>+</sup>.

**9c: 5-hydroxymethyl-3-(4-methoxyphenyl)-4,5-dihydroisoxazole methanesulfonate**

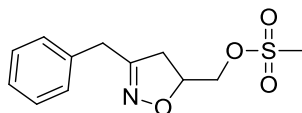


White solid; mp: (EtOAc) 146–148 °C. <sup>1</sup>H NMR (300 MHz, CDCl<sub>3</sub>):  $\delta$  7.60 (d,  $J = 8.8$  Hz, 2H), 6.93 (d,  $J = 8.8$  Hz, 2H), 5.04–4.94 (m, 1H), 4.40 (dd,  $J = 11.3, 4.1$  Hz, 1H), 4.34 (dd,  $J = 11.3, 5.0$  Hz, 1H), 3.85 (s, 3H), 3.48 (dd,  $J = 16.8, 11.0$  Hz, 1H), 3.28 (dd,  $J = 16.8, 7.2$  Hz, 1H), 3.09 (s, 3H). ESI-MS  $m/z$ : 286 (M+H)<sup>+</sup>.

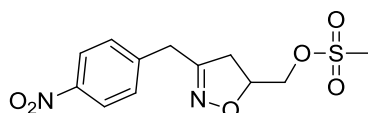
**9d: 5-hydroxymethyl-3-(4-(tosyloxy)phenyl)-4,5-dihydroisoxazole methanesulfonate**



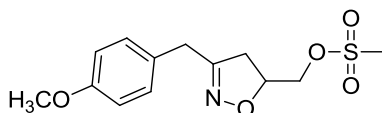
White solid; mp: (i-PrOH) 123–125 °C. <sup>1</sup>H NMR (300 MHz, CDCl<sub>3</sub>):  $\delta$  7.69 (d,  $J = 8.5$  Hz, 2H), 7.57 (d,  $J = 8.5$  Hz, 2H), 7.32 (d,  $J = 8.5$  Hz, 2H), 7.02 (d,  $J = 8.5$  Hz, 2H), 5.07–4.95 (m, 1H), 4.38 (dd,  $J = 11.6, 3.9$  Hz, 1H), 4.31 (dd,  $J = 11.6, 3.9$  Hz, 1H), 3.44 (dd,  $J = 17.1, 11.0$  Hz, 1H), 3.24 (dd,  $J = 17.1, 7.1$  Hz, 1H), 3.06 (s, 3H), 2.44 (s, 3H). ESI-MS  $m/z$ : 426 (M+H)<sup>+</sup>.

**9h: 3-benzyl-5-hydroxymethyl-4,5-dihydroisoxazole methanesulfonate**

White solid; mp (i-PrOH): 43–44 °C.  $^1\text{H}$  NMR (300 MHz,  $\text{CDCl}_3$ ):  $\delta$  7.38–7.20 (m, 5H), 4.82–4.72 (m, 1H), 4.22 (dd,  $J = 11.3, 3.9$  Hz, 1H), 4.15 (dd,  $J = 11.3, 5.0$  Hz, 1H), 3.66 (s, 2H), 2.98 (s, 3H), 2.96 (dd,  $J = 17.6, 10.9$  Hz, 1H), 2.71 (dd,  $J = 17.6, 7.0$  Hz, 1H). ESI-MS  $m/z$ : 270 ( $\text{M}+\text{H}$ ) $^+$ .

**9i: 5-hydroxymethyl-3-(4-nitrobenzyl)-4,5-dihydroisoxazole methanesulfonate**

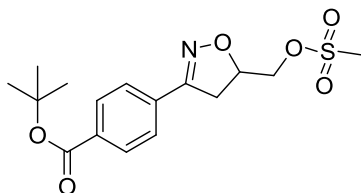
Pale-yellow solid; mp (i-PrOH): 107–109 °C.  $^1\text{H}$  NMR (300 MHz,  $\text{CDCl}_3$ ):  $\delta$  8.24 (d,  $J = 8.8$  Hz, 2H), 7.45 (d,  $J = 8.8$  Hz, 2H), 4.92–4.81 (m, 1H), 4.29 (dd,  $J = 11.3, 3.8$  Hz, 1H), 4.21 (dd,  $J = 11.3, 4.4$  Hz, 1H), 3.83 (s, 2H), 3.08 (s, 3H), 3.02 (dd,  $J = 17.4, 10.8$  Hz, 1H), 2.82 (dd,  $J = 17.4, 6.8$  Hz, 1H). ESI-MS  $m/z$ : 315 ( $\text{M}+\text{H}$ ) $^+$ .

**9j: 5-hydroxymethyl-3-(4-methoxybenzyl)-4,5-dihydroisoxazole methanesulfonate**

White solid; mp (i-PrOH): 104–105 °C.  $^1\text{H}$  NMR (300 MHz,  $\text{CDCl}_3$ ):  $\delta$  7.12 (d,  $J = 8.7$  Hz, 2H), 6.83 (d,  $J = 8.7$  Hz, 2H), 4.83–4.72 (m, 1H), 4.24 (dd,  $J = 11.3, 3.9$  Hz, 1H), 4.17 (dd,  $J = 11.3, 5.0$  Hz, 1H), 3.79 (s, 3H), 3.62 (s, 2H),

3.03 (s, 3H), 2.96 (dd, J = 17.3, 11.0 Hz, 1H), 2.72 (dd, J = 17.3, 7.1 Hz, 1H). ESI-MS  $m/z$ : 300 (M+H)<sup>+</sup>.

**9l: 3-(4-*tert*-butyloxycarbonylphenyl)-5-hydroxymethyl-4,5-dihydroisoxazole methanesulfonate**



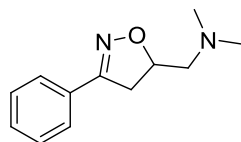
White solid; mp (i-PrOH): 128–129 °C. <sup>1</sup>H NMR (300 MHz, CDCl<sub>3</sub>): δ 8.02 (d, J = 8.8 Hz, 2H), 7.68 (d, J = 8.8 Hz, 2H), 5.12–4.99 (m, 1H), 4.42 (dd, J = 11.7, 4.1 Hz, 1H), 4.35 (dd, J = 11.7, 5.0 Hz, 1H), 3.52 (dd, J = 17.0, 11.1 Hz, 1H), 3.30 (dd, J = 17.0, 7.3 Hz, 1H), 3.08 (s, 3H), 1.60 (s, 9H). ESI-MS  $m/z$ : 356 (M+H)<sup>+</sup>.

**General procedure for the synthesis of 3-substituted-5-(*N,N*-dimethylaminomethyl)-4,5-dihydroisoxazoles (5)**

The proper mesylate (1.30 mmol) was dissolved in a 2 M THF solution of dimethylamine (20 mL, 39.0 mmol) under N<sub>2</sub> atmosphere. The vessel was sealed, and the reaction was stirred at 100 °C for 12h and then concentrated in vacuo. The residue was purified by silica gel chromatography (EtOAc/hexane) to give the title compounds. Compounds **5c,d** and **5l** were recrystallized from the appropriate solvent. Compounds **5a,b**, and **5h-j** were dissolved in 4N HCl in dioxane, and the mixture was stirred at room temperature for 10 min. The solvent was concentrated in vacuo, and the resulting solid was recrystallized from the appropriate solvent to yield title compounds as hydrochloride salts.

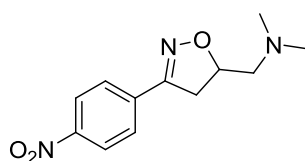


**5a: 5-(*N,N*-dimethylaminomethyl)-3-phenyl-4,5-dihydroisoxazole hydrochloride**



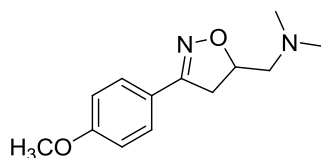
White solid, 79% yield; mp (i-PrOH) 188–190 °C; free base. <sup>1</sup>H NMR (300 MHz, CDCl<sub>3</sub>): δ 7.62–7.51 (m, 2H), 7.35–7.23 (m, 3H), 4.86–4.72 (m, 1H), 3.30 (dd, J = 16.5, 10.5 Hz, 1H), 3.05 (dd, J = 16.5, 8.0 Hz, 1H), 2.53 (dd, J = 12.7, 6.6 Hz, 1H), 2.46 (dd, J = 12.7, 5.2 Hz, 1H), 2.24 (s, 6H). ESI-MS *m/z*: 205 (M+H)<sup>+</sup>.

**5b: 5-(*N,N*-dimethylaminomethyl)-3-(4-nitrophenyl)-4,5-dihydroisoxazole hydrochloride**



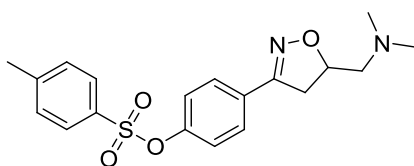
White solid, 78% yield; mp (MeOH) 262 °C (decomp); free base. <sup>1</sup>H NMR (300 MHz, CDCl<sub>3</sub>): δ 8.26 (d, J = 8.7 Hz, 2H), 7.84 (d, J = 8.7 Hz, 2H), 5.06–4.90 (m, 1H), 3.43 (dd, J = 16.7, 10.6 Hz, 1H), 3.24 (dd, J = 16.7, 8.1 Hz, 1H), 2.66 (dd, J = 12.8, 6.4 Hz, 1H), 2.55 (dd, J = 12.8, 6.0 Hz, 1H), 2.34 (s, 6H). ESI-MS *m/z*: 250 (M+H)<sup>+</sup>.

**5c: 5-(*N,N*-dimethylaminomethyl)-3-(4-methoxyphenyl)-4,5-dihydroisoxazole**



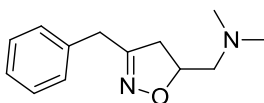
White solid, 75% yield; mp (isopropyl ether) 75–76 °C. <sup>1</sup>H NMR (300 MHz, CDCl<sub>3</sub>): δ 7.61 (d, J = 8.8 Hz, 2H), 6.91 (d, J = 8.8 Hz, 2H), 4.93–4.80 (m, 1H), 3.83 (s, 3H), 3.40 (dd, J = 16.7, 10.5 Hz, 1H), 3.14 (dd, J = 16.7, 7.6 Hz, 1H), 2.63 (dd, J = 12.9, 6.7 Hz, 1H), 2.55 (dd, J = 12.9, 5.6 Hz, 1H), 2.35 (s, 6H). ESI-MS *m/z*: 235 (M+H)<sup>+</sup>.

**5d: 5-(*N,N*-dimethylaminomethyl)-3-(4-(tosyloxy)phenyl)-4,5-dihydroisoxazole**



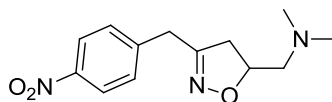
White solid, 78% yield; mp (i-PrOH) 123–124 °C. <sup>1</sup>H NMR (300 MHz, CDCl<sub>3</sub>): δ 7.70 (d, J = 8.2 Hz, 2H), 7.57 (d, J = 8.2 Hz, 2H), 7.31 (d, J = 8.2 Hz, 2H), 7.00 (d, J = 8.2 Hz, 2H), 4.93–4.82 (m, 1H), 3.32 (dd, J = 16.8, 10.5 Hz, 1H), 3.12 (dd, J = 16.8, 8.0 Hz, 1H), 2.60 (dd, J = 12.9, 6.3 Hz, 1H), 2.49 (dd, J = 12.9, 6.3 Hz, 1H), 2.43 (s, 3H), 2.31 (s, 6H). ESI-MS *m/z*: 375 (M+H)<sup>+</sup>.

**5h: 3-benzyl-5-(*N,N*-dimethylaminomethyl)-4,5-dihydroisoxazole hydrochloride**



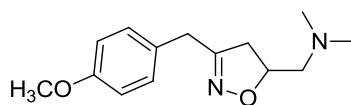
White solid, 76% yield; mp (EtOAc) 80–82 °C; free base. <sup>1</sup>H NMR (300 MHz, CDCl<sub>3</sub>): δ 7.35–7.22 (m, 5H), 4.70–4.60 (m, 1H), 3.68 (s, 2H), 2.86 (dd, J = 17.0, 10.4 Hz, 1H), 2.60 (dd, J = 17.0, 8.0 Hz, 1H), 2.50 (dd, J = 12.8, 6.5 Hz, 1H), 2.33 (dd, J = 12.8, 5.7 Hz, 1H), 2.25 (s, 6H). ESI-MS *m/z*: 219 (M+H)<sup>+</sup>.

**5i: 5-(*N,N*-dimethylaminomethyl)-3-(4-nitrobenzyl)-4,5-dihydroisoxazole hydrochloride**



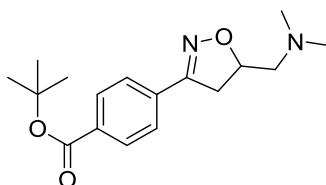
White solid, 79% yield; mp (EtOH/Et<sub>2</sub>O) 164–167 °C; free base. <sup>1</sup>H NMR (300 MHz, CDCl<sub>3</sub>): δ 8.20 (d, J = 8.8 Hz, 2H), 7.42 (d, J = 8.8 Hz, 2H), 4.78–4.66 (m, 1H), 3.78 (s, 2H), 2.89 (dd, J = 17.0, 10.4 Hz, 1H), 2.65 (dd, J = 17.0, 8.0 Hz, 1H), 2.52 (dd, J = 12.9, 6.5 Hz, 1H), 2.40 (dd, J = 12.9, 5.5 Hz, 1H), 2.27 (s, 6H). ESI-MS *m/z*: 264 (M+H)<sup>+</sup>.

**5j: 5-(*N,N*-dimethylaminomethyl)-3-(4-methoxybenzyl)-4,5-dihydroisoxazole hydrochloride**



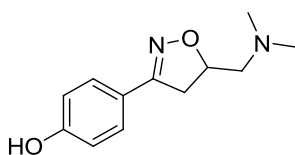
White solid, 79% yield; mp (acetone/Et<sub>2</sub>O) 126–128 °C; free base. <sup>1</sup>H NMR (300 MHz, CDCl<sub>3</sub>): δ 7.14 (d, J = 8.5 Hz, 2H), 6.86 (d, J = 8.5 Hz, 2H), 4.69–4.59 (m, 1H), 3.79 (s, 3H), 3.61 (s, 2H), 2.86 (dd, J = 16.9, 10.3 Hz, 1H), 2.59 (dd, J = 16.9, 8.0 Hz, 1H), 2.49 (dd, J = 12.8, 6.6 Hz, 1H), 2.33 (dd, J = 12.8, 5.7 Hz, 1H), 2.25 (s, 6H). ESI-MS *m/z*: 249 (M+H)<sup>+</sup>.

**5l: 5-(*N,N*-dimethylaminomethyl)-3-(4-*tert*-butyloxycarbonylphenyl)-4,5-dihydroisoxazole**

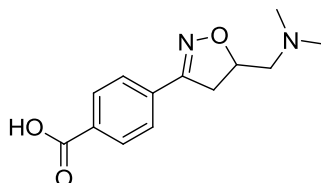


White solid, 81% yield; mp (i-PrOH) 75–76 °C. <sup>1</sup>H NMR (300 MHz, CDCl<sub>3</sub>): δ 8.00 (d, J = 8.8 Hz, 2H), 7.70 (d, J = 8.8 Hz, 2H), 4.98–4.84 (m, 1H), 3.41 (dd, J = 16.7, 10.6 Hz, 1H), 3.18 (dd, J = 16.7, 8.2 Hz, 1H), 2.63 (dd, J = 12.9, 6.2 Hz, 1H), 2.52 (dd, J = 12.9, 6.2 Hz, 1H), 2.32 (s, 6H), 1.60 (s, 9H). ESI-MS *m/z*: 305 (M+H)<sup>+</sup>.

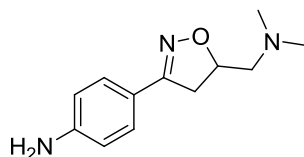
**Synthesis of 5-(*N,N*-dimethylaminomethyl)-3-(4-hydroxyphenyl)-4,5-dihydroisoxazole hydrochloride (5g)**



To a solution of **5d** (0.11 g, 0.29 mmol) in EtOH (5 mL) an aqueous solution of 1N NaOH (1.45 mL, 1.45 mmol) was added. The mixture was heated at reflux and stirred for 1h. The reaction mixture was then cooled to room temperature, treated with HCl 1N to pH 9, and concentrated in vacuo. The residue was treated with water (30 mL) and extracted with EtOAc (3 x 30 mL). The combined organic phases were washed with brine (10 mL), dried (Na<sub>2</sub>SO<sub>4</sub>), filtered, and concentrated in vacuo to give the title compound as a free base (61.2 mg, 96%), which was converted in the corresponding hydrochloride salt following the general procedure described for compounds **5a,b**, and **5h-j**; mp 232–235 °C (decomp); free base. <sup>1</sup>H NMR (300 MHz, DMSO-*d*<sub>6</sub>): δ 9.90 (br s, 1H), 7.47 (d, J = 8.5 Hz, 2H), 6.80 (d, J = 8.5 Hz, 2H), 4.77–4.66 (m, 1H), 3.37 (dd, J = 16.9, 11.7 Hz, 1H), 3.07 (dd, J = 16.9, 8.0 Hz, 1H), 2.51–2.39 (m, 2H), 2.20 (s, 6H). ESI-MS *m/z*: 221 (M+H)<sup>+</sup>.

**Synthesis of 5-(*N,N*-dimethylaminomethyl)-3-(4-carboxyphenyl)-4,5-dihydroisoxazole (5e)**

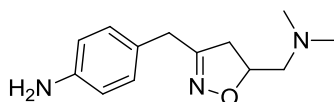
A mixture of TFA and DCM (1:3, 12 mL) was added to compound **5l** (0.31 g, 1.03 mmol). The reaction was stirred at room temperature overnight and then concentrated in vacuo to give the title compound as a white solid (0.26 g, 99%), which was recrystallized from MeOH/H<sub>2</sub>O. White solid; mp 249–251 °C (decomp). <sup>1</sup>H NMR (300 MHz, DMSO-*d*<sub>6</sub>): δ 9.96 (br s, 1H), 8.0 (d, J = 8.2 Hz, 2H), 7.78 (d, J = 8.2 Hz, 2H), 5.25–5.15 (m, 1H), 3.80–3.63 (m, 1H), 3.50–3.23 (m, 3H), 2.84 (s, 6H). ESI-MS *m/z*: 249 (M+H)<sup>+</sup>.

**Synthesis of 5-(*N,N*-dimethylaminomethyl)-3-(4-aminophenyl)-4,5-dihydroisoxazole hydrochloride (5f).**

To an ice cooled solution of **5b** free base (0.16 g, 0.64 mmol) in AcOH (36 mL) zinc powder (0.340g, 5.13 mmol) was added. The resulting mixture was stirred at room temperature for 1h, the solid was filtered off, and the solvent was evaporated. The residue was taken up with EtOAc (20 mL) and washed with NaHCO<sub>3</sub> saturated aqueous solution twice. The organic phase was dried (Na<sub>2</sub>SO<sub>4</sub>), filtered, and concentrated in vacuo. The residue was purified by silica gel chromatography (CH<sub>2</sub>Cl<sub>2</sub>/MeOH) to give the title compound (0.12 g, 63%), which was converted in the corresponding hydrochloride salt following

the general procedure described for compounds **5a,b**, and **7h-j**. White solid; mp 268–270 °C (decomp); free base. <sup>1</sup>H NMR (300 MHz, CDCl<sub>3</sub>): δ 7.47 (d, J = 8.8 Hz, 2H), 6.67 (d, J = 8.8 Hz, 2H), 4.86–4.76 (m, 1H), 3.87 (br s, 2H); 3.36 (dd, J = 16.5, 10.3 Hz, 1H), 3.11 (dd, J = 16.5, 7.8 Hz, 1H), 2.60 (dd, J = 12.8, 6.4 Hz, 1H), 2.50 (dd, J = 12.8, 6.1 Hz, 1H), 2.32 (s, 6H). ESI-MS *m/z*: 220 (M+H)<sup>+</sup>.

**Synthesis of 5-(*N,N*-dimethylaminomethyl)-3-(4-aminobenzyl)-4,5-dihydroisoxazole hydrochloride (5k).**



Reduction of compound **5i** (0.15 g, 0.58 mmol) according to the procedure used for **5f** yielded the free amine (0.10 g, 75%), which was converted to the hydrochloride salt following the general procedure described for compounds **5a,b**, and **5h-j**. White solid; mp (EtOH/Et<sub>2</sub>O) 211–212 °C (decomp); free base. <sup>1</sup>H NMR (300 MHz, CDCl<sub>3</sub>): δ 6.99 (d, J = 8.2 Hz, 2H), 6.62 (d, J = 8.2 Hz, 2H), 4.79–4.46 (m, 1H), 3.75 (br s, 2H), 3.54 (s, 2H), 2.86 (dd, J = 17.0, 10.3 Hz, 1H), 2.58 (dd, J = 17.0, 10.3 Hz, 1H), 2.50 (dd, J = 12.8, 7.0 Hz, 1H), 2.35 (dd, J = 12.8, 5.5 Hz, 1H), 2.26 (s, 6H). ESI-MS *m/z*: 234 (M+H)<sup>+</sup>.

**General procedures for the synthesis of *tert*-Butyl 3-substituted-6,6a-dihydro-3a*H*-pyrrolo[3,4-*d*]isoxazole-5(4*H*)-carboxylates (12a-d, 12h-j, 12l).**

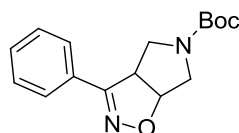
*Conventional conditions.* To a solution of *N*-Boc-Δ<sup>3</sup>-pyrroline **11** (0.17 g, 1.00 mmol) in EtOAc (5 mL) were added solid NaHCO<sub>3</sub> (0.42 g, 5.00 mmol) and the proper chloroxime **10** (4 equiv added portionwise: 1 equiv the first day, 0.5 equiv/day for the next six days). The mixture was vigorously stirred at room temperature for 7 days. Water was added to the reaction mixture, and the

organic layer was separated. The aqueous layer was further extracted with EtOAc, and the combined organic phase was dried over anhydrous sodium sulfate. The solvent was evaporated, and the crude material was purified by silica gel chromatography (cyclohexane/EtOAc 7:3) to give the corresponding cycloadduct.

*Microwave batch conditions.* The proper chloroxime **10** (1.00 mmol) was dissolved in EtOAc (5 mL) at room temperature in a 10 mL CEM pressure vessel equipped with a stirrer bar. *N*-Boc- $\Delta^3$ -pyrroline **11** (0.17 g, 1.00 mmol), solid NaHCO<sub>3</sub> (0.34 g, 4.00 mmol), and H<sub>2</sub>O (50  $\mu$ L) were added, and the vial was sealed and heated in a CEM Discover microwave synthesizer to 80 °C (measured by the vertically focused IR temperature sensor) for 30 min. The reaction cycle was repeated another two times, each time adding additional 0.5 equiv of chloroxime **10** (2 equiv total). The solid was filtered off, and the solution was dried over anhydrous sodium sulfate. The solvent was evaporated, and the crude material was purified by silica gel column chromatography (cyclohexane/EtOAc 7:3) to give the corresponding cycloadduct.

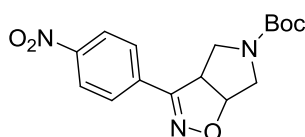
*Continuous flow conditions.* A 0.25M solution of *N*-Boc- $\Delta^3$ -pyrroline **11** (0.17 g, 1.00 mmol) in EtOAc (4 mL) and a 0.37M solution of the proper chloroxime **10** (1.50 mmol) in EtOAc (4 mL) were prepared. The two reactant streams were mixed using a simple T-piece and delivered to an Omnifit glass column (6.6 mm id by 100 mm length) filled with K<sub>2</sub>CO<sub>3</sub> (0.54 g, 4.00 mmol) heated at 90 °C at a total flow rate of 0.1 mL min<sup>-1</sup>, equivalent to a residence time of about 10 min. A 100 psi backpressure regulator was applied to the system. The solvent was evaporated, and the product was purified by silica gel column chromatography (hexane/EtOAc 7:3) to give the title compound **12**.

**12a: *tert*-Butyl 3-Phenyl-6,6a-dihydro-3a*H*-pyrrolo[3,4-*d*]isoxazole-5(4*H*)-carboxylate**



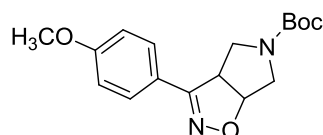
White solid, 69% yield; mp (EtOAc/hexane) 146–147 °C (decomp). <sup>1</sup>H NMR (300 MHz, CDCl<sub>3</sub>): δ 7.65–7.55 (m, 2H), 7.45–7.35 (m, 3H), 5.28 (ddd, J = 9.3, 5.5, 1.1 Hz, 1H), 4.25–4.15 (m, 1H), 3.90 (d, J = 12.6 Hz, 1H), 3.51–3.70 (m, 3H), 1.40 (s, 9H). ESI-MS *m/z*: 233 (M+H – <sup>t</sup>Bu)<sup>+</sup>.

**12b: *tert*-Butyl 3-(4-nitrophenyl)-6,6a-dihydro-3a*H*-pyrrolo[3,4-*d*]isoxazole-5(4*H*)-carboxylate**



Pale-yellow solid, 60% yield; mp (EtOAc/hexane) 189–190 °C (decomp). <sup>1</sup>H NMR (300 MHz, CDCl<sub>3</sub>): δ 8.28 (d, J = 8.8 Hz, 2H), 7.80 (d, J = 8.8 Hz, 2H), 5.40 (dd, J = 8.3, 4.1 Hz, 1H), 4.30–4.20 (m, 1H), 4.03 (d, J = 13.2 Hz, 1H), 3.85–3.55 (m, 3H), 1.42 (s, 9H). ESI-MS *m/z*: 278 (M+H – <sup>t</sup>Bu)<sup>+</sup>.

**12c: *tert*-Butyl 3-(4-methoxyphenyl)-6,6a-dihydro-3a*H*-pyrrolo[3,4-*d*]isoxazole-5(4*H*)-carboxylate**

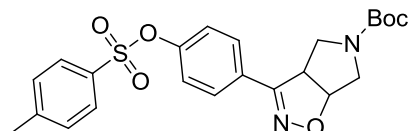


White solid, 73% yield; mp (EtOAc/hexane) 137–138 °C. <sup>1</sup>H NMR (300 MHz, CDCl<sub>3</sub>): δ 7.56 (d, J = 8.8 Hz, 2H), 6.93 (d, J = 8.8 Hz, 2H), 5.26 (dd, J = 9.3,



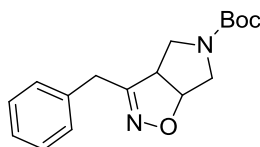
5.2 Hz, 1H), 4.25–4.15 (m, 1H), 3.95 (d,  $J = 12.6$  Hz, 1H), 3.83 (s, 3H), 3.72–.58 (m, 3H), 1.40 (s, 9H). ESI-MS  $m/z$ : 263 ( $M+H - tBu$ )<sup>+</sup>.

**12d: *tert*-Butyl 3-(4-(tosyloxy)phenyl)-6,6a-dihydro-3a*H*-pyrrolo[3,4-*d*]isoxazole-5(4*H*)-carboxylate**



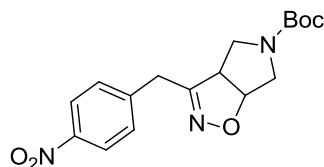
Pale-yellow solid, 58% yield; mp (EtOAc/hexane) 189–190 °C. <sup>1</sup>H NMR (300 MHz, CDCl<sub>3</sub>):  $\delta$  7.72 (d,  $J = 8.2$  Hz, 2H), 7.56 (d,  $J = 8.2$  Hz, 2H), 7.33 (d,  $J = 7.8$  Hz, 2H), 7.04 (d,  $J = 7.8$  Hz, 2H), 5.34 (dd,  $J = 9.5, 5.1$  Hz, 1H), 4.25–4.13 (m, 1H), 4.00 (d,  $J = 12.9$  Hz, 1H), 3.85–3.55 (m, 3H), 2.46 (s, 3H), 1.42 (s, 9H). ESI-MS  $m/z$ : 403 ( $M+H - tBu$ )<sup>+</sup>.

**12h: *tert*-Butyl 3-benzyl-6,6a-dihydro-3a*H*-pyrrolo[3,4-*d*]isoxazole-5(4*H*)-carboxylate**



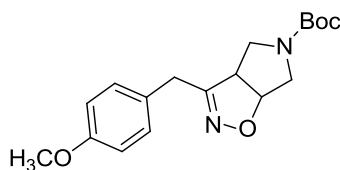
Pale-yellow oil, 71% yield. <sup>1</sup>H NMR (300 MHz, CDCl<sub>3</sub>):  $\delta$  7.21–7.37 (m, 5H), 5.08 (ddd,  $J = 9.1, 5.6, 1.5$  Hz, 1H), 3.95–3.80 (m, 3H), 3.62–3.50 (m, 2H), 3.45 (dd,  $J = 13.5, 5.6$  Hz, 1H), 3.29 (dd,  $J = 11.7, 8.5$  Hz, 1H), 1.45 (s, 9H). ESI-MS  $m/z$ : 325 ( $M+Na$ )<sup>+</sup>.

**12i:** *tert*-Butyl 3-(4-nitrobenzyl)-6,6a-dihydro-3a*H*-pyrrolo[3,4-*d*]isoxazole-5(4*H*)-carboxylate



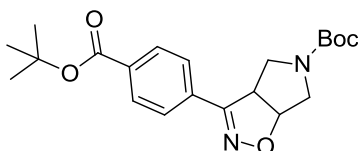
Yellow solid, 67% yield; mp (EtOAc/hexane) 108–110 °C. <sup>1</sup>H NMR (300 MHz, CDCl<sub>3</sub>): δ 8.20 (d, J = 8.5 Hz, 2H), 7.45 (d, J = 8.5 Hz, 2H), 5.12 (dd, J = 8.2, 4.8 Hz, 1H), 4.00–3.80 (m, 2H), 3.75–3.55 (m, 3H), 3.45 (dd, J = 12.6, 4.8 Hz, 1H), 3.32 (dd, J = 11.8, 8.2 Hz, 1H), 1.42 (s, 9H). ESI-MS *m/z*: 292 (M+H – <sup>t</sup>Bu)<sup>+</sup>.

**12j:** *tert*-Butyl 3-(4-methoxybenzyl)-6,6a-dihydro-3a*H*-pyrrolo[3,4-*d*]isoxazole-5(4*H*)-carboxylate



Pale-yellow oil, 64% yield. <sup>1</sup>H NMR (300 MHz, CDCl<sub>3</sub>): δ 7.15 (d, J = 8.5 Hz, 2H), 6.88 (d, J = 8.5 Hz, 2H), 5.07 (ddd, J = 9.1, 5.8, 1.6 Hz, 1H), 3.80 (s, 3H), 3.85–3.75 (m, 2H), 3.60–3.40 (m, 4H), 3.30 (dd, J = 11.8, 8.5 Hz, 1H), 1.45 (s, 9H). ESI-MS *m/z*: 355 (M+Na)<sup>+</sup>.

**12l:** *tert*-Butyl 3-(4-(*tert*-butoxycarbonyl)phenyl)-6,6a-dihydro-3a*H*-pyrrolo[3,4-*d*]isoxazole-5(4*H*)-carboxylate



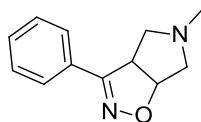
White solid, 69% yield; mp (EtOAc/hexane) 143–145 °C. <sup>1</sup>H NMR(300 MHz, CDCl<sub>3</sub>): δ 8.02 (d, J = 8.2 Hz, 2H), 7.67 (d, J = 8.2 Hz, 2H), 5.34 (dd, J = 9.4, 5.6 Hz, 1H), 4.27–4.18 (m, 1 H), 4.00 (d, J = 12.9 Hz, 1H), 3.80–3.58 (m, 3H), 1.65 (s, 9H), 1.40 (s, 9H). ESI-MS *m/z*: 389 (M+H)<sup>+</sup>.

**General procedure for the synthesis of 5-methyl-3-substituted-4,5,6,6a-tetrahydro-3aH-pyrrolo[3,4-*d*]isoxazoles (6).**

A solution of the proper *N*-Boc protected derivative **12** (1.00 mmol) in 4 M HCl solution in dioxane (5.0 mL, 20.0 mmol) was stirred for 1 h and then concentrated in vacuo. The residue was treated with water (10 mL) and washed with CH<sub>2</sub>Cl<sub>2</sub> twice. The aqueous phase was basified with NaHCO<sub>3</sub> and extracted with EtOAc (3 x 30 mL). The combined organic phases were washed with brine (10 mL), dried (Na<sub>2</sub>SO<sub>4</sub>), filtered, and concentrated in vacuo to afford the crude, unprotected derivative, which was used for the next step without further purification.

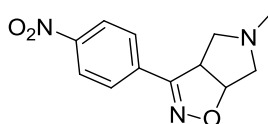
To a solution of the proper unprotected 4,5,6,6a-tetrahydro-3aH-pyrrolo[3,4-*d*]isoxazole (0.80 mmol) in acetone (8 mL), K<sub>2</sub>CO<sub>3</sub> (0.44 g, 3.20 mmol) and methyl iodide (49 μL, 0.80 mmol) were added. The resulting mixture was stirred at room temperature for 12h, the solid was filtered off, and the solvent was evaporated. The residue was purified by silica gel chromatography (CH<sub>2</sub>Cl<sub>2</sub>/MeOH) to give the title compounds. Derivatives **6a-d** were recrystallized from the appropriate solvent. Compounds **6h** and **6i** were converted in the corresponding hydrochloride salts following the general procedure described for compounds **5a,b** and **5h-j**. Compound **6j** (53.0 mg, 0.21 mmol) was dissolved in EtOH (3 mL), and a solution of oxalic acid (30.0 mg, 0.24 mmol) in EtOH (1 mL) was added. The mixture was stirred at room temperature for 10 min, and the resulting solid was recrystallized from EtOH/Et<sub>2</sub>O to yield title compounds as oxalate salt.

**6a: 5-methyl-3-phenyl-4,5,6,6a-tetrahydro-3aH-pyrrolo[3,4-d]isoxazole**



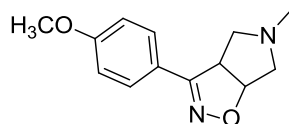
White solid, 48% yield; mp (EtOAc/hexane) 119–121 °C (decomp). <sup>1</sup>H NMR (300 MHz, CDCl<sub>3</sub>): δ 7.50–7.68 (m, 2H), 7.28–7.40 (m, 3H), 5.22 (dd, J = 9.1, 4.5 Hz, 1H), 4.21–4.16 (ddd, J = 9.1, 7.4, 1.7 Hz, 1H), 3.26 (d, J = 11.0 Hz, 1H), 3.09 (d, J = 9.6 Hz, 1H), 2.51 (dd, J = 9.6, 7.4 Hz, 1H), 2.45 (dd, J = 11.0, 4.5 Hz, 1H), 2.33 (s, 3H). ESI-MS *m/z*: 203 (M+H)<sup>+</sup>.

**6b: 5-methyl-3-(4-nitrophenyl)-4,5,6,6a-tetrahydro-3aH-pyrrolo[3,4-d]isoxazole**



White solid, 38% yield; mp (EtOAc/hexane) 161–162 °C. <sup>1</sup>H NMR (300 MHz, CDCl<sub>3</sub>): δ 8.27 (d, J = 7.7 Hz, 2H), 7.85 (d, J = 7.7 Hz, 2H), 5.33 (dd, J = 4.3, 9.5, 1H), 4.23–4.17 (m, 1H), 3.33 (d, J = 11.2 Hz, 1H), 3.08 (d, J = 9.7, 1H), 2.66–2.43 (m, 2H), 2.37 (s, 3H). ESI-MS *m/z*: 248 (M+H)<sup>+</sup>.

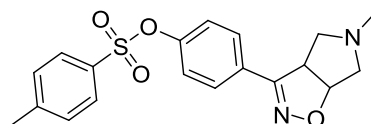
**6c: 5-methyl-3-(4-methoxyphenyl)-4,5,6,6a-tetrahydro-3aH-pyrrolo[3,4-d]isoxazole**



White solid, 33% yield; mp (EtOAc/hexane) 158–160 °C. <sup>1</sup>H NMR (300 MHz, CDCl<sub>3</sub>): δ 7.61 (d, J = 8.8 Hz, 2H), 6.91 (d, J = 8.8 Hz, 2H), 5.19 (dd, J = 10.0,

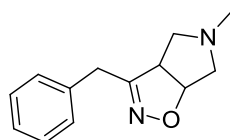
4.6 Hz, 1H), 4.17–4.12 (m, 1H), 3.84 (s, 3H), 3.25 (d,  $J = 10.9$  Hz, 1H), 3.07 (d,  $J = 9.0$ , 1H), 2.59–2.40 (m, 2H), 2.32 (s, 3H). ESI-MS  $m/z$ : 233 (M+H)<sup>+</sup>.

**6d: 5-methyl-3-(4-(tosyloxy)phenyl)-4,5,6,6a-tetrahydro-3aH-pyrrolo-[3,4-d]isoxazole**



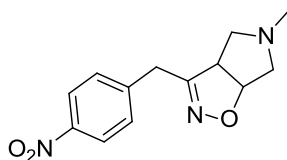
White solid, 32% yield; mp (EtOAc/hexane) 122–123 °C. <sup>1</sup>H NMR (300 MHz, CDCl<sub>3</sub>):  $\delta$  7.70 (d,  $J = 8.5$  Hz, 2H), 7.59 (d,  $J = 8.5$  Hz, 2H), 7.32 (d,  $J = 8.5$  Hz, 2H), 7.00 (d,  $J = 8.5$  Hz, 2H), 5.22 (dd,  $J = 9.4, 4.1$  Hz, 1H), 4.14–4.08 (m, 1H), 3.28 (d,  $J = 11.9$  Hz, 1H), 3.07 (d,  $J = 9.4$ , 1H), 2.49–2.38 (m, 5H), 2.33 (s, 3H). ESI-MS  $m/z$ : 373 (M+H)<sup>+</sup>.

**6h: 3-benzyl-5-methyl-4,5,6,6a-tetrahydro-3aH-pyrrolo[3,4-d]isoxazole hydrochloride**



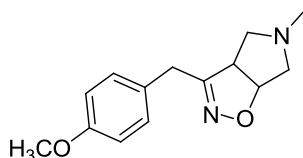
White solid, 31% yield; mp (EtOH/Et<sub>2</sub>O) 122–123 °C; free base. <sup>1</sup>H NMR (300 MHz, CDCl<sub>3</sub>):  $\delta$  7.37–7.16 (m, 5H), 4.97 (dd,  $J = 4.6, 9.3$  Hz, 1H), 3.89 (d,  $J = 15.1$  Hz, 1H), 3.50 (d,  $J = 15.1$  Hz, 1H), 3.55–3.42 (m, 1H), 3.20 (d,  $J = 10.9$  Hz, 1H), 2.96 (d,  $J = 9.4$  Hz, 1H), 2.31 (s, 3H), 2.26 (dd,  $J = 10.9, 4.6$  Hz, 1H), 2.17 (dd,  $J = 9.4, 7.3$  Hz, 1H). ESI-MS  $m/z$ : 217 (M+H)<sup>+</sup>.

**6i: 5-methyl-3-(4-nitrobenzyl)-4,5,6,6a-tetrahydro-3aH-pyrrolo[3,4-d]isoxazole hydrochloride**

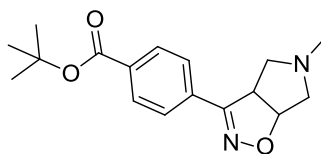


Pale-yellow solid, 40% yield; mp (EtOH/Et<sub>2</sub>O) 239–240 °C (decomp); free base. <sup>1</sup>H NMR (300 MHz, CDCl<sub>3</sub>): δ 8.20 (d, J = 8.5 Hz, 2H), 7.45 (d, J = 8.5 Hz, 2H), 5.03 (dd, J = 9.3, 4.6 Hz, 1H), 3.93 (d, J = 15.5 Hz, 1H), 3.64 (d, J = 15.5 Hz, 1H), 3.55–3.45 (m, 1H), 3.23 (d, J = 10.9 Hz, 1H), 2.94 (d, J = 9.7 Hz, 1H), 2.31 (s, 3H), 2.27 (dd, J = 10.9, 4.6 Hz, 1H), 2.20 (dd, J = 9.7, 7.2 Hz, 1H). ESI-MS *m/z*: 262 (M+H)<sup>+</sup>.

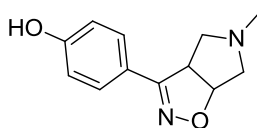
**6j: 3-(4-methoxybenzyl)-5-methyl-4,5,6,6a-tetrahydro-3aH-pyrrolo-[3,4-d]isoxazole oxalate**



White solid, 34% yield; mp (Et<sub>2</sub>O/EtOH) 138–140 °C; free base. <sup>1</sup>H NMR (300 MHz, CDCl<sub>3</sub>): δ 7.14 (d, J = 8.4 Hz, 2H), 6.83 (d, J = 8.4 Hz, 2H), 4.94 (dd, J = 9.2, 4.6 Hz, 1H), 3.86–3.75 (m, 1H), 3.77 (s, 3H), 3.53–3.39 (m, 2H), 3.17 (d, J = 10.9 Hz, 1H), 2.93 (d, J = 9.4 Hz, 1H), 2.29 (s, 3H), 2.23 (dd, J = 10.9, 4.6 Hz, 1H), 2.14 (dd, J = 9.4, 7.4 Hz, 1H). ESI-MS *m/z*: 247 (M+H)<sup>+</sup>.

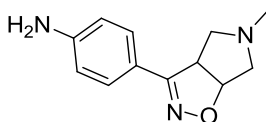
**6l: 5-methyl-3-(4-(tert-butoxycarbonyl)phenyl)-4,5,6,6a-tetrahydro-3aH-pyrrolo[3,4-d]isoxazole**

Colorless oil, 45% yield.  $^1\text{H}$  NMR (300 MHz,  $\text{CDCl}_3$ ):  $\delta$  8.00 (d,  $J = 8.8$  Hz, 2H), 7.70 (d,  $J = 8.8$  Hz, 2H), 5.25 (dd,  $J = 9.6, 4.4$  Hz, 1H), 4.22–4.15 (m, 1H), 3.28 (d,  $J = 11.0$  Hz, 1H), 3.06 (d,  $J = 9.3$  Hz, 1H), 2.51 (dd,  $J = 9.3, 7.4$  Hz, 1H), 2.45 (dd,  $J = 11.0, 4.4$  Hz, 1H), 2.32 (s, 3 H), 1.58 (s, 9 H). ESI-MS  $m/z$ : 303 ( $\text{M}+\text{H}$ ) $^+$ .

**6g: 3-(4-hydroxyphenyl)-5-methyl-4,5,6,6a-tetrahydro-3aH-pyrrolo[3,4-d]isoxazole**

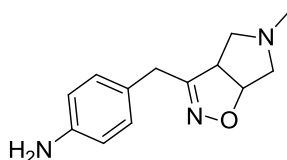
Deprotection of compound **6d** (70.0 mg, 0.19 mmol) according to the procedure used for **5g** yielded the title compound as a white solid (40.5 mg, 95%), which was recrystallized from EtOAc/hexane; mp 126–127 °C.  $^1\text{H}$  NMR (300 MHz,  $\text{DMSO}-d_6$ ):  $\delta$  9.87 (s, 1H), 7.46 (d,  $J = 8.5$  Hz, 2H), 6.79 (d,  $J = 8.5$  Hz, 2H), 5.05 (dd,  $J = 9.4, 4.3$  Hz, 1H), 4.25–4.20 (m, 1H), 3.01 (d,  $J = 10.8$  Hz, 1H), 2.85 (d,  $J = 9.5$  Hz, 1H), 2.33 (dd,  $J = 9.5, 7.4$  Hz, 1H), 2.25 (dd,  $J = 10.8, 4.3$  Hz, 1H), 2.15 (s, 3H). ESI-MS  $m/z$ : 219 ( $\text{M}+\text{H}$ ) $^+$ .

**6f:** 3-(4-aminophenyl)-5-methyl-4,5,6,6a-tetrahydro-3aH-pyrrolo[3,4-*d*]isoxazole hydrochloride



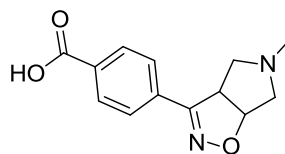
Reduction of compound **6b** (0.14 g, 0.55 mmol) according to the procedure used for **5l** yielded the free amine (0.10 g, 85%), which was converted to the hydrochloride salt following the general procedure described for compounds **5a,b**, and **5h-j**. White solid; mp (EtOH/Et<sub>2</sub>O) 211–212 °C (decomp); free base. <sup>1</sup>H NMR (300 MHz, CDCl<sub>3</sub>): δ 7.47 (d, J = 8.5 Hz, 2H), 6.67 (d, J = 8.5 Hz, 2H), 5.15 (dd, J = 9.3, 4.4 Hz, 1H), 4.15–4.08 (m, 1H), 3.87 (br s, 2H), 3.22 (d, J = 10.7 Hz, 1H), 3.06 (d, J = 9.6 Hz, 1H), 2.55–2.40 (m, 2H), 2.32 (s, 3H). ESIMS *m/z*: 218 (M+H)<sup>+</sup>.

**6k:** 3-(4-aminobenzyl)-5-methyl-4,5,6,6a-tetrahydro-3aH-pyrrolo[3,4-*d*]isoxazole oxalate



Reduction of compound **6i** (0.14 g, 0.54 mmol) according to the procedure used for **5f** yielded the free amine (0.10 g, 83%), which was converted to the oxalate salt following the general procedure described for compound **6j**. White solid; mp (EtOH/Et<sub>2</sub>O) 164–165 °C; free base. <sup>1</sup>H NMR (300 MHz, CDCl<sub>3</sub>): δ 7.02 (d, J = 8.5 Hz, 2H), 6.64 (d, J = 8.5 Hz, 2H), 4.96 (dd, J = 9.3, 4.6 Hz, 1H), 3.77 (d, J = 15.1 Hz, 1H), 3.64 (br s, 2H), 3.49 (dd, 9.3, 7.5 Hz, 1H), 3.38 (d, J = 15.1 Hz, 1H), 3.19 (d, J = 10.9 Hz, 1H), 2.94 (d, J = 9.7 Hz, 1H), 2.31 (s, 3H), 2.31–2.25 (m, 1H), 2.18 (dd, J = 9.7, 7.5 Hz, 1H). ESI-MS *m/z*: 232 (M+H)<sup>+</sup>.

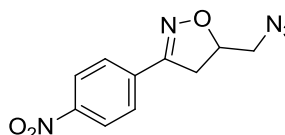


**6e: 3-(4-carboxyphenyl)-5-methyl-4,5,6,6a-tetrahydro-3aH-pyrrolo[3,4-d]isoxazole**

Deprotection of compound **6i** (0.20 g, 0.66 mmol) according to the procedure used for **5e** yielded the title compounds (0.16 g, 99%). White solid; mp (methanol/H<sub>2</sub>O) 255–257 °C (decomp). <sup>1</sup>H NMR (300 MHz, DMSO-*d*<sub>6</sub>): δ 10.20 (br s, 1H), 8.02 (d, J = 8.5 Hz, 2 H), 7.84 (d, J = 8.5 Hz, 2H), 5.50 (dd, J = 9.6, 4.4 Hz, 1H), 4.82–4.70 (m, 1H), 3.98–3.80 (m, 1H), 3.78–3.60 (m, 1H), 3.58–3.25 (m, 2H), 2.78 (s, 3H). ESI-MS *m/z*: 247 (M+H)<sup>+</sup>.

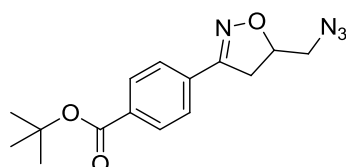
**General procedure for the synthesis of 5-(azidomethyl)-3-(4-substitutedphenyl)-4,5-dihydroisoxazoles (14)**

To a solution of methanesulfonates **9** (6.67 mmol) in dry DMF (13 mL) sodium azide (1.30 g, 19.9 mmol) was added. The reaction mixture was stirred at 80 °C for 3h and then water (20 mL) was added. The aqueous layer was extracted with EtOAc (3 × 20 mL). The combined organic phases were washed with NaHCO<sub>3</sub> saturated aqueous (20 mL) and brine (20 mL), dried (Na<sub>2</sub>SO<sub>4</sub>), filtered, and concentrated in vacuo to give the desired which was used without further purification in the subsequent reaction.

**14a: 5-(azidomethyl)-3-(4-nitrophenyl)-4,5-dihydroisoxazole**

Yellow solid, 90% yield; mp 109–111 °C.  $^1\text{H}$  NMR (300 MHz,  $\text{CDCl}_3$ ):  $\delta$  8.28 (d,  $J = 8.8$  Hz, 2H), 7.85 (d,  $J = 8.8$  Hz, 2H), 5.04–5.00 (m, 1H), 3.63 (dd,  $J = 11.1, 4.3$  Hz, 1H), 3.53–3.42 (m, 2H), 3.27 (dd,  $J = 16.8, 7.3$  Hz, 1H). ESI-MS  $m/z$ : 248 ( $\text{M}+\text{H}$ ) $^+$ .

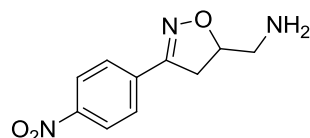
**14b: tert-butyl 4-(5-(azidomethyl)-4,5-dihydroisoxazol-3-yl)benzoate**



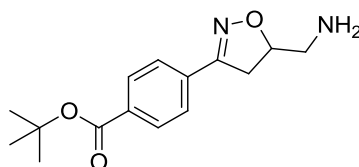
Yellow solid, 92% yield; mp 82–84 °C.  $^1\text{H}$  NMR (300 MHz,  $\text{CDCl}_3$ ):  $\delta$  8.02 (d,  $J = 8.1$  Hz, 2H), 7.71 (d,  $J = 8.1$  Hz, 2H), 5.03–4.84 (m, 1H), 3.57 (dd,  $J = 12.9, 4.4$  Hz, 1H), 3.52–3.39 (m, 2H), 3.24 (dd,  $J = 16.7, 7.2$  Hz, 1H), 1.60 (s, 9H). ESI-MS  $m/z$ : 303 ( $\text{M}+\text{H}$ ) $^+$ .

**General procedure for the synthesis of 5-(aminomethyl)-3-(4-substitutedphenyl)-4,5-dihydroisoxazoles (15)**

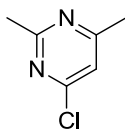
To a solution of azides **14** (8.09 mmol) and water (2 mL) in MeOH (160 mL), triphenylphosphine (3.18 g, 12.1 mmol) was added. The reaction mixture was stirred at room temperature for 12h and then methanol was evaporated. The mixture was diluted with 1N HCl (30 mL), and washed with hexane ( $3 \times 20$  mL). The aqueous phase was basified with  $\text{NaHCO}_3$  and extracted with EtOAc ( $3 \times 30$  mL). The combined organic phases were washed with brine (10 mL), dried ( $\text{Na}_2\text{SO}_4$ ), filtered, and concentrated in vacuo to give the corresponding amine, which was used for the next steps without further purification.

**15a: (3-(4-nitrophenyl)-4,5-dihydroisoxazol-5-yl)methanamine**

Yellow solid, 73% yield; mp 156–158 °C.  $^1\text{H}$  NMR (300 MHz,  $\text{CDCl}_3$ ):  $\delta$  8.26 (d,  $J = 8.8$  Hz, 2H), 7.84 (d,  $J = 8.8$  Hz, 2H), 4.95–4.87 (m, 1H), 3.40 (dd,  $J = 16.6, 10.7$  Hz, 1H), 3.23 (dd,  $J = 16.6, 7.9$  Hz, 1H), 3.07 (dd,  $J = 13.4, 3.6$  Hz, 1H), 2.91 (dd,  $J = 13.4, 5.7$  Hz, 1H), 1.40 (br s, 2H). ESI-MS  $m/z$ : 222 ( $\text{M}+\text{H}$ ) $^+$ .

**15b: *tert*-butyl 4-(5-(aminomethyl)-4,5-dihydroisoxazol-3-yl)benzoate**

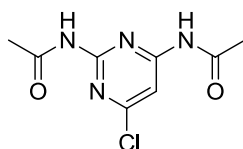
Yellow solid, 82% yield; mp 110–112 °C.  $^1\text{H}$  NMR (300 MHz,  $\text{CDCl}_3$ ):  $\delta$  7.98 (d,  $J = 8.8$  Hz, 2H), 7.65 (d,  $J = 8.8$  Hz, 2H), 5.07–5.01 (m, 1H), 4.78 (br s, 2H), 3.40 (dd,  $J = 16.6, 10.7$  Hz, 1H), 3.23 (dd,  $J = 16.6, 7.9$  Hz, 1H), 3.00–2.88 (m, 2H), 1.59 (s, 9H). ESI-MS  $m/z$ : 277 ( $\text{M}+\text{H}$ ) $^+$ .

**Synthesis of 4-chloropyrimidines 22 and 24****22: 4-chloro-2,6-dimethylpyridine**

Triphenylphosphine (0.84 g, 1.60 mmol) and NCS (0.21 g, 1.60 mmol) were dissolved in dry 1,4-dioxane (5 mL) at room temperature in a 10 mL CEM pressure vessel equipped with a stirrer bar. After 30 minutes, 4-hydroxy-2,6-dimethylpyridine (0.10 g, 0.80 mmol) was added, and the vial was sealed

and heated in a CEM Discover microwave synthesizer to 105 °C (measured by the vertically focused IR temperature sensor) for 15 min. The mixture was basified with triethylamine (1 mL) and the solvent was evaporated. The crude material was purified by silica gel column chromatography (hexane/EtOAc 7:3) to give the desired product. Pale-yellow oil, 87% yield. <sup>1</sup>H NMR (300 MHz, CDCl<sub>3</sub>): δ 7.04 (s, 1H); 2.69 (s, 3H); 2.48 (s, 3H). ESI-MS *m/z*: 143 (M+H)<sup>+</sup>; 145 (30%) (M+2H)<sup>+</sup>.

**24: *N,N'*-(4-chloropyrimidine-2,6-diyl)diacetamide**



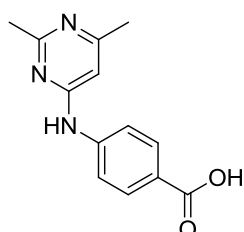
A suspension of 2,6-diamino-4-chloropyrimidine (1.00 g, 6.92 mmol) in acetic anhydride (5 mL) was refluxed for 3h. The solvent was removed and 10 mL of methanol were added. The yellow suspension was stirred at room temperature for 1h. The solvent was removed under reduced pressure, then 10 mL of water were added. The mixture was basified with 5% Na<sub>2</sub>CO<sub>3</sub> to pH 8. The solid was filtered and washed with cold water. Yellow solid, 90% yield; mp 244–246 °C. <sup>1</sup>H NMR (300 MHz, DMSO-*d*<sub>6</sub>): δ 10.95 (s, 1H); 10.63 (s, 1H); 7.74 (s, 1H); 2.19 (s, 3H); 2.15 (s, 3H). ESI-MS *m/z*: 229 (M+H)<sup>+</sup>; 231 (30%) (M+2H)<sup>+</sup>.

**General procedure for the synthesis of pyrimidin-amino benzoic acids (25-27)**

The proper 6-chloropyrimidine (0.88 mmol) and *p*-aminobenzoic acid (0.14 g, 1.06 mmol) were dissolved in 2-propanol (1 mL) at room temperature in a 10 mL CEM pressure vessel equipped with a stirrer bar. The vial was sealed and heated in a CEM Discover microwave synthesizer to 120 °C (measured by the vertically focused IR temperature sensor) for 30 min. The suspension was

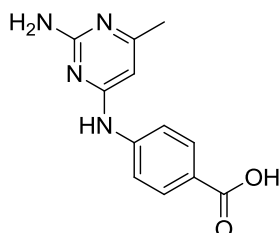
filtered off, and washed with 2-propanol and acetone to give the corresponding product.

**25: 4-((2,6-dimethylpyrimidin-4-yl)amino)benzoic acid**



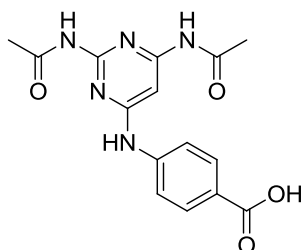
White solid, 99% yield; mp 348–350 °C (decomp.);  $^1\text{H}$  NMR (300 MHz, DMSO- $d_6$ ):  $\delta$  11.52 (br s, 1H); 8.00–7.95 (m, 2H); 7.90–7.79 (m, 2H); 6.92 (s, 1H); 3.74 (s, 1H); 2.59 (s, 3H); 2.44 (s, 3H). ESI-MS  $m/z$ : 244 (M+H) $^+$ .

**26: 4-((2-amino-6-methylpyrimidin-4-yl)amino)benzoic acid**



White solid, 99% yield; mp 340–342 °C (decomp.);  $^1\text{H}$  NMR (300 MHz, DMSO- $d_6$ ):  $\delta$  12.89 (m, 2H); 10.92 (s, 1H); 8.25–7.75 (m, 4H); 6.27 (s, 1H); 2.30 (s, 3H). ESI-MS  $m/z$ : 245 (M+H) $^+$ .

**27: 4-((2,6-diacetamidopyrimidin-4-yl)amino)benzoic acid**

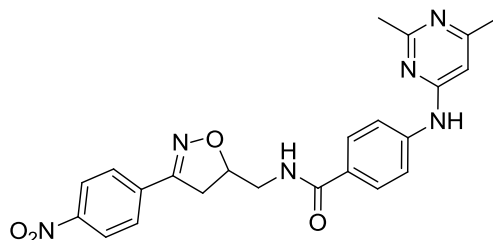


For the synthesis of **27**, the vial was heated to 120 °C for 1.5h. Pale-yellow solid, 99% yield; mp 345–347 °C (decomp.); <sup>1</sup>H NMR (300 MHz, DMSO-*d*<sub>6</sub>): δ 11.87 (s, 1H); 11.61 (s, 1H); 11.06 (s, 1H); 8.10–7.74 (m, 4H); 6.86 (s, 1H); 2.27 (s, 3H); 2.20 (s, 3H). ESI-MS *m/z*: 230 (M+H)<sup>+</sup>.

**General procedure for the synthesis of 4-((2,6-substitutedpyrimidin-4-yl)amino)-*N*-((3-(4-substitutedphenyl)-4,5-dihydroisoxazol-5-yl)methyl)benzamides (16-19)**

To a solution of amines **15** (0.27 mmol) in dry 1:2 DMF/THF (1.5 mL), a mixture of 4-(2,6-substitutedpyrimidin-4-ylamino)benzoic acids **25-27** (0.27 mmol), HOBt (10 mg, 0.65 mmol), HBTU (10 mg, 0.65 mmol), and DIPEA (*N,N*-Diisopropylethylamine) (0.23 mL, 1.29 mmol), in dry 1:3 DMF/THF (6.0 mL) was added dropwise at room temperature. The reaction mixture was stirred for 12h at room temperature and the solvents were then removed under vacuum. The residue was taken up with EtOAc (20 mL) and washed with NaHCO<sub>3</sub> saturated aqueous solution (2 × 20 mL) and brine (20 mL). The organic phase was dried (Na<sub>2</sub>SO<sub>4</sub>), filtered, and concentrated in vacuo. The residue was purified by silica gel chromatography (CH<sub>2</sub>Cl<sub>2</sub>/MeOH) to give the title compound.

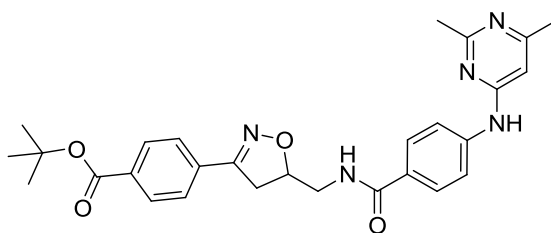
**16a: 4-((2,6-dimethylpyrimidin-4-yl)amino)-*N*-((3-(4-nitrophenyl)-4,5-dihydroisoxazol-5-yl)methyl)benzamide**



White solid, 80% yield; mp 287–289 °C (decomp.). <sup>1</sup>H NMR (300 MHz, DMSO-*d*<sub>6</sub>): δ 9.67 (s, 1H), 8.62 (t, *J* = 5.7 Hz, 1H), 8.30 (d, *J* = 8.6 Hz, 2H),

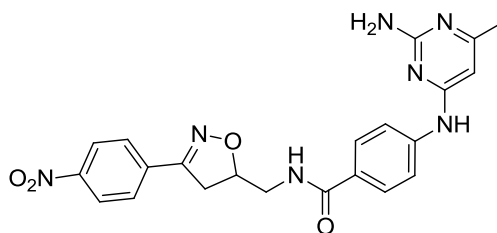
7.93 (d,  $J = 8.6$  Hz, 2H), 7.82 (d,  $J = 8.6$  Hz, 2H), 7.76 (d,  $J = 8.6$  Hz, 2H), 6.50 (s, 1H), 5.02–4.96 (m, 1H), 3.65–3.25 (m, 4H), 2.44 (s, 3H), 2.27 (s, 3H). ESI-MS  $m/z$ : 447 (M+H)<sup>+</sup>.

**16b:** *tert*-butyl 4-(5-((4-((2,6-dimethylpyrimidin-4-yl)amino)benzamido)methyl)-4,5-dihydroisoxazol-3-yl)benzoate



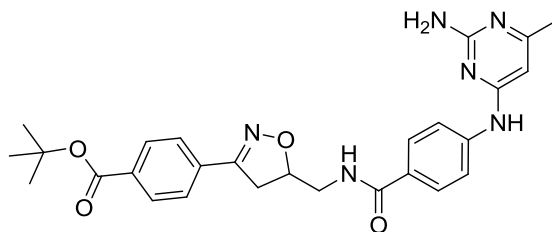
White solid, 80% yield; mp 228–230 °C. <sup>1</sup>H NMR (300 MHz, CDCl<sub>3</sub>):  $\delta$  7.95 (d,  $J = 7.8$  Hz, 2H), 7.73 (d,  $J = 7.8$  Hz, 2H), 7.64 (d,  $J = 7.8$  Hz, 2H), 7.46 (d,  $J = 7.8$  Hz, 2H), 7.40 (s, 1H), 6.77 (t,  $J = 5.5$  Hz, 1H), 6.41 (s, 1H), 5.01–4.92 (m, 1H), 3.83–3.67 (m, 2H), 3.43 (dd,  $J = 16.8, 10.7$  Hz, 1H), 3.18 (dd,  $J = 16.8, 7.2$  Hz, 1H), 2.52 (s, 3H), 2.31 (s, 3H), 1.56 (s, 9H). ESI-MS  $m/z$ : 500 (M+H)<sup>+</sup>.

**17a:** 4-((2-amino-6-methylpyrimidin-4-yl)amino)-N-((3-(4-nitrophenyl)-4,5-dihydroisoxazol-5-yl)methyl)benzamide



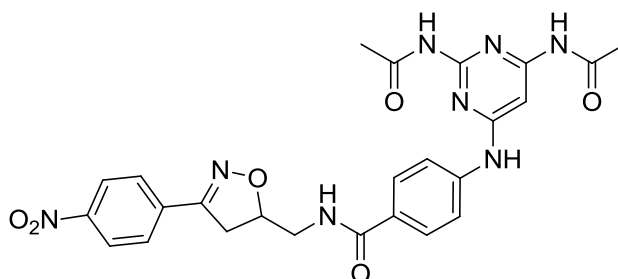
Pale-yellow solid, 71% yield; mp 245–248 °C (decomp.). <sup>1</sup>H NMR (300 MHz, DMSO-*d*<sub>6</sub>):  $\delta$  9.29 (s, 1H), 8.57 (t,  $J = 5.7$  Hz, 1H), 8.30 (d,  $J = 8.9$  Hz, 2H), 7.92 (d,  $J = 8.9$  Hz, 2H), 7.81–7.74 (m, 4H), 6.27 (s, 2H), 5.93 (s, 1H), 5.01–4.96 (m, 1H), 3.63–3.49 (m, 4H), 2.10 (s, 3H). ESI-MS  $m/z$ : 448 (M+H)<sup>+</sup>.

**17b:** *tert*-butyl 4-(5-((4-((2-amino-6-methylpyrimidin-4-yl)amino)benzamido)methyl)-4,5-dihydroisoxazol-3-yl)benzoate



Pale-yellow solid, 73% yield; mp 218–220 °C.  $^1\text{H}$  NMR (300 MHz, DMSO- $d_6$ ):  $\delta$  9.24 (s, 1H), 8.56 (t,  $J$  = 5.5 Hz, 1H), 7.98 (d,  $J$  = 8.2 Hz, 2H), 7.85–7.76 (m, 6H), 6.25 (s, 2H), 5.94 (s, 1H), 5.00–4.88 (m, 1H), 3.64–3.32 (m, 4H), 2.11 (s, 3H), 1.55 (s, 9H). ESI-MS  $m/z$ : 503 (M+H) $^+$ .

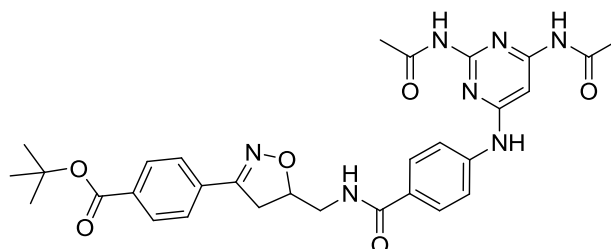
**18a:**  $N,N'$ -(6-((4-(((3-(4-nitrophenyl)-4,5-dihydroisoxazol-5-yl)methyl)carbamoyl)phenyl)amino)pyrimidine-2,4-diyl)diacetamide



White solid, 74% yield; mp 280–282 °C.  $^1\text{H}$  NMR (300 MHz, DMSO- $d_6$ ):  $\delta$  10.26 (s, 1H); 10.03 (s, 1H); 9.85 (s, 1H); 8.56 (t,  $J$  = 5.5 Hz, 1H); 8.32 (d,  $J$  = 8.4 Hz, 2H); 7.99–7.93 (m, 4H); 7.80 (d,  $J$  = 8.4 Hz, 2H); 7.32 (s, 1H); 5.15–4.91 (m, 1H); 3.70–3.32 (m, 4H); 2.24 (s, 3H); 2.14 (s, 3H). ESI-MS  $m/z$ : 533 (M+H) $^+$ .

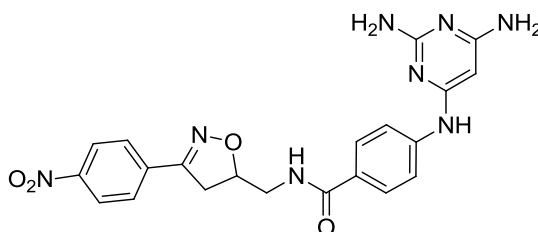


**18b:** *tert*-butyl 4-(5-((4-((2,6-diacetamidopyrimidin-4-yl)amino)benzamido)methyl)-4,5-dihydroisoxazol-3-yl)benzoate



White solid, 73% yield; mp 235–237 °C.  $^1\text{H}$  NMR (300 MHz,  $\text{DMSO-}d_6$ ):  $\delta$  10.25 (s, 1H); 10.02 (s, 1H); 9.83 (s, 1H); 8.59 (t,  $J = 5.5$  Hz, 1H); 8.03–7.91 (m, 4H); 7.86–7.71 (m, 4H); 7.30 (s, 1H); 5.06–4.79 (m, 1H); 3.72–3.43 (m, 4H); 2.22 (s, 3H); 2.12 (s, 3H); 1.55 (s, 9H). ESI-MS  $m/z$ : 588 ( $\text{M}+\text{H}$ ) $^+$ .

**Synthesis of 4-((2,6-diaminopyrimidin-4-yl)amino)-*N*-((3-(4-nitrophenyl)-4,5-dihydroisoxazol-5-yl)methyl)benzamide (19a)**



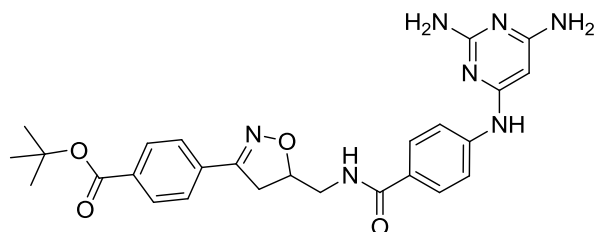
To a suspension of **18a** (0.21 g, 0.40 mmol) in EtOH (6.7 mL), 7.7 mL of NaOH 1M were added. The mixture was stirred at reflux for 4h, then  $\text{H}_2\text{O}$  (30 ml) was added and the solution was acidified with diluted  $\text{H}_3\text{PO}_4$  to pH 4-5. The aqueous phase was washed with EtOAc (3 x 10 ml) and basified with NaOH 2N. The suspension was filtered off to recover the pale-yellow solid (0.12 g, 70%); mp 227–229 °C.  $^1\text{H}$  NMR (300 MHz,  $\text{DMSO-}d_6$ ):  $\delta$  8.81 (s, 1H); 8.51 (t,  $J = 4.7$  Hz, 1H); 8.30 (d,  $J = 8.5$  Hz, 2H); 7.92 (d,  $J = 8.5$  Hz,

2H); 7.79–7.61 (m, 4H); 5.71 (br s, 2H); 5.87 (br s, 2H); 5.23 (s, 1H); 5.07–4.81 (m, 1H); 3.67–3.40 (m, 4H). ESI-MS  $m/z$ : 449 (M+H)<sup>+</sup>.

**Synthesis of *tert*-butyl 4-(5-((4-((2,6-diaminopyrimidin-4-yl)amino)benzamido)methyl)-4,5-dihydroisoxazol-3-yl)benzoate and its acid (19b and 19c)**

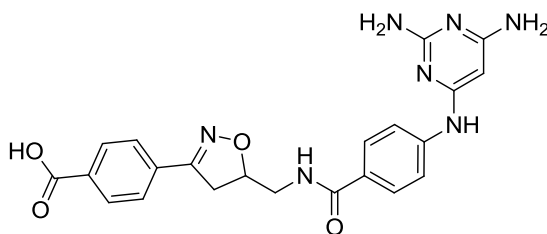
To a suspension of **18b** (0.21 g, 0.40 mmol) in EtOH (6.7 mL), 7.7 mL of NaOH 1M were added. The mixture was stirred at room temperature for 4h, then H<sub>2</sub>O (30 ml) was added and the solution was acidified with diluted H<sub>3</sub>PO<sub>4</sub> to pH 4-5. The aqueous phase was extracted with EtOAc (3 x 10 ml), dried (Na<sub>2</sub>SO<sub>4</sub>), and filtered. The solvent was concentrated in vacuo and the residue was purified by silica gel chromatography (CH<sub>2</sub>Cl<sub>2</sub>/MeOH) to give the title compound.

**19b: *tert*-butyl 4-(5-((4-((2,6-diaminopyrimidin-4-yl)amino)benzamido)methyl)-4,5-dihydroisoxazol-3-yl)benzoate**



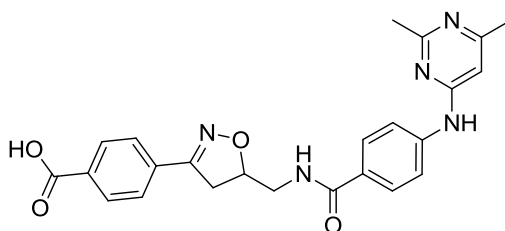
White solid, 43% yield; mp 206–208 °C. <sup>1</sup>H NMR (300 MHz, DMSO-*d*<sub>6</sub>):  $\delta$  8.84 (s, 1H); 8.50 (t, J = 5.1 Hz, 1H); 7.96 (d, J = 8.2 Hz, 2H); 7.77 (d, J = 8.2 Hz, 2H); 7.75 – 7.62 (m, 4H); 5.92 (br s, 2H); 5.77 (br s, 2H); 5.24 (s, 1H); 4.99–4.86 (m, 1H); 3.62–3.38 (m, 4H); 1.55 (s, 9H). ESI-MS  $m/z$ : 504 (M+H)<sup>+</sup>.

**19c: 4-(5-((4-((2,6-diaminopyrimidin-4-yl)amino)benzamido)methyl)-4,5-dihydroisoxazol-3-yl)benzoic acid**



Derivative **19c** is obtained by partial hydrolysis of *tert*-butyl ester **19b** during the deprotection reaction. The product was recovered by acidification of the aqueous phase with HCl 1N and filtration of the white precipitate (40%); mp 283–285 °C. <sup>1</sup>H NMR (300 MHz, DMSO-*d*<sub>6</sub>): δ 13.14 (s, 1H); 11.47 (s, 1H); 9.90 (s, 1H); 8.67 (t, J = 5.3 Hz, 1H); 8.00 (d, J = 8.2 Hz, 2H); 7.80 (dd, J = 13.9, 8.2 Hz, 4H); 7.68 (d, J = 8.2 Hz, 2H); 7.60 (br s, 2H); 7.41 (br s, 2H); 5.42 (s, 1H); 5.14–4.82 (m, 1H); 3.67–3.40 (m, 4H). ESI-MS *m/z*: 448 (M+H)<sup>+</sup>.

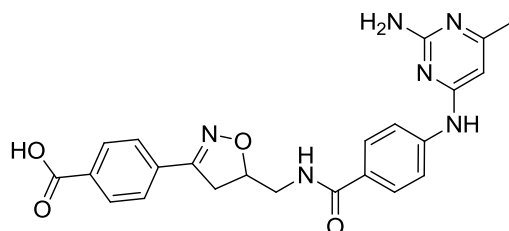
**Synthesis of 4-(5-((4-((2,6-dimethylpyrimidin-4-yl)amino)benzamido)methyl)-4,5-dihydroisoxazol-3-yl)benzoic acid (17c)**



A mixture of TFA and DCM (1:3, 8 mL) was added to compound **17b** (60 mg, 0.12 mmol). The reaction was stirred at room temperature overnight and then concentrated in vacuo to give the title compound as a white solid (50 mg, 99%) which was recrystallized from ethanol/Et<sub>2</sub>O. Mp 295–298 °C (decomp.). <sup>1</sup>H NMR (300 MHz, DMSO-*d*<sub>6</sub>): δ 10.78 (br s, 1H), 8.72 (t, J = 5.2 Hz, 1H); 8.00 (d, J = 8.2 Hz, 2H), 7.89 (d, J = 8.2 Hz, 2H), 7.83–7.65 (m, 4H), 6.72 (s,

1H); 5.09–4.80 (m, 1H), 3.67–3.43 (m, 4H), 2.55 (s, 3H); 2.41 (s, 3H). ESI-MS  $m/z$ : 446 (M+H)<sup>+</sup>.

**Synthesis of 4-(5-((4-((2-amino-6-methylpyrimidin-4-yl)amino)benzamido)methyl)-4,5-dihydroisoxazol-3-yl)benzoic acid (18c)**



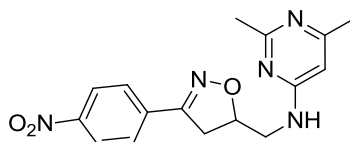
A mixture of TFA and DCM (1:3, 9 mL) was added to compound **18b** (70 mg, 0.14 mmol). The reaction was stirred at room temperature overnight and then concentrated in vacuo to give the title compound as a white solid (50 mg, 99%) which was recrystallized from ethanol/Et<sub>2</sub>O. Mp 255–258 °C (decomp.). <sup>1</sup>H NMR (300 MHz, DMSO-*d*<sub>6</sub>):  $\delta$  10.50 (br s, 1H), 8.72 (t, *J* = 5.2 Hz, 1H); 8.00 (d, *J* = 8.2 Hz, 2H), 7.85 (dd, *J* = 13.9, 8.1 Hz, 4H), 7.78 (d, *J* = 8.2 Hz, 2H), 6.15 (s, 1H); 5.17–4.77 (m, 1H), 3.77–3.39 (m, 4H), 2.29 (s, 3H). ESI-MS  $m/z$ : 447 (M+H)<sup>+</sup>.

**General procedure for the synthesis of 2,6-substituted-*N*-((3-(4-substitutedphenyl)-4,5-dihydroisoxazol-5-yl)methyl)pyrimidin-4-amine (20-21)**

The proper amine **15** (0.36 mmol) and 6-chloropyrimidine (0.30 mmol) were dissolved in 2-propanol (3 mL) at room temperature in a 3 CEM pressure vessels equipped with a stirrer bar. The vials were sealed and heated in a CEM Discover microwave synthesizer to 180 °C (measured by the vertically focused IR temperature sensor) for 30 min. The solvent was evaporated, the crude material was taken up with EtOAc (20 mL), washed with NaHCO<sub>3</sub> saturate aqueous solution (3 x 10 mL) and with brine (10 mL), dried (Na<sub>2</sub>SO<sub>4</sub>),

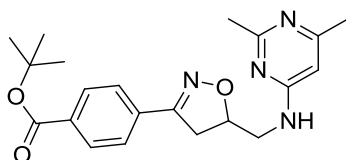
filtered and concentrated in vacuo. The residue was purified by silica gel chromatography (CH<sub>2</sub>Cl<sub>2</sub>/MeOH) to give the title compound.

**20a: 2,6-dimethyl-N-((3-(4-nitrophenyl)-4,5-dihydroisoxazol-5-yl)methyl)pyrimidin-4-amine**



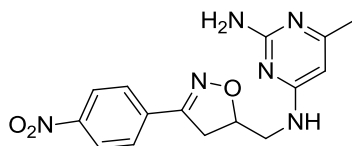
Pale-yellow solid, 80% yield; mp 129–131 °C. <sup>1</sup>H NMR (300 MHz, CDCl<sub>3</sub>): δ 8.26 (d, J = 8.6 Hz, 2H); 7.80 (d, J = 8.6 Hz, 2H); 6.05 (s, 1H); 5.11–5.06 (m, 1H); 5.03–4.98 (m, 1H); 3.79–3.72 (m, 2H); 3.45 (dd, J = 16.7, 10.6 Hz, 1H); 3.21 (dd, J = 16.8, 7.8 Hz, 1H); 2.48 (s, 3H); 2.29 (s, 3H). ESI-MS *m/z*: 328 (M+H)<sup>+</sup>.

**20b: tert-butyl 4-(5-(((2,6-dimethylpyrimidin-4-yl)amino)methyl)-4,5-dihydroisoxazol-3-yl)benzoate**



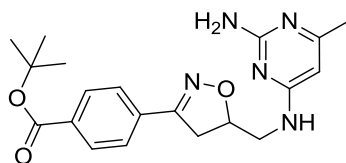
Pale-yellow solid, 80% yield; mp 135–138 °C. <sup>1</sup>H NMR (300 MHz, CDCl<sub>3</sub>): δ 8.01 (d, J = 7.9 Hz, 2H); 7.68 (d, J = 7.9 Hz, 2H); 6.05 (s, 1H); 5.13–4.82 (m, 2H); 3.88–3.60 (m, 2H); 3.45 (dd, J = 16.2, 10.7 Hz, 1H); 3.18 (dd, J = 17.0, 8.2 Hz, 1H); 2.48 (s, 3H); 2.30 (s, 3H); 1.60 (s, 9H). ESI-MS *m/z*: 383 (M+H)<sup>+</sup>.

**21a:** 6-methyl-*N*<sup>4</sup>-((3-(4-nitrophenyl)-4,5-dihydroisoxazol-5-yl)methyl)pyrimidine-2,4-diamine



Pale-yellow solid, 70% yield; mp 159–162 °C. <sup>1</sup>H NMR (300 MHz, CDCl<sub>3</sub>): δ 8.26 (d, J = 8.6 Hz, 2H); 7.81 (d, J = 8.6 Hz, 2H); 5.66 (s, 1H); 5.14–5.00 (m, 3H); 4.87–4.98 (m, 1H); 3.76–3.69 (m, 2H); 3.43 (dd, J = 16.8, 10.7 Hz, 1H); 3.19 (dd, J = 16.8, 7.8 Hz, 1H); 2.18 (s, 3H). ESI-MS *m/z*: 329 (M+H)<sup>+</sup>.

**21b:** *tert*-butyl 4-(5-(((2-amino-6-methylpyrimidin-4-yl)amino)methyl)-4,5-dihydroisoxazol-3-yl)benzoate

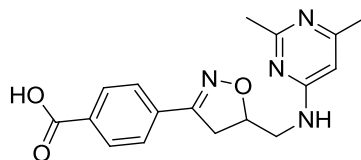


Pale-yellow solid, 67% yield; mp 128–130 °C. <sup>1</sup>H NMR (300 MHz, CDCl<sub>3</sub>): δ 7.98 (d, J = 8.1 Hz, 2H); 7.66 (d, J = 8.1 Hz, 2H); 5.67 (s, 1H); 5.51–5.36 (m, 1H), 5.26–5.12 (m, 2H); 5.06–4.90 (m, 1H); 3.87–3.59 (m, 2H); 3.40 (dd, J = 16.7, 10.7 Hz, 1H); 3.16 (dd, J = 16.8, 7.5 Hz, 1H); 2.18 (s, 3H); 1.59 (s, 9H). ESI-MS *m/z*: 384 (M+H)<sup>+</sup>.

**General procedure for the synthesis of the acids 20c and 21c**

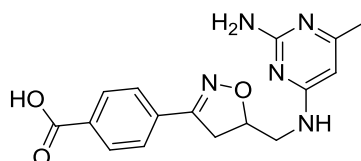
A mixture of TFA and DCM (1:3, 9 mL) was added to compounds **20-21** (0.18 mmol). The reaction was stirred at room temperature overnight and then concentrated in vacuo to give the title compound as a white solid, which was recrystallized from EtOH/Et<sub>2</sub>O.

**20c: 4-(5-(((2,6-dimethylpyrimidin-4-yl)amino)methyl)-4,5-dihydroisoxazol-3-yl)benzoic acid**



White solid, 99% yield; mp 204–207 °C.  $^1\text{H}$  NMR (300 MHz,  $\text{DMSO-}d_6$ ):  $\delta$  9.24 (br s, 1H); 8.01 (d,  $J = 8.2$  Hz, 2H); 7.78 (d,  $J = 8.2$  Hz, 2H); 6.49 (s, 1H); 5.05–4.90 (m, 1H); 3.85–3.65 (m, 1H); 3.60–3.48 (m, 4H); 2.48 (s, 3H); 2.33 (s, 3H). ESI-MS  $m/z$ : 327 ( $\text{M}+\text{H}$ ) $^+$ .

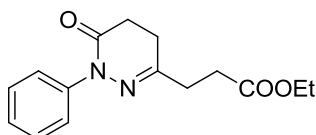
**21c: 4-(5-(((2-amino-6-methylpyrimidin-4-yl)amino)methyl)-4,5-dihydroisoxazol-3-yl)benzoic acid**



White solid, 99% yield; mp 208–210 °C.  $^1\text{H}$  NMR (300 MHz,  $\text{DMSO-}d_6$ ):  $\delta$  8.86 (t,  $J = 5.0$  Hz, 1H); 8.01 (d,  $J = 8.2$  Hz, 2H); 7.78 (d,  $J = 8.2$  Hz, 2H); 7.83–7.25 (m, 2H); 5.95 (s, 1H); 5.15–4.67 (m, 1H); 3.74–3.42 (m, 3H); 3.23 (dd,  $J = 17.2, 7.2$  Hz, 1H); 2.19 (s, 3H). ESI-MS  $m/z$ : 328 ( $\text{M}+\text{H}$ ) $^+$ .

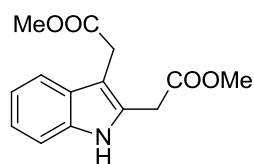
## 7.2. Synthesis of NSC derivatives

### Synthesis of ethyl 3-(6-oxo-1-phenyl-1,4,5,6-tetrahydropyridazin-3-yl)propanoate (28)



A suspension of phenylhydrazine hydrochloride (4.00 g, 27.7 mmol) and diethyl 4-oxopimelate (6.44 g, 27.9 mmol) was heated in toluene (35 mL) under N<sub>2</sub> in a Dean-Stark apparatus until the full consumption of the starting material. After evaporation of the solvent, the residue was purified by flash chromatography on silica gel (CH<sub>2</sub>Cl<sub>2</sub>) to afford the pyridazinone **28** (6.84 g, 90%). Yellowish viscous oil. <sup>1</sup>H NMR (300 MHz, CDCl<sub>3</sub>): δ 7.49 (d, J = 8.0 Hz, 2H); 7.36 (t, J = 8.0 Hz, 2H); 7.21 (t, J = 8.0 Hz, 1H); 4.11 (q, J = 7.0 Hz, 2H); 2.71–2.59 (m, 8H); 1.23 (t, J = 7.0 Hz, 3H). ESI-MS *m/z*: 275 (M+H)<sup>+</sup>.

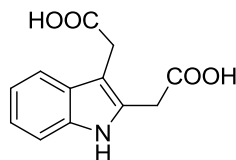
### Synthesis of methyl 3-(3-methoxycarbonylmethyl-1*H*-indol-2-yl)propanoate (**29**)



A solution of **28** (3.13 g, 11.41 mmol) in methanol (50 mL) saturated with HCl gas was heated under reflux with continuous bubbling of HCl for 2h. After evaporation of solvent, the residue was dissolved in CH<sub>2</sub>Cl<sub>2</sub> (50 mL), washed with H<sub>2</sub>O (30 mL), Na<sub>2</sub>CO<sub>3</sub> aqueous saturated solution (30 mL), dried (Na<sub>2</sub>SO<sub>4</sub>) and evaporated to dryness under reduced pressure. The residue was filtered through a short silica gel pad (CH<sub>2</sub>Cl<sub>2</sub>) to give the diester **29** (2.54 g, 81%). White crystals; mp (Et<sub>2</sub>O) 73–74 °C. <sup>1</sup>H NMR (300 MHz, CDCl<sub>3</sub>): δ 8.61 (s, 1H); 7.54 (d, J = 8.0 Hz, 1H); 7.25 (d, J = 8.0 Hz, 1H); 7.13 (t, J = 8.0 Hz, 1H); 7.07 (t, J = 8.0 Hz, 1H); 3.69 (s, 1H); 3.68 (s, 1H); 3.63 (s, 3H); 3.04 (t, J = 7.4 Hz, 2H); 2.68 (t, J = 7.4 Hz, 3H). ESI-MS *m/z*: 262 (M+H)<sup>+</sup>.

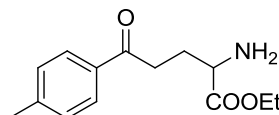


### Synthesis of 3-(3-methoxycarbonylmethyl-1*H*-indol-2-yl)propanoic acid (30)



To a solution of ester **29** (0.07 g, 0.25 mmol) in MeOH (0.5 mL), 0.5 mL of NaOH 1N were added. The solution was stirred for 3h at room temperature. The crude material was concentrated in vacuo and the aqueous phase was washed with Et<sub>2</sub>O (3 x 10 mL). The residue was acidified with HCl 2N. The white precipitate was filtered to obtain the pure product. Glossy white crystals, 99% yield; mp 186–188 °C. <sup>1</sup>H NMR (300 MHz, CDCl<sub>3</sub>): δ 12.47 (br s, 2H); 10.84 (s, 1H); 7.45 (d, J = 8.0 Hz, 1H); 7.31 (d, J = 8.0 Hz, 1H); 7.06 (t, J = 8.0 Hz, 1H); 6.98 (t, J = 8.0 Hz, 1H); 3.65 (s, 2H); 2.98 (t, J = 7.7 Hz, 2H); 2.64 (t, J = 7.7 Hz, 2H). ESI-MS *m/z*: 234 (M+H)<sup>+</sup>.

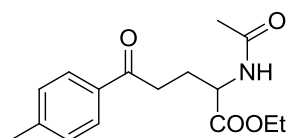
### Synthesis of ethyl 2-amino-5-oxo-5-(*p*-tolyl)pentanoate (31)



A solution of DIPEA (0.39 mL, 2.74 mmol) in dry THF (6 mL) was prepared and cooled to -78 °C, then BuLi (1.6 M sol., 1.72 mL) and DMPU (0.83 mL, 6.85 mmol) were added. After 10 min, a solution of ethyl 2-((diphenylmethylene)amino)acetate (0.73 g, 2.74 mmol) in dry THF (6 mL) was added. After further 10 min, a solution of 3-chloro-1-(*p*-tolyl)propan-1-one (0.50 g, 2.74 mmol) in dry THF (4 mL) was added, and the mixture was stirred at -78 °C. After 2h, the mixture was quenched with NH<sub>4</sub>Cl saturated aqueous solution (50 mL) and extracted with CH<sub>2</sub>Cl<sub>2</sub> (3 x 50 mL). The organic phase was dried (Na<sub>2</sub>SO<sub>4</sub>), filtered and concentrated in vacuo. The crude

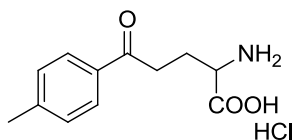
mixture was dissolved in Et<sub>2</sub>O (5 mL) and 5 mL of HCl 2N were added. The solution was basified with solid K<sub>2</sub>CO<sub>3</sub> and extracted with EtOAc (3 x 20 mL). The organic phase was dried, filtered and concentrated in vacuoto obtain the derivative **31** (0.41 g, 60%). White solid, mp (hexane) 49–50 °C. <sup>1</sup>H NMR (300 MHz, CDCl<sub>3</sub>): δ 7.80 (d, J = 7.4 Hz, 2H); 7.24 (d, J = 7.4 Hz, 2H); 4.16 (q, J = 5.9 Hz, 2H); 3.81 (t, J = 7.6 Hz, 1H); 2.86 (t, J = 5.9 Hz, 2H); 2.35 (s, 3H); 2.13 (dq, J = 7.4, 6.1 Hz, 2H); 1.58 (s, 1H); 1.49 (s, 1H); 1.33 (t, J = 5.9 Hz, 3H). ESI-MS *m/z*: 250 (M+H)<sup>+</sup>.

### Synthesis of ethyl 2-amino-5-oxo-5-(*p*-tolyl)pentanoate (**32**)



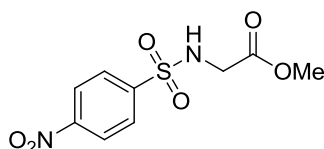
To a solution of **31** (0.41 g, 1.64 mmol) in dry CH<sub>2</sub>Cl<sub>2</sub> (20 mL), acetic anhydride (0.77 mL, 8.20 mmol) was added and the reaction was stirred at reflux. After 4h, 20 mL of HCl 1N were added and the mixture was extracted with CH<sub>2</sub>Cl<sub>2</sub> (3 x 20 mL), dried (Na<sub>2</sub>SO<sub>4</sub>), filtered and concentrated in vacuoto have the desired product **32**. White solid, 99% yield; mp 90–92 °C. <sup>1</sup>H NMR (300 MHz, CDCl<sub>3</sub>): δ 7.78 (d, J = 7.5 Hz, 2H); 7.23 (d, J = 7.4 Hz, 2H); 5.86 (s, 1H); 4.60 (t, J = 7.5 Hz, 1H); 4.19 (q, J = 6.0 Hz, 2H); 2.82 (t, J = 8.1 Hz, 2H); 2.35 (s, 3H); 2.23 – 1.94 (m, 5H); 1.38 (t, J = 6.0 Hz, 3H). ESI-MS *m/z*: 292 (M+H)<sup>+</sup>.

### Synthesis of 2-amino-5-oxo-5-(*p*-tolyl)pentanoic acid hydrochloride (**34**)



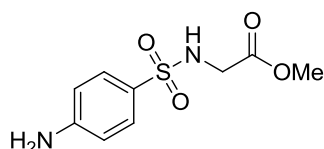
After the dissolution of **32** (0.46 g, 1.60 mmol) in EtOH (2.5 mL), H<sub>2</sub>O (2.5 mL) and Amb. 900 OH (2 equiv) were added. After 3h at room temperature, the resin was filtered off, washed with EtOH and H<sub>2</sub>O, then suspended in HCl 1N. After 30 min at room temperature, the suspension was filtered and the filtrate was concentrated in vacuo and lyophilized to obtain derivative **34**. White solid, 99 % yield; mp 150–152 °C; free base. <sup>1</sup>H NMR (300 MHz, DMSO-*d*<sub>6</sub>): δ 7.75 (d, J = 7.5 Hz, 2H); 7.24 (d, J = 7.5 Hz, 2H); 3.44 (t, J = 7.8 Hz, 1H); 2.79 (t, J = 5.9 Hz, 2H); 2.46 (s, 1H); 2.33 (s, 1H); 2.05 (s, 1H); 2.03–1.89 (m, 2H). ESI-MS *m/z*: 222 (M+H)<sup>+</sup>.

#### Synthesis of methyl 2-(4-nitrophenylsulfonamido)acetate (**35**)



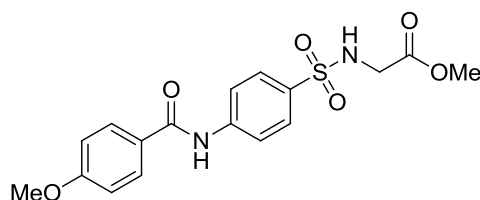
To a solution of 4-nitrobenzene-1-sulfonyl chloride (0.58 g, 2.63 mmol) and GlyOMe·HCl (0.30 g, 2.39 mmol) in dry CH<sub>2</sub>Cl<sub>2</sub> (13 mL), triethylamine (1.2 mL, 8.60 mmol) was added and the mixture was stirred at room temperature for 1.5h. the organic phase was washed with HCl 1N (3x 10 mL), NaHCO<sub>3</sub> aqueous saturated solution (3 x 10 mL) and brine (1 x 10 mL). The organic phase was dried (Na<sub>2</sub>SO<sub>4</sub>), filtered and concentrated in vacuo to give the pure product (0.41 g, 57%). White solid; mp (CH<sub>2</sub>Cl<sub>2</sub>/hexane): 87– 89 °C. <sup>1</sup>H NMR (300 MHz, CDCl<sub>3</sub>): δ 8.44 (d, J = 7.4 Hz, 2H); 8.22 (d, J = 7.4 Hz, 2H); 5.23 (s, 1H); 4.07 (d, J = 19.0 Hz, 2H); 3.76 (s, 3H). ESI-MS *m/z*: 275 (M+H)<sup>+</sup>.

#### Synthesis of methyl 2-(4-aminophenylsulfonamido)acetate (**36**)



Pd/C (5 wt % palladium on activated carbon, 0.1 eq) was added to a solution of **35** (0.31 g, 1.14 mmol) in EtOH (180 mL), and the reaction was stirred under 1 atm of H<sub>2</sub> (balloon) for 2h. The reaction mixture was filtered and, after solvent evaporation, a colourless oil was recollected (0.27 g, 99%). <sup>1</sup>H NMR (300 MHz, CDCl<sub>3</sub>):  $\delta$  7.73 (d, J = 7.4 Hz, 2H); 6.86 (d, J = 7.5 Hz, 2H); 5.60 (s, 2H); 4.97 (s, 1H); 4.07 (d, J = 12.2 Hz, 2H); 3.76 (s, 3H). ESI-MS *m/z*: 245 (M+H)<sup>+</sup>.

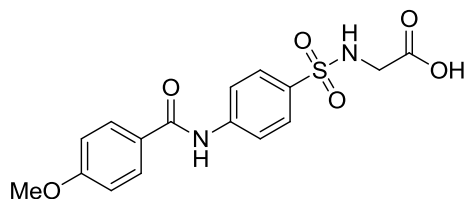
**Synthesis of methyl 2-(4-(4-methoxybenzamido)phenylsulfonamido)acetate (**37**)**



A solution of 4-methoxybenzoic acid (0.10 g, 1.25 mmol) in thionyl chloride (5 mL) was refluxed for 2h under nitrogen atmosphere. After cooling at room temperature, the excess thionyl chloride was removed at reduced pressure and the crude material dried under vacuum. To the residue, dissolved in dry THF (5 mL) and cooled to 0 °C, a mixture of the amine **36** (0.27 g, 1.14 mmol) and triethylamine (0.17 mL, 1.25 mmol) in dry THF (5 mL) was added dropwise. The reaction mixture was stirred at room temperature for 12h, filtered and evaporated. The residue was taken up with EtOAc (20 mL) and washed with NaHCO<sub>3</sub> saturated aqueous solution (2 × 20 mL) and brine (20 mL). The organic phase was dried (Na<sub>2</sub>SO<sub>4</sub>), filtered, and concentrated in vacuo to give the title compound (0.33 g, 77%) as a white solid. Mp (MeOH/Et<sub>2</sub>O) 150– 152 °C. <sup>1</sup>H NMR (300 MHz, CDCl<sub>3</sub>):  $\delta$  8.39 (s, 1H); 8.07 (d, J = 7.4 Hz, 2H); 7.84 (d, J = 7.5 Hz, 2H); 7.77 (d, J = 7.4 Hz, 2H); 7.05 (d, J = 7.5 Hz, 2H); 5.19 (s,

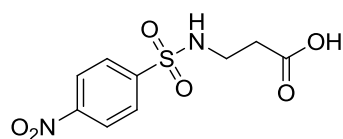
H); 4.10 (d,  $J = 6.3$  Hz, 2H); 3.82 (s, 3H); 3.76 (s, 3H). ESI-MS  $m/z$ : 379 (M+H)<sup>+</sup>.

**Synthesis of 2-(4-(4-methoxybenzamido)phenylsulfonamido)acetic acid (38)**



To a suspension of **37** (0.15 g, 0.39 mmol) in MeOH (10 mL), a solution of LiOH (0.04 g, 1.54 mmol) in H<sub>2</sub>O (10 mL) was added and stirred at room temperature. After 2.5h, the solvent was removed under reduced pressure, taken up with water and washed with CH<sub>2</sub>Cl<sub>2</sub> (3 x 10 mL). The aqueous phase was acidified with HCl 6N to pH 1. The white precipitate was filtered to recover the pure compound. White solid (0.13 g, 90%); mp 178–180 °C. <sup>1</sup>H NMR (300 MHz, DMSO-*d*<sub>6</sub>):  $\delta$  10.46 (s, 1H); 10.20 (s, 1H); 8.04 (d,  $J = 7.5$  Hz, 2H); 7.84 (d,  $J = 7.5$  Hz, 2H); 7.72 (d,  $J = 7.5$  Hz, 2H); 7.04 (d,  $J = 7.4$  Hz, 2H); 5.69 (s, 1H); 4.24 (s, 1H); 4.03 (s, 1H); 3.79 (s, 3H). ESI-MS  $m/z$ : 365 (M+H)<sup>+</sup>.

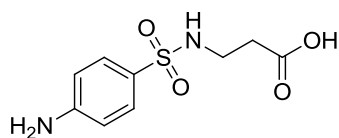
**Synthesis of 3-(4-nitrophenylsulfonamido)propanoic acid (39)**



To a cold solution (0 °C) of  $\beta$ -Alanine (0.30 g, 3.37 mmol) in 1M NaOH (3.5 mL) was added 4-nitrobenzylsulfonyl chloride (0.75 g, 3.37 mmol). The reaction mixture was stirred for 3 h at room temperature. The pH was kept at 9. The crude mixture was then washed with EtOAc (3 x 20 mL). The pH of the

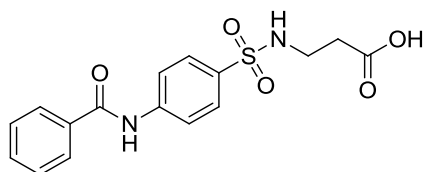
aqueous phase was adjusted to 2 by the addition of 1N HCl. This solution was extracted with EtOAc (3 x 20 mL). The combined organic phases were washed with H<sub>2</sub>O and brine. The organic layer was then dried (Na<sub>2</sub>SO<sub>4</sub>) and the excess solvent removed under reduced pressure. The product (0.35 g, 37%) was afforded as a white solid. Mp: 154–155 °C. <sup>1</sup>H NMR (300 MHz, CDCl<sub>3</sub>): δ 9.50 (s, 1H); 8.40 (d, J = 7.4 Hz, 2H); 8.22 (d, J = 7.5 Hz, 2H); 6.00 (s, 1H); 3.49 (t, J = 5.3 Hz, 1H); 3.43 (t, J = 5.3 Hz, 1H); 2.52 (t, J = 5.3 Hz, 2H). ESI-MS *m/z*: 275 (M+H)<sup>+</sup>.

### Synthesis of 3-(4-aminophenylsulfonamido)propanoic acid (40)



Pd/C (5 wt % palladium on activated carbon, 0.1 eq) was added to a solution of **39** (0.35 g, 1.26 mmol) in EtOH (180 mL), and the reaction was stirred under 1 atm of H<sub>2</sub> (balloon) for 2h. The reaction mixture was filtered and, after solvent evaporation, a colourless oil was recollected (0.30 g, 99%). <sup>1</sup>H NMR (300 MHz, CDCl<sub>3</sub>): δ 9.51 (s, 1H); 7.74 (d, J = 7.5 Hz, 2H); 6.86 (d, J = 7.5 Hz, 2H); 5.66 (s, 2H); 4.28 (s, 1H); 3.55 (t, J = 7.9 Hz, 1H); 3.46 (t, J = 7.9 Hz, 1H); 2.57 (t, J = 7.9 Hz, 2H). ESI-MS *m/z*: 245 (M+H)<sup>+</sup>.

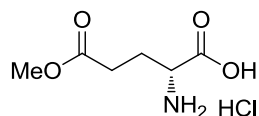
### Synthesis of 3-(4-benzamidophenylsulfonamido)propanoic acid (41)



A solution of benzoic acid (0.08 g, 0.69 mmol) in thionyl chloride (4 mL) was refluxed for 2h under nitrogen atmosphere. After cooling at room temperature, the excess thionyl chloride was removed at reduced pressure and the crude

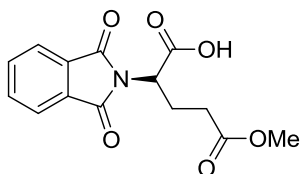
material dried under vacuum. To the residue, dissolved in THF (4 mL) and cooled to 0 °C, a mixture of the amine **40** (0.30 g, 1.26 mmol) in THF (4 mL) and NaHCO<sub>3</sub> (0.11 mL, 1.26 mmol) in H<sub>2</sub>O (8 mL) was added dropwise. The reaction mixture was stirred at reflux for 48 h and evaporated. The residue was taken up with NaOH 2N to pH 10 and washed with EtOAc (3 × 20 mL). The aqueous phase was acidified with HCl 3N to pH 2 and the solid was filtered to obtain the pure product (0.17 g, 70%) as a white solid. Mp 185–187 °C. <sup>1</sup>H NMR (300 MHz, DMSO-*d*<sub>6</sub>): δ 10.87 (s, 1H); 9.77 (s, 1H); 8.07 (d, J = 7.5 Hz, 2H); 7.93–7.80 (m, 2H); 7.61 (d, J = 7.4 Hz, 2H); 7.53–7.31 (m, 3H); 5.27 (s, 1H); 3.57 (t, J = 5.6 Hz, 1H); 3.49 (t, J = 5.6 Hz, 1H); 3.49 (t, J = 5.6 Hz, 1H). ESI-MS *m/z*: 349 (M+H)<sup>+</sup>.

#### Synthesis of (*R*)-2-amino-5-methoxy-5-oxopentanoic acid hydrochloride (**42**)



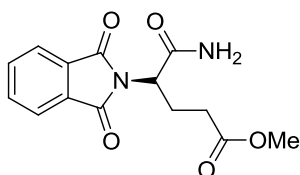
To a cooled suspension (-10 °C) of *D*-glutamic acid (1.00 g, 6.80 mmol) in MeOH (5 mL) thionyl chloride (0.76 mL, 10.9 mmol) was added dropwise. The mixture was stirred at room temperature for 30 min, then Et<sub>2</sub>O (20 mL) was added. The white precipitate was filtered to obtain the pure product (1.34 g, 99%). Mp 257–259 °C. <sup>1</sup>H NMR (300 MHz, DMSO-*d*<sub>6</sub>): δ 12.34 (s, 1H); 3.80 (s, 3H); 3.22 (t, J = 7.4 Hz, 1H); 2.44 (t, J = 7.9 Hz, 2H); 2.24–2.07 (m, 4H). ESI-MS *m/z*: 162 (M+H)<sup>+</sup>.

**Synthesis of (S)-2-(1,3-dioxoisindolin-2-yl)-5-methoxy-5-oxopentanoic acid (43)**



To a solution of **42** (1.00 g, 5.06 mmol) in 0.55 mol/l aqueous  $\text{Na}_2\text{CO}_3$  (20 mL, 11.13 mmol) was added *N*-ethoxycarbonylphtalimide (1.60 g, 7.33 mmol) at 0 °C. the reaction mixture was stirred at 0 °C for 10 min and at room temperature for 50 min, then insoluble material was removed by filtration and HCl 2N was added to the filtrate until the pH reached about 2. Then the mixture was stirred at 0 °C for 30 min, the solution was extracted with EtOAc (2 x 50 mL). The organic phase was dried ( $\text{Na}_2\text{SO}_4$ ), filtered and concentrated in vacuo to afford the desired compound (1.47 g, 99%). White solid, mp 102–104 °C.  $^1\text{H}$  NMR (300 MHz,  $\text{CDCl}_3$ ):  $\delta$  9.13 (s, 1H); 8.02–7.63 (m, 2H); 7.63–7.30 (m, 2H); 4.78 (t,  $J = 3.1$  Hz, 1H); 3.82 (s, 3H); 2.50–2.37 (m, 2H); 2.35–2.20 (m, 2H). ESI-MS  $m/z$ : 292 ( $\text{M}+\text{H}$ ) $^+$ .

**Synthesis of (S)-methyl 5-amino-4-(1,3-dioxoisindolin-2-yl)-5-oxopentanoate (44)**

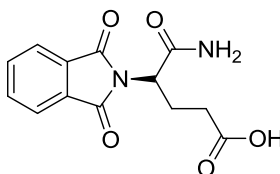


To a cooled solution (-10 °C) of **43** (0.15 g, 0.51 mmol) in THF (2 mL), NMM (56.0  $\mu\text{L}$ , 0.51 mmol), isobutyl chloroformate (78.0  $\mu\text{L}$ , 0.76 mmol) and  $\text{NH}_3$  were added. The reaction was stirred 30 min at -10 °C and 1h at room temperature. The mixture was concentrated in vacuo, the  $\text{H}_2\text{O}$  (30 mL) was



added and extracted with EtOAc (3 x 20 mL). The organic phase was washed with 5% NaHCO<sub>3</sub> solution (1 x 20 mL) and H<sub>2</sub>O (1 x 20 mL). The crude mixture was purified by silica gel chromatography (cyclohexane/EtOAc) to obtain the pure product (0.07 g, 51%). White solid, mp 96–98 °C. <sup>1</sup>H NMR (300 MHz, CDCl<sub>3</sub>): δ 7.83–7.70 (m, 2H); 7.70–7.43 (m, 2H); 5.13 (s, 2H); 4.84 (t, J = 3.0 Hz, 1H); 3.81 (s, 3H); 2.47–2.19 (m, 4H). ESI-MS *m/z*: 291 (M+H)<sup>+</sup>.

**Synthesis of (S)-5-amino-4-(1,3-dioxoisindolin-2-yl)-5-oxopentanoic acid (45)**



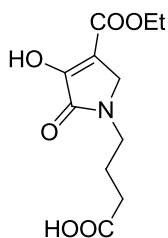
Derivative **44** (0.05 g, 0.17 mmol) was dissolved in HCl 2N in dioxane (85.0 μL) and stirred at room temperature overnight. The solution was concentrated in vacuo to obtain the final product (0.04 g, 99%) as a white solid. Mp 119–121 °C. <sup>1</sup>H NMR (300 MHz, DMSO-*d*<sub>6</sub>): δ 12.04 (s, 1H); 7.83–7.88 (m, 4H); 7.57 (s, 1H); 7.16 (s, 1H); 4.56 (dd, J = 10.3, 4.3 Hz, 1H); 2.37–2.29 (m, 1H); 2.20–1.09 (m, 3H). ESI-MS *m/z*: 277 (M+H)<sup>+</sup>.

**General synthesis of 1-(ω-carboxyalkyl)-1-carbethoxy-2,3-dioxopyrrolidines (46, 49)**

To a cooled stirred solution of amino acid (29.1 mmol) in ethanolic sodium ethoxide (25 mL, 29.1 mmol) was added ethyl acrylate (29.1 mmol) in small portions and the mixture was stirred overnight. The resulting solution of the adduct was heated with an ethanolic sodium ethoxide solution (10 mL, 29.1 mmol) mixed with diethyl oxalate (29.1 mmol) under reflux for 3h. The

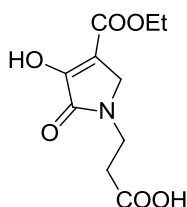
reaction mixture was poured into ice-cold water and acidified with concentrated HCl to precipitate the product, filtered off.

**46: 4-(4-(ethoxycarbonyl)-3-hydroxy-2-oxo-2,5-dihydro-1H-pyrrol-1-yl)butanoic acid**

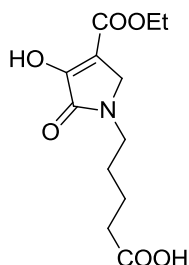


White solid, 52% yield; mp 182–186 °C.  $^1\text{H}$  NMR (300 MHz, DMSO- $d_6$ ):  $\delta$  11.25 (s, 1H); 4.15 (q,  $J = 7.1$  Hz, 2H); 3.95 (s, 2H); 3.39 (t,  $J = 6.9$  Hz, 2H); 2.20 (t,  $J = 7.2$  Hz, 2H); 1.80–1.71 (m, 2H); 1.23 (t,  $J = 7.1$  Hz, 3H). ESI-MS  $m/z$ : 258 (M+H) $^+$ .

**49': 3-(4-(ethoxycarbonyl)-3-hydroxy-2-oxo-2,5-dihydro-1H-pyrrol-1-yl)propanoic acid**



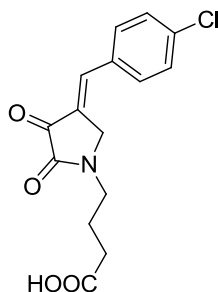
White solid, 66% yield; mp 195–200 °C.  $^1\text{H}$  NMR (300 MHz, DMSO- $d_6$ ):  $\delta$  11.25 (s, 1H); 4.11 (q,  $J = 7.1$  Hz, 2H); 3.93 (s, 2H); 3.54 (t,  $J = 6.9$  Hz, 2H); 2.48 (t,  $J = 6.9$  Hz, 2H); 1.17 (t,  $J = 7.1$  Hz, 3H). ESI-MS  $m/z$ : 244 (M+H) $^+$ .

**49'': 5-(4-(ethoxycarbonyl)-3-hydroxy-2-oxo-2,5-dihydro-1H-pyrrol-1-yl)pentanoic acid**

White solid, 60% yield; mp 118–120 °C.  $^1\text{H}$  NMR (300 MHz,  $\text{DMSO-}d_6$ ):  $\delta$  11.25 (s, 1H); 4.16 (q,  $J = 7.1$  Hz, 2H); 3.95 (s, 2H); 3.38 (t,  $J = 12.1$  Hz, 2H); 2.23 (t,  $J = 7.1$  Hz, 2H); 1.58–1.40 (m, 4H); 1.22 (t,  $J = 7.1$  Hz, 3H). ESI-MS  $m/z$ : 272 ( $\text{M}+\text{H}$ ) $^+$ .

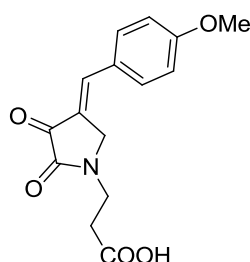
**General procedure for the synthesis of 4-arylidene-1-( $\omega$ -carboxyalkyl)-3,4-dioxopyrrolidines (47, 50a-h)**

The 1-( $\omega$ -carboxyalkyl)-1-carbethoxy-2,3-dioxopyrrolidine (10.0 mmol) was refluxed with HCl 6N (50 mL) for 30 min. To the solution was added dropwise the aromatic aldehyde (15.0 mmol) in 5 mL of formic acid. The mixture was refluxed for an additional 2.5h. The solution was poured onto crushed ice and the precipitate solid was collected by filtration and washed with water.

**47: 4-(4-(4-chlorobenzylidene)-2,3-dioxopyrrolidin-1-yl)butanoic acid**

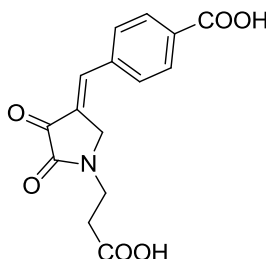
White solid, 43% yield; mp 206–207 °C.  $^1\text{H}$  NMR (300 MHz,  $\text{DMSO-}d_6$ ):  $\delta$  7.71 (d,  $J = 7.9$  Hz, 2H), 7.59 (d,  $J = 7.9$  Hz, 2H), 7.54 (s, 1H), 4.64 (s, 2H), 3.68 (t,  $J = 7.1$  Hz, 2H), 2.68 (t,  $J = 7.1$  Hz, 2H); 1.93–1.84 (m, 2H). ESI-MS  $m/z$ : 308 ( $\text{M}+\text{H}$ ) $^+$ , 310 ( $\text{M}+2\text{H}$ ) $^+$ .

**50a: 3-(4-(4-methoxybenzylidene)-2,3-dioxopyrrolidin-1-yl)propanoic acid**



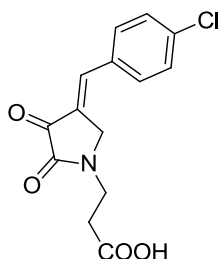
Yellow solid, 71% yield; mp 236–240 °C (decomp).  $^1\text{H}$  NMR (300 MHz,  $\text{DMSO-}d_6$ ):  $\delta$  7.66 (d,  $J = 7.8$  Hz, 2H); 7.53 (s, 1H); 7.09 (d,  $J = 8.0$  Hz, 2H); 4.65 (s, 2H); 3.89 (s, 3H); 3.70 (t,  $J = 7.0$  Hz, 2H); 2.67 (t,  $J = 7.1$  Hz, 2H). ESI-MS  $m/z$ : 290 ( $\text{M}+\text{H}$ ) $^+$ .

**50b: 4-((1-(2-carboxyethyl)-4,5-dioxopyrrolidin-3-ylidene)methyl)benzoic acid**



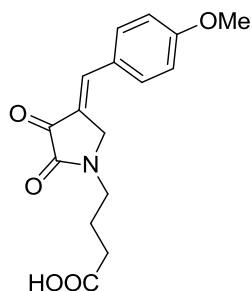
Yellow solid, 86% yield; mp 298–300 °C (decomp).  $^1\text{H}$  NMR (300 MHz,  $\text{DMSO-}d_6$ ):  $\delta$  8.02 (d,  $J = 9.3$  Hz, 2H), 7.80 (d,  $J = 9.3$  Hz, 2H), 7.56 (s, 1H), 4.67 (s, 2H), 3.70 (t,  $J = 7.1$  Hz, 2H), 2.68 (t,  $J = 7.1$  Hz, 2H). ESI-MS  $m/z$ : 304 ( $\text{M}+\text{H}$ ) $^+$ .

**50c: 3-(4-(4-chlorobenzylidene)-2,3-dioxopyrrolidin-1-yl)propanoic acid**



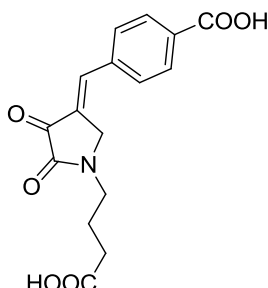
Yellow solid, 66% yield; mp 200–202 °C.  $^1\text{H}$  NMR (300 MHz,  $\text{DMSO-}d_6$ ):  $\delta$  7.71 (d,  $J = 7.9$  Hz, 2H), 7.59 (d,  $J = 7.9$  Hz, 2H), 7.54 (s, 1H), 4.64 (s, 2H), 3.68 (t,  $J = 7.1$  Hz, 2H), 2.68 (t,  $J = 7.1$  Hz, 2H). ESI-MS  $m/z$ : 294 ( $\text{M}+\text{H}$ ) $^+$ , 296 ( $\text{M}+2\text{H}$ ) $^+$ .

**50d: 4-(4-(4-methoxybenzylidene)-2,3-dioxopyrrolidin-1-yl)butanoic acid**



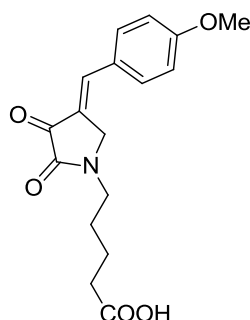
Yellow solid, 43% yield; mp 194–197 °C.  $^1\text{H}$  NMR (300 MHz,  $\text{DMSO-}d_6$ ):  $\delta$  7.67 (d,  $J = 8.7$  Hz, 2H); 7.52 (s, 1H), 7.08 (d,  $J = 8.7$  Hz, 2H), 4.58 (s, 2H); 3.84 (s, 3H); 3.52 (t,  $J = 6.9$  Hz, 2H); 2.28 (t,  $J = 7.2$  Hz, 2H); 1.93-1.84 (m, 2H). ESI-MS  $m/z$ : 304 ( $\text{M}+\text{H}$ ) $^+$ .

**50e:** 4-((1-(3-carboxypropyl)-4,5-dioxopyrrolidin-3-ylidene)methyl)benzoic acid



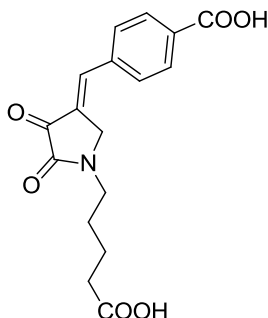
Yellow solid, 60% yield; mp 272–276 °C (decomp).  $^1\text{H}$  NMR (300 MHz, DMSO- $d_6$ ):  $\delta$  8.03 (d,  $J = 8.3$  Hz, 2H); 7.80 (d,  $J = 8.3$  Hz, 2H); 7.60 (s, 1H); 4.65 (s, 2H); 3.53 (t,  $J = 7.0$  Hz, 2H); 2.30 (t,  $J = 7.0$  Hz, 2H); 1.89 (m,  $J = 1.92$ – $1.87$  Hz, 2H). ESI-MS  $m/z$ : 318 (M+H) $^+$ .

**50f:** 5-(4-(4-methoxybenzylidene)-2,3-dioxopyrrolidin-1-yl)pentanoic acid



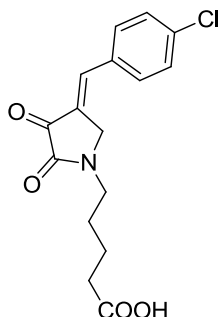
Yellow solid, 30% yield; mp 148–150 °C (decomp).  $^1\text{H}$  NMR (300 MHz, DMSO- $d_6$ ):  $\delta$  7.67 (d,  $J = 8.7$  Hz, 2H); 7.51 (s, 1H); 7.08 (d,  $J = 8.7$  Hz, 2H); 4.58 (s, 2H); 3.85 (s, 3H); 3.50 (t,  $J = 6.8$  Hz, 2H); 2.27 (t,  $J = 7.2$  Hz, 2H); 1.74–1.61 (m, 2H), 1.55–1.45 (m, 2H). ESI-MS  $m/z$ : 318 (M+H) $^+$ .

**0g: 4-((1-(4-carboxybutyl)-4,5-dioxopyrrolidin-3-ylidene)methyl)benzoic acid**



Yellow solid, 60% yield; mp 270–273 °C (decomp).  $^1\text{H}$  NMR (300 MHz,  $\text{DMSO-}d_6$ ):  $\delta$  8.01 (d,  $J = 8.2$  Hz, 2H); 7.80 (d,  $J = 8.2$  Hz, 2H); 7.58 (s, 1H); 4.65 (s, 2H); 3.49 (t,  $J = 6.9$  Hz, 2H); 2.27 (t,  $J = 7.1$  Hz, 2H); 1.79–1.40 (m, 4H). ESI-MS  $m/z$ : 332 ( $\text{M}+\text{H}$ ) $^+$ .

**50h: 5-(4-(4-chlorobenzylidene)-2,3-dioxopyrrolidin-1-yl)pentanoic acid**

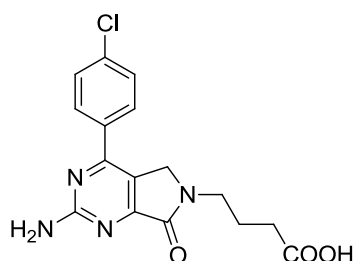


Yellow solid, 38% yield; mp 210–212 °C (decomp).  $^1\text{H}$  NMR (300 MHz,  $\text{DMSO-}d_6$ ):  $\delta$  7.73 (d,  $J = 7.3$  Hz, 2H); 7.60 (s, 1H); 7.56 (d,  $J = 7.3$  Hz, 2H); 4.61 (s, 2H); 3.47 (t,  $J = 7.1$  Hz, 2H); 2.26 (t,  $J = 7.1$  Hz, 2H); 1.72–1.60 (m, 2H); 1.55 – 1.42 (m, 2H). ESI-MS  $m/z$ : 322 ( $\text{M}+\text{H}$ ) $^+$ , 324 ( $\text{M}+2\text{H}$ ) $^+$ .

**General procedure for the synthesis of 2-amino-4-aryl-6-( $\omega$ -carboxyalkyl)-5H-pyrrolo[3,4-d]pyrimidin-7-(6H)ones (48 and 51a-h)**

A solution of guanidine in absolute ethanol was prepared by addition of 3.80 g (40.0 mmol) of guanidine hydrochloride to 100 mL of 0.4N ethanolic sodium ethoxide, followed by filtration to remove precipitated sodium chloride. A 10 mmol quantity of the benzylidene compound (**47** or **49**) and 0.50 g of guanidine hydrochloride were added and the mixture was stirred for 72h at room temperature. The solution was cooled in an ice bath and the product was collected by filtration, then dissolved in 20 mL of water. Following precipitation by dropwise addition of 50% acetic acid, the product was collected by filtration, washed with ice-cold water.

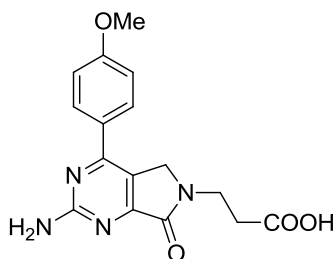
**48: 4-(2-amino-4-(4-chlorophenyl)-7-oxo-5H-pyrrolo[3,4-d]pyrimidin-6(7H)-yl)butanoic acid**



White solid, 30% yield; mp 253–255 °C.  $^1\text{H}$  NMR (300 MHz,  $\text{D}_2\text{O}/\text{NaOD}$ ):  $\delta$  7.36 (d,  $J = 8.0$  Hz, 2H); 7.18 (d,  $J = 8.0$  Hz, 2H); 3.70 (t,  $J = 6.4$  Hz, 2H); 2.51 (t,  $J = 6.4$  Hz, 2H); 1.70–1.54 (m, 2H). ESI-MS  $m/z$ : 347 ( $\text{M}+\text{H}$ ) $^+$ , 349 ( $\text{M}+2\text{H}$ ) $^+$ .

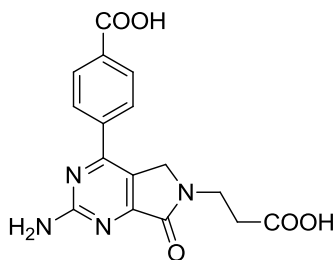


**51a: 3-(2-amino-4-(4-methoxyphenyl)-7-oxo-5H-pyrrolo[3,4-d]pyrimidin-6(7H)-yl)propanoic acid**



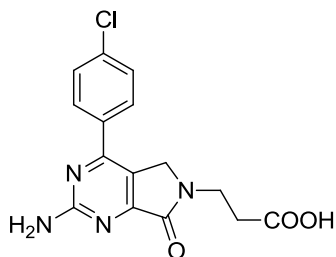
Yellow solid, 35% yield; mp 218–220 °C.  $^1\text{H}$  NMR (300 MHz,  $\text{D}_2\text{O}/\text{NaOD}$ ):  $\delta$  7.38 (d,  $J = 8.0$  Hz, 2H); 6.68 (d,  $J = 8.0$  Hz, 2H); 3.75 (s, 3H); 3.69 (t,  $J = 6.2$  Hz, 2H); 2.51 (t,  $J = 6.2$  Hz, 2H). ESI-MS  $m/z$ : 329 ( $\text{M}+\text{H}$ ) $^+$ .

**51b: 4-(2-amino-6-(2-carboxyethyl)-7-oxo-6,7-dihydro-5H-pyrrolo[3,4-d]pyrimidin-4-yl)benzoic acid**



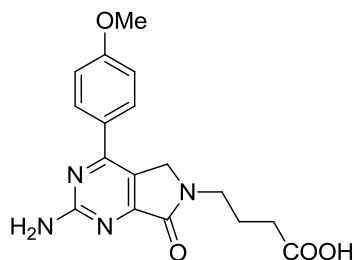
Yellow solid, 34% yield; mp 275–277 °C.  $^1\text{H}$  NMR (300 MHz,  $\text{D}_2\text{O}/\text{NaOD}$ ):  $\delta$  7.99 (d,  $J = 8.2$  Hz, 2H); 7.88 (d,  $J = 8.2$  Hz, 2H); 3.86 (t,  $J = 7.0$  Hz, 2H); 2.58 (t,  $J = 7.0$  Hz, 2H). ESI-MS  $m/z$ : 343 ( $\text{M}+\text{H}$ ) $^+$ .

**51c: 3-(2-amino-4-(4-chlorophenyl)-7-oxo-5H-pyrrolo[3,4-d]pyrimidin-6(7H)-yl)propanoic acid**



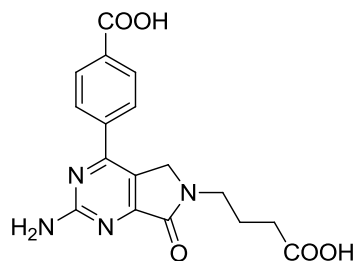
White solid, 37% yield; mp 232–234 °C. <sup>1</sup>H NMR (300 MHz, D<sub>2</sub>O/NaOD): δ 7.36 (d, J = 8.0 Hz, 2H); 7.18 (d, J = 8.0 Hz, 2H); 3.70 (t, J = 6.4 Hz, 2H); 2.51 (t, J = 6.4 Hz, 2H). ESI-MS *m/z*: 333 (M+H)<sup>+</sup>, 335 (M+2H)<sup>+</sup>.

**51d: 4-(2-amino-4-(4-methoxyphenyl)-7-oxo-5H-pyrrolo[3,4-d]pyrimidin-6(7H)-yl)butanoic acid**



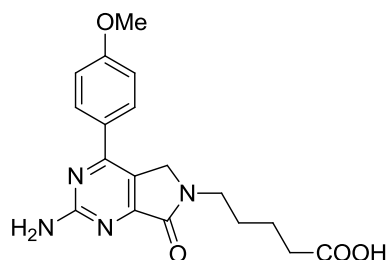
Yellow solid, 30% yield; mp 236–240 °C. <sup>1</sup>H NMR (300 MHz, DMSO-*d*<sub>6</sub>): δ 12.06 (s, 1H); 7.98 (d, J = 8.6 Hz, 2H); 7.11 (d, J = 8.6 Hz, 2H); 6.91 (s, 2H); 4.68 (s, 2H); 3.85 (s, 3H); 3.55 (t, J = 7.2 Hz, 2H); 2.27 (t, J = 7.1 Hz); 1.92–1.75 (m, 2H). ESI-MS *m/z*: 343 (M+H)<sup>+</sup>.

**51e: 4-(2-amino-6-(3-carboxypropyl)-7-oxo-6,7-dihydro-5H-pyrrolo[3,4-*d*]pyrimidin-4-yl)benzoic acid**



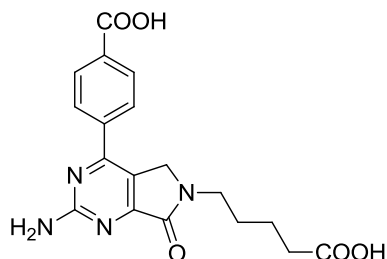
Yellow solid, 34% yield; mp 292–296 °C.  $^1\text{H}$  NMR (300 MHz,  $\text{D}_2\text{O}/\text{NaOD}$ ):  $\delta$  7.97 (d,  $J = 8.1$  Hz, 2H); 7.84 (d,  $J = 8.1$  Hz, 2H); 3.61 (t,  $J = 7.1$  Hz, 2H); 2.20 (t,  $J = 7.1$  Hz, 2H); 1.95–1.89 (m, 2H). ESI-MS  $m/z$ : 357 ( $\text{M}+\text{H}$ ) $^+$ .

**51f: 5-(2-amino-4-(4-methoxyphenyl)-7-oxo-5H-pyrrolo[3,4-*d*]pyrimidin-6(7*H*)-yl)pentanoic acid**



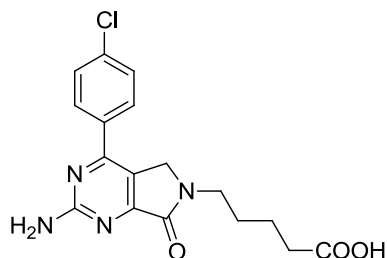
Yellow solid, 38% yield; mp 243–245 °C.  $^1\text{H}$  NMR (300 MHz,  $\text{D}_2\text{O}/\text{NaOD}$ ):  $\delta$  7.69 (d,  $J = 8.0$  Hz, 2H); 6.97 (d,  $J = 8.0$  Hz, 2H); 3.87 (s, 3H); 3.60 (t,  $J = 6.9$  Hz, 2H); 2.24 (t,  $J = 6.9$  Hz, 2H); 1.70–1.54 (m, 4H). ESI-MS  $m/z$ : 357 ( $\text{M}+\text{H}$ ) $^+$ .

**51g: 4-(2-amino-6-(4-carboxybutyl)-7-oxo-6,7-dihydro-5H-pyrrolo[3,4-d]pyrimidin-4-yl)benzoic acid**



Yellow solid, 37% yield; mp 301–303 °C.  $^1\text{H}$  NMR (300 MHz,  $\text{D}_2\text{O}/\text{NaOD}$ ):  $\delta$  7.87 (d,  $J = 8.1$  Hz, 2H); 7.72 (d,  $J = 8.1$  Hz, 2H); 3.47 (t,  $J = 6.9$  Hz, 2H); 2.13 (t,  $J = 6.9$  Hz, 2H); 1.59–1.48 (m, 4H). ESI-MS  $m/z$ : 371 ( $\text{M}+\text{H}$ ) $^+$ .

**51h: 5-(2-amino-4-(4-chlorophenyl)-7-oxo-5H-pyrrolo[3,4-d]pyrimidin-6(7H)-yl)pentanoic acid**

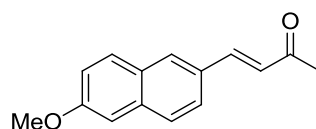


Yellow solid, 32% yield; mp 260–262 °C.  $^1\text{H}$  NMR (300 MHz,  $\text{D}_2\text{O}/\text{NaOD}$ ):  $\delta$  7.56 (d,  $J = 7.9$  Hz, 2H); 7.36 (d,  $J = 7.9$  Hz, 2H); 3.54 (t,  $J = 5.6$  Hz, 2H); 2.19 (t,  $J = 5.6$  Hz, 2H); 1.65–1.55 (m, 4H). ESI-MS  $m/z$ : 361 ( $\text{M}+\text{H}$ ) $^+$ , 363 ( $\text{M}+2\text{H}$ ) $^+$ .

### 7.3. Synthesis of 4-aryl-2-butanones (52-53)

**Microwave and Continuous Flow Equipment.** Microwave irradiation experiments were carried out in Pyrex or silicon carbide (SiC) process vials in an Anton Paar Monowave 300 single-mode microwave instrument (IR and/or internal fiberoptic temperature monitoring). Laboratory scale flow experiments were performed using a FlowSyn (Uniqsis), or X-Cube Flash/H-Cube (ThalesNano Nanotechnology Inc.) flow reactors.

#### Synthesis of 4-(6-methoxynaphthalen-2-yl)-3-buten-2-one (52a).



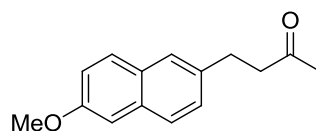
**Batch Microwave Synthesis: Wittig Reaction.** To a solution of (acetylmethylene)triphenylphosphorane **56** (0.19 g, 0.61 mmol) in 3 mL of DMF, 6-methoxy-2-naphthaldehyde **55a** (0.07 g, 0.36 mmol) was added, and the mixture was stirred for 30 s in a 10-mL Pyrex vial. The solution was capped with a Teflon septum and heated by microwave irradiation at 210 °C for 10 min. After cooling the vessel to ambient conditions, the crude reaction mixture was concentrated under reduced pressure and transferred to a silica-samplet, dried for 1 h at 50 °C in a drying oven, and subjected to automated flash chromatography with petroleum ether/ethyl acetate (0 to 45% gradient) as eluent to provide 0.08 g (94%) of 4-(6-methoxynaphthalen-2-yl)-3-buten-2-one (**52a**). Yellow solid, mp 118–120 °C. <sup>1</sup>H NMR (300 MHz, CDCl<sub>3</sub>): δ 7.89–7.63 (m, 5H); 7.69 (d, J = 16.2 Hz, 1H); 7.19–7.13 (m, 2H); 3.94 (s, 3H); 2.41 (s, 3H). ESI-MS *m/z*: 227 (M+H)<sup>+</sup>.

*Batch Microwave Synthesis: Aldol Reaction.* To a solution of **55a** (0.56 g, 2.50 mmol) in 2 mL of acetone, 60  $\mu$ L of NaOH 10% solution and 1 mL of distilled water were added, and the mixture was stirred for 30 s in a 10 mL Pyrex vial. The solution was capped with a Teflon septum and heated by microwave irradiation at 70 °C for 450 s. After cooling the vessel to ambient conditions, the crude reaction mixture was concentrated under reduced pressure and transferred to a silica-samplet, dried for 1h at 50 °C in a drying oven, and subjected to automated flash chromatography with petroleum ether/ethyl acetate (0 to 45% gradient) as eluent to provide 0.55 g (97%) of **52a** identical in all respects to the sample prepared above.

*Continuous Flow Synthesis: Wittig Reaction.* To a solution of **56** (0.65 g, 2.04 mmol) in 10 mL of DMF, **55a** (0.22 g, 1.20 mmol) was added, and the mixture was stirred for 30 s in a 15-mL Pyrex vial. At the same time the FlowSyn reactor was equipped with a stainless steel reaction coil (10 mL volume, 10 min residence time at 1 mL/min flow rate). The reaction parameters, temperature (210 °C) and 1 mL/min flow rate, were selected on the flow reactor, and processing was started, whereby initially only DMF solvent was pumped through the system until the instrument had achieved the desired reaction parameters and stable processing was achieved. At that point the inlet tube was switched from the solvent flask to the 15-mL glass vial containing the reaction mixture. After processing through the flow reactor, the inlet flow was dipped back into the flask containing solvent and was processed for an additional 1min, thus washing from the system any remaining reaction mixture. The reaction was concentrated under vacuum, and the product **52a** was isolated as described above in 97% yield.

*Continuous Flow Synthesis: Aldol Reaction.* To a solution of **55a** (0.26 g, 1.37 mmol) in 6.5 mL of acetone were added 33  $\mu$ L of a 10% aqueous NaOH solution and 3.5 mL of distilled water, and the mixture was stirred for 30 s. At the same time the FlowSyn reactor was equipped with a stainless steel reaction coil (10 mL volume, 450 s residence time at 1.34 mL/min flow rate). The reaction parameters, temperature (70 °C) and 1.34 mL/min flow rate, were selected on the flow reactor, and processing was started, whereby initially only solvent acetone was pumped through the system until the instrument had achieved the desired reaction parameters and stable processing was achieved. At that point the inlet tube was switched from the solvent flask to the 15-mL glass vial containing the freshly prepared reaction mixture (a slow aldol condensation occurs also at room temperature). After processing through the flow reactor, the inlet flow was dipped back into the flask containing solvent and processed for an additional min, thus washing from the system any remaining reaction mixture. The reaction was concentrated under vacuum, and the product was isolated as described above in 94% yield.

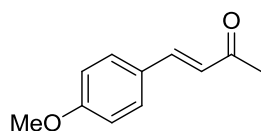
**Synthesis of 4-(6-methoxynaphthalen-2-yl)-butan-2-one (53a).**



A 10-mL stock solution of 4-(6-methoxynaphthalen-2-yl)-3-buten-2-one **52a** of 0.5M concentration in DMF was prepared in a glass vial. The reaction parameters (Full-H<sub>2</sub> mode, 100 °C and 1mL/min flow rate) were selected on the H-Cube hydrogenator. The instrument was fitted with a 30 mm Ra/Ni CatCart and the processing was started, whereby initially only pure solvent was pumped through the system until the instrument had achieved the desired reaction parameters and stable processing was achieved. At that point the sample inlet line was switched to the vial containing the substrate. A total

reaction volume of 15 mL was collected and the cartridge subsequently washed with pure solvent for 5 min to remove any substrate/product still adsorbed on the catalyst. Evaporation of the solvent afforded 4-(6-methoxynaphthalen-2-yl)-butan-2-one (**53a**) as a colorless oil (97% crude yield), which was purified by flash chromatography to provide 1.02 g of pure product as a white solid (90%). Mp 77–79 °C. <sup>1</sup>H NMR (300 MHz, CDCl<sub>3</sub>): δ 7.68–7.11 (m, 6H); 3.91 (s, 3H); 3.05–3.00 (m, 2H); 2.86–2.81 (m, 2H); 2.15 (s, 3H). ESI-MS *m/z*: 229 (M+H)<sup>+</sup>.

#### Synthesis of 4-(4-methoxyphenyl)-3-buten-2-one (**52b**)



*Batch Microwave Synthesis: Mizoraki–Heck Reaction.* To 1 mL of DMF/H<sub>2</sub>O (3:1) solvent in a 10 mL Pyrex microwave vial 4-iodoanisole (0.10 g, 0.43 mmol), methyl vinyl ketone (52.0 μL, 0.64 mmol) and Cs<sub>2</sub>CO<sub>3</sub> (0.15 g, 0.47 mmol) were added, followed by 2 mL of a 0.0004 M stock solution of Pd(OAc)<sub>2</sub> in DMF/H<sub>2</sub>O (3:1) (0.19 mg, 0.2 mol %). The reaction mixture was stirred for 30 s, capped with a Teflon septum and subjected to microwave heating for 20 min (hold time) at 160 °C. After cooling to ambient temperature, the crude reaction mixture was concentrated in vacuo and the residue subjected to automated flash chromatography with petroleum ether/ethyl acetate (0 to 45% gradient) as eluent to provide 0.06 g (74%) of **52b**. Yellow solid, mp 73–75 °C. <sup>1</sup>H NMR (300 MHz, CDCl<sub>3</sub>): δ 7.52–7.45 (m, 3H); 6.94–6.89 (m, 2H); 6.61 (d, J = 16.2 Hz, 1H); 3.85 (s, 3H); 2.36 (s, 3H). ESI-MS *m/z*: 177 (M+H)<sup>+</sup>.



*Batch Microwave Synthesis: Wittig Reaction.* To a solution of (acetylmethylene)triphenylphosphorane (0.19 g, 0.61 mmol) in 3 mL of DMF, 44.0  $\mu$ L of *p*-anisaldehyde (0.36 mmol) were added and the mixture was stirred for 30 s in a 10 mL Pyrex vial. The solution was capped with a Teflon septum and heated by microwave irradiation at 210 °C for 10 min. After cooling the vessel to ambient conditions, the crude reaction mixture was concentrated in vacuo and transferred to a silica-samplet, dried for 1h at 50 °C in a drying oven and subjected to automated flash chromatography with petroleum ether/ethyl acetate (0 to 45% gradient) as eluent to provide 0.06 g (95%) of **52b** in all respects identical to a sample prepared above.

*Batch Microwave Synthesis: Aldol Condensation.* To a solution of *p*-anisaldehyde (0.30 mL, 2.50 mmol) in 2 mL of acetone, were added 60.0  $\mu$ L of NaOH 10% solution and 1 mL of distilled water, and the mixture was stirred for 30 s in a 10 mL Pyrex vial. The solution was capped with a Teflon septum and heated by microwave irradiation at 120 °C for 1 min. After cooling the vessel to ambient conditions, the crude reaction mixture was concentrated under reduced pressure and transferred to a silica-samplet, dried for 1h at 50 °C in a drying oven and subjected to automated flash chromatography with petroleum ether/ethyl acetate (0 to 45% gradient) as eluent to provide 0.41 g (94%) of **52b**.

*Continuous Flow Synthesis: Mizoroki–Heck Reaction.* To a stirred mixture of 4-iodoanisole (0.33 g, 1.43 mmol), methyl vinyl ketone (0.17 mL, 2.14 mmol), Cs<sub>2</sub>CO<sub>3</sub> (0.51 g, 1.57 mmol) and DMF/H<sub>2</sub>O (3:1) (5 mL) was added 5 mL of a 0.0008 M stock solution of Pd(OAc)<sub>2</sub> in DMF/ H<sub>2</sub>O (3:1) (0.64 mg, 0.2 mol %) and stirred for 30 s. At the same time the X-Cube Flash reactor was

equipped with a stainless steel reaction coil (16 mL volume, 10 min residence time at 1.6 mL/min flow rate). The reaction parameters temperature (180 °C), pressure (60 bar) and 1.6 mL/min flow rate were selected on the flow reactor, and processing was started, whereby initially only solvent DMF/H<sub>2</sub>O (3:1) was pumped through the system until the instrument had achieved the desired reaction parameters and stable processing was achieved. At that point the inlet tube was switched from the solvent flask to the 15-mL glass vial containing the reaction mixture. After processing through the flow reactor, the inlet flow was dipped back into the flask containing solvent and processed for an additional 10 min, thus washing from the system any remaining reaction mixture. Workup as above provided 0.17 g (67%) of **52b**.

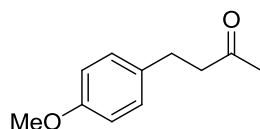
*Continuous Flow Synthesis: Wittig Reaction.* To a solution of (acetylmethylene)triphenylphosphorane (0.65 g, 2.04 mmol) in 10 mL of DMF was added 0.13 mL of *p*-anisaldehyde (1.20 mmol), and the mixture was stirred for 30 s in a 15-mL Pyrex vial. At the same time the FlowSyn reactor was equipped with a stainless steel reaction coil (10 mL volume, 10 min residence time at 1 mL/min flow rate). The reaction parameters temperature (210 °C) and 1 mL/min flow rate were selected on the flow reactor, and processing was started, whereby initially only solvent DMF was pumped through the system until the instrument had achieved the desired reaction parameters and stable processing was achieved. At that point the inlet tube was switched from the solvent flask to the 15-mL glass vial containing the reaction mixture. After processing through the flow reactor, the inlet flow was dipped back into the flask containing solvent and processed for an additional 1 min, thus washing from the system any remaining reaction mixture. The reaction was concentrated under vacuum, and 0.20 g (97%) of product was isolated.

*Continuous Flow Synthesis: Aldol Reaction.* To a solution of *p*-anisaldehyde (0.97 mL, 8.00 mmol) in 6.5 mL of acetone were added 0.19 mL of NaOH 10% solution and 3.5 mL of distilled water and stirred for 30 s. At the same time the FlowSyn reactor was equipped with a stainless steel reaction coil (5 mL volume, 1 min residence time at 5 mL/min flow rate). The reaction parameters temperature (120 °C) and 5 mL/min flow rate were selected on the flow reactor, and processing was started, whereby initially only acetone solvent was pumped through the system until the instrument had achieved the desired reaction parameters and stable processing was achieved. At that point the inlet tube was switched from the solvent flask to the 15 mL glass vial containing the freshly prepared reaction mixture (a slow aldol condensation occurs also at room temperature). After processing through the flow reactor, the inlet flow was dipped back into the flask containing solvent and processed for an additional min, thus washing from the system any remaining reaction mixture. The reaction was concentrated under vacuum and 1.27 g (90%) of product **52b** was isolated as described above.

*Continuous Mesofluidic Flow Synthesis: Aldol Reaction.* The flow rate was set to 40 g/min (~45 mL/min). The starting solution was prepared from *p*-anisaldehyde (486 mL, 4.0 mol, 4.47 g/min, 0.033 mol/min) and NaOH (96 mL 10% aqueous solution, 0.2 mol, 0.09 g/min, 0.002 mol/min) in 3.25 L acetone (21.08 g/min, 0.36 mol/min) and 1.75 L deionized water (14.37 g/min). With pure acetone the pressure maintaining valve was adjusted to 7 bar. Together with 2 bar pressure drop from the residence time tubing an overall pressure of 9 bar was achieved. The silicon oil bath was heated to 120 °C. The process was started by feeding the starting solution into the system and putting the residence time tubing into the preheated silicon oil bath. A total volume of 4.65 L of output stream was collected. Two 100 mL samples

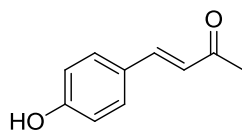
were collected after 3 and 5.5 min from process start. Then four larger samples (~1.1 L) were collected in about 25 min each (after 8, 33, 58, and 82 min). All samples have been analyzed as mentioned previously via HPLC and showed full conversion and the same selectivity as achieved in the small-scale experiments. A 1.1 L fraction was worked up. The solvent was evaporated, and the obtained precipitate was washed with a total volume of 1 L of distilled water and subsequently dried in a desiccator under vacuum to give **52b** in almost quantitative yield.

### Synthesis of 4-(4-methoxyphenyl)-butan-2-one (**53b**)



A 10 mL stock solution of **52b** with a 0.5 M concentration in EtOH was prepared in a glass vial. The reaction parameters (Full-H<sub>2</sub> mode, room temperature and 1.5 mL/min flow rate) were selected on the H-Cube hydrogenator. The instrument was fitted with a 30 mm Ra/Ni CatCart and the processing was started, whereby initially only pure solvent was pumped through the system until the instrument had achieved the desired reaction parameters and stable processing was achieved. At that point the sample inlet line was switched to the vial containing the substrate. A total reaction volume of 15 mL was collected and the cartridge subsequently washed with pure solvent for 5 min to remove any substrate/product still adsorbed on the catalyst. Evaporation of the solvent afforded **53b** as a yellow oil (97% crude yield), which was purified by flash chromatography to provide 0.84 g of a pale-yellow oil (94%). <sup>1</sup>H NMR (300 MHz, CDCl<sub>3</sub>): δ 7.11–7.08 (m, 2H); 6.84–6.81 (m, 2H); 3.78 (s, 3H); 2.87–2.81 (m, 2H); 2.75–2.70 (m, 2H); 2.13 (s, 3H). ESI-MS *m/z*: 179 (M+H)<sup>+</sup>.

**Synthesis of 4-(4-hydroxyphenyl)-3-buten-2-one (52c)**



*Batch Microwave Synthesis: Mizoroki–Heck Reaction.* To 1 mL of DMF/ H<sub>2</sub>O (3:1) as solvent in a 10-mL Pyrex microwave vial were added 4-iodoanisole (0.09 g, 0.43 mmol), methyl vinyl ketone (52.0  $\mu$ L, 0.64 mmol) and Cs<sub>2</sub>CO<sub>3</sub> (0.15 g, 0.47 mmol), followed by 2 mL of 0.0004 M stock solution of Pd(OAc)<sub>2</sub> in DMF/H<sub>2</sub>O (3:1) (0.19 mg, 0.2 mol %). The reaction mixture was stirred for 30 s, capped with a Teflon septum, and subjected to microwave heating for 20 min (hold time) at 160 °C. After cooling to ambient temperature, the crude reaction mixture was concentrated under reduced pressure and the residue subjected to automated flash chromatography with petroleum ether/ethyl acetate (0 to 45% gradient) as eluent to provide 0.05 g (78%) of **52c**. White solid, mp 111–113 °C. <sup>1</sup>H NMR (300 MHz, CDCl<sub>3</sub>):  $\delta$  7.52–7.43 (m, 3H); 6.91–6.86 (m, 2H); 6.61 (d, J = 16.2 Hz, 1H); 6.09 (br s, 1H); 2.38 (s, 3H). ESI-MS m/z: 163 (M+H)<sup>+</sup>.

*Batch Microwave Synthesis: Wittig Reaction.* To a solution of (acetylmethylene)triphenylphosphorane (0.19 g, 0.61 mmol) in 3 mL of DMF, was added 4-hydroxybenzaldehyde (0.04 g, 0.36 mmol), and the mixture was stirred for 30 s in a 10-mL Pyrex vial. The solution was capped with a Teflon septum and heated by microwave irradiation at 210 °C for 10 min. After cooling the vessel to ambient conditions, the crude reaction mixture was concentrated under reduced pressure and transferred to a silica-samplet, dried for 1 h at 50 °C in a drying oven, and subjected to automated flash

chromatography with petroleum ether/ethyl acetate (0 to 45% gradient) as eluent to provide 0.04 mg (70%) of **52c**.

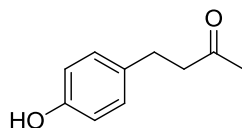
*Batch Microwave Synthesis: Aldol Condensation.* To a solution of 4-hydroxybenzaldehyde (0.30 g, 2.50 mmol) in 2 mL of acetone was added 2 mL of a 10% aqueous NaOH solution, and the mixture was stirred for 30 s in a 10-mL Pyrex vial. The solution was capped with a Teflon septum and heated by microwave irradiation at 70 °C for 450 s. After cooling the vessel to ambient conditions, the crude reaction mixture was concentrated under reduced pressure and transferred to a silica-samplet, dried for 1 h at 50 °C in a drying oven, and subjected to automated flash chromatography with petroleum ether/ethyl acetate (0 to 45% gradient) as eluent to provide 0.28 g (69%) of **52c**.

*Continuous Flow Synthesis: Wittig Reaction.* To a solution of (acetylmethylene)triphenylphosphorane (0.65 g, 2.04 mmol) in 10 mL of DMF was added 4-hydroxybenzaldehyde (0.15 g, 1.20 mmol), and the mixture was stirred for 30 s in a 15-mL Pyrex vial. At the same time the FlowSyn reactor was equipped with a stainless steel reaction coil (10 mL volume, 10 min residence time at 1 mL/min flow rate). The reaction parameters temperature (210 °C) and 1 mL/min flow rate were selected on the flow reactor, and processing was started, whereby initially only solvent DMF was pumped through the system until the instrument had achieved the desired reaction parameters and stable processing was achieved. At that point the inlet tube was switched from the solvent flask to the 15 mL glass vial containing the reaction mixture. After processing through the flow reactor, the inlet flow was dipped back into the flask containing solvent and processed for an additional 1 min,

thus washing from the system any remaining reaction mixture. The reaction was concentrated under vacuum and 0.19 g (98%) of product.

*Continuous Flow Synthesis: Aldol Reaction.* To a solution of 4-hydroxybenzaldehyde (0.76, 6.25 mmol) in 5 mL of acetone was added 5 mL of a 10% aqueous NaOH solution, and the solution was stirred for 30 s. At the same time the FlowSyn reactor was equipped with a stainless steel reaction coil (10 mL volume, 450 s residence time at 1.34 mL/min flow rate). The reaction parameters temperature (70 °C) and 1.34 mL/min flow rate were selected on the flow reactor, and processing was started, whereby initially only solvent acetone was pumped through the system until the instrument had achieved the desired reaction parameters and stable processing was achieved. At that point the inlet tube was switched from the solvent flask to the 15 mL glass vial containing the freshly prepared reaction mixture (a slow aldol condensation occurs also at room temperature). After processing through the flow reactor, the inlet flow was dipped back into the flask containing solvent and processed for an additional 1 min, thus washing from the system any remaining reaction mixture. The reaction was concentrated under vacuum and 0.79 mg (78%) of product.

#### Synthesis of 4-(4-hydroxyphenyl)-butan-2-one (53c)



A 10 mL stock solution of **52c** with a 0.7 M concentration in DMF was prepared in a glass vial. The reaction parameters (Full-H<sub>2</sub> mode, 35 °C and 1 mL/min flow-rate) were selected on the H-Cube hydrogenator. The instrument was fitted with a 30 mm Ra/Ni CatCart and the processing was started,

whereby initially only pure solvent was pumped through the system until the instrument had achieved the desired reaction parameters and stable processing was achieved. At that point the sample inlet line was switched to the vial containing the substrate. A total reaction volume of 15 mL was collected and the cartridge subsequently washed with pure solvent for 5 min to remove any substrate/product still adsorbed on the catalyst. Evaporation of the solvent affords **53c** as a yellow oil (97% crude yield), which was purified by flash chromatography to provide 1.04 g of a pale yellow oil (91%). <sup>1</sup>H NMR (300 MHz, CDCl<sub>3</sub>): δ 7.07–7.02 (m, 2H); 6.76–6.73 (m, 2H); 4.86 (br s, 1H); 2.86–2.80 (m, 2H); 2.75–2.70 (m, 2H); 2.14 (s, 3H). ESI-MS *m/z*: 165 (M+H)<sup>+</sup>.

#### **7.4. DNMT1 expression, purification, and assay**

*Cloning and purification of recombinant DNMT1.* Briefly, proteins were expressed in Sf9 insect cells (derived from *Spodoptera frugiperda*) and purified by affinity chromatography and gel filtration. The protein concentration of purified DNMT was determined by Bradford assay and verified by using Coomassie blue stained SDS/polyacrylamide gels and suitable molecular mass markers of known concentration. Protein identity was confirmed by immunoblotting using a DNMT1-specific antibody (Santa Cruz) according to the manufacturer's protocol.

*Biochemical DNMT activity assay and dose-response assays.* DNA methylation assays were carried out in total reaction volume of 25 μL containing 0.4 μM hemimethylated or unmethylated oligonucleotide substrate purchased from MWG (upper strand: 5'-GATCGCXGATGCGXGAATXGCGATXGATGCGAT-3', X = 5mC for hemimethylated or X = C for unmethylated substrate, and lower strand: 5'-



ATCGCATCGATCGCGATTTCGCGCATCGGCGATC-3'), purified DNMT (500 nM) in reaction buffer (100 mM KCl, 10 mM TrisCl pH 7.5, 1 mM EDTA), and BSA (1 mg/mL). All reactions were carried out at 37 °C in the presence of 0.7  $\mu$ M [methyl-<sup>3</sup>H] AdoMet (2.6 TBq/mmol, PerkinElmer). After 3 h, the reaction was stopped by adding 10  $\mu$ L of 20% SDS and spotting of the whole volume onto DE81 cellulose paper. Filters were baked at 80 °C for 2 h and washed three times with cold 0.2M NH<sub>4</sub>HCO<sub>3</sub>, three times with distilled water, and once with 100% ethanol. After drying, filters were transferred into Mini-Poly Q vial (PerkinElmer) and 5 mL of Ultima Gold LSC Cocktail was added per vial. Analysis was done in a scintillation counter, each measurement was repeated once.

*Competition assay.* For the determination of the mode of action of **5b** in the catalytic domain of DNMT1, we used the model of Lai and Wu as recommended by the NIH Chemical Genomics Center (<http://www.ncgc.nih.gov/guidance>) and adapted it to our biochemical DNMT activity assay. The conditions of the biochemical DNMT activity assay (see above) were slightly modified for the competition experiments: the inhibitor concentration was held constant at 150  $\mu$ M, the reaction time at 37 °C was decreased to 1 h. The concentrations of either SAM substrate or oligo substrate were increased to test for competition with **5b**, which should result in a decreasing inhibition.

*Cell culture.* HCT116 cells were obtained directly from the American Type Culture Collection (ATCC, [www.atcc.org](http://www.atcc.org)) and passaged for fewer than 6 months after resuscitation. HCT116 were cultured in DMEM/Ham's F12 (BIOCHROM) supplemented with 10% FCS (Invitrogen). Cell proliferation and viability was assessed by counting trypan blue stained cells by TC10 automated cell counter (Bio-Rad).



## **CHAPTER 8**

## **REFERENCES**

- 
- <sup>1</sup> Waddington, C.H. The epigenotype. *Endeavour* 1942, 1, 18–20.
- <sup>2</sup> Egger, G.; Liang G.; Aparicio A.; Jones P.A. Epigenetics in human disease and prospects for epigenetic therapy. *Nature* **2004**, *429*, 457–463.
- <sup>3</sup> Jones, P.A.; Baylin, S. B. The fundamental role of epigenetic events in cancer. *Nat. Rev. Genet.* **2002**, *3*, 415–428.
- <sup>4</sup> Jones, P. A.; Martienssen, R. A blueprint for a Human Epigenome Project: the AACR Human Epigenome Workshop. *Cancer Res.* **2005**, *65*, 11241–11246.
- <sup>5</sup> Yoo, C. B.; Jones, P. A. Epigenetic therapy of cancer: past, present and future. *Nat. Rev. Drug Discov.* **2006**, *5*, 37–50.
- <sup>6</sup> Jones, P. A.; Baylin, S. B. The epigenomics of cancer. *Cell* **2007**, *128*, 683–692.
- <sup>7</sup> Lister, R.; Pelizzola, M.; Dowen, R. H.; Hawkins, R. D.; Hon, G.; Tonti-Filippini, J.; Nery, J. R.; Lee, L.; Ye, Z.; Ngo, Q. M.; Edsall, L.; Antosiewicz-Bourget, J.; Stewart, R.; Ruotti, V.; Millar, A. H.; Thomson, J. A.; Ren, B.; Ecker, J. R. Human DNA methylomes at base resolution show widespread epigenomic differences. *Nature* **2009**, *462*, 315–322.
- <sup>8</sup> Laurent, L.; Wong, E.; Li, G.; Huynh, T.; Tsirigos, A.; Ong, C. T.; Low, H. M.; Kin Sung, K. W.; Rigoutsos, I.; Loring, J.; Wei, C.-L. Dynamic changes in the human methylome during differentiation. *Genome Res.* **2010**, *20*, 320–321.
- <sup>9</sup> Portela, A.; Esteller, M. Epigenetic modifications and human disease. *Nat. Biotechnol.* **2010**, *28*, 1057–1068..
- <sup>10</sup> Doi, A.; Park, I.-H.; Wen, B.; Murakami, P.; Aryee, M. J.; Irizarry, R.; Herb, B.; Ladd-Acosta, C.; Rho, J.; Loewer, S.; Miller, J.; Schlaeger, T.; Daley, G. Q.; Feinberg, A. P. Differential methylation of tissue- and cancer-specific CpG island shores distinguishes human induced pluripotent stem cells, embryonic stem cells and fibroblasts. *Nat. Genet.* **2009**, *41*, 1350–1353.
- <sup>11</sup> Irizarry, R. A.; Ladd-Acosta, C.; Wen, B.; Wu, Z.; Montano, C.; Onyango, P.; Cui, H.; Gabo, K.; Rongione, M.; Webster, M.; Ji, H.; Potash, J. B.; Sabunciyan, S.; Feinberg, A. P. The human colon cancer methylome shows similar hypo- and hypermethylation at conserved tissue-specific CpG island shores. *Nat. Genet.* **2009**, *41*, 178–186.
- <sup>12</sup> Razin, A.; Riggs, A.D. DNA methylation and gene function. *Science* **1980**, *210*, 604–610.
- <sup>13</sup> Comb, M.; Goodman, H. M. CpG methylation inhibits proenkephalin gene expression and binding of the transcription factor AP-2. *Nucleic Acids Res.* **1990**, *18*, 3975–3982.
- <sup>14</sup> Inamdar, N.M.; Ehrlich, K.C.; Ehrlich, M. CpG methylation inhibits binding of several sequence specific DNA-binding proteins from pea, wheat, soybean and cauliflower. *Plant Mol. Biol.* **1991**, *17*, 111–123.
- <sup>15</sup> Ehrlich, M. DNA methylation in cancer: too much, but also too little. *Oncogene* **2002**, *21*, 5400–5413.

- 
- <sup>16</sup> Robertson, K. D.; Jones, P. A. DNA methylation: past, present and future directions. *Carcinogenesis* 2000, *21*, 461–467.
- <sup>17</sup> Yan, J.; Zierath, J. R.; Barres, R. Evidence for non-CpG methylation in mammals. *Exp. Cell Res.* **2011**, *317*, 2555–2561.
- <sup>18</sup> Klimasauskas, S.; Kumar, S.; Roberts, R. J.; Cheng, X. HhaI methyltransferase flips its target base out of the DNA helix. *Cell* **1994**, *76*, 357–369.
- <sup>19</sup> Svedruzic, Z. M.; Reich, N. O. Mechanism of allosteric regulation of DNMT1's processivity. *Biochemistry* **2005**, *44*, 14977–14988.
- <sup>20</sup> Okano, M.; Bell, D. W.; Haber, D. A.; Li, E. DNA methyltransferases DNMT3A and DNMT3B are essential for de novo methylation and mammalian development. *Cell* **1999**, *99*, 247–257.
- <sup>21</sup> Leonhardt, H.; Page, A. W.; Weier, H.U.; Bestor, T. H. A targeting sequence directs DNA methyltransferase to sites of DNA replication in mammalian nuclei. *Cell* **1992**, *71*, 865–873.
- <sup>22</sup> Okano, M.; Xie, S.; Li, E. Cloning and characterization of a family of novel mammalian DNA (cytosine-5) methyltransferases. *Nat. Genet.* **1998**, *19*, 219–220.
- <sup>23</sup> Lauster, R.; Trautner, T. A.; Noyer-Weidner, M. Cytosine-specific type II DNA methyltransferases. A conserved enzyme core with variable target recognizing domains. *J. Mol. Biol.* **1989**, *206*, 305–312.
- <sup>24</sup> Robertson, K. D. DNA methylation, methyltransferases, and cancer. *Oncogene* **2001**, *20*, 3139–3155.
- <sup>25</sup> Bestor, T. H.; Verdine, G. L. DNA methyltransferases. *Curr. Opin. Cell Biol.* **1994**, *6*, 380–389.
- <sup>26</sup> Bestor, T. H.; Laudano, A.; Mattaliano, R.; Ingram, V. Cloning and sequencing of a cDNA encoding DNA methyltransferase of mouse cells. The carboxylterminal domain of the mammalian enzymes is related to bacterial restriction methyltransferases. *J. Mol. Biol.* **1988**, *203*, 971–983.
- <sup>27</sup> Bestor, T. H. Cloning of a mammalian DNA methyltransferase. *Gene* **1988**, *74*, 9–12.
- <sup>28</sup> Robertson, K. D.; Uzvolgyi, E.; Liang, G.; Talmadge, C.; Sumegi, J.; Gonzales, F. A.; Jones, P. A. The human DNA methyltransferases (DNMTs) 1, 3A and 3B: coordinate mRNA expression in normal tissues and overexpression in tumors. *Nucleic Acids Res.* **1999**, *27*, 2291–2298.
- <sup>29</sup> Mertineit, C.; Yoder, J. A.; Taketo, T.; Laird, D. W.; Trasler, J. M.; Bestor, T. H. Sex-specific exons control DNA methyltransferase in mammalian germ cells. *Development* **1998**, *125*, 889–897.
- <sup>30</sup> Pradhan, S.; Talbot, D.; Sha, M.; Benner, J.; Hornstra, L.; Li, E.; Jaenisch, R.; Roberts, R. J. Baculovirus-mediated expression and characterization of the full-length murine DNA methyltransferase. *Nucleic Acids Res.* **1997**, *25*, 4666–4673.

- 
- <sup>31</sup> Pradhan, S.; Bacolla, A.; Wells, R. D.; Roberts, R. J. Recombinant human DNA (cytosine-5) methyltransferase. I. Expression, purification, and comparison of de novo and maintenance methylation. *J. Biol. Chem.* **1999**, *274*, 33002–33010.
- <sup>32</sup> Prokhortchouk, E.; Defossez, P. A. The cell biology of DNA methylation in mammals, *Biochim. Biophys. Acta* **2008**, *1783*, 2167–2173.
- <sup>33</sup> Takashima, S.; Takehashi, M.; Lee, J.; Chuma, S.; Okano, M.; Hata, K.; Suetake, I.; Nakatsuji, N.; Miyoshi, H.; Tajima, S.; Tanaka, Y.; Toyokuni, S.; Sasaki, H.; Kanatsu-Shinohara, M.; Shinohara, T. Abnormal DNA methyltransferase expression in mouse germ-line stem cells results in spermatogenic defects. *Biol. Reprod.* **2009**, *81*, 155–164.
- <sup>34</sup> Chen, T.; Hevi, S.; Gay, F.; Tsujimoto, N.; He, T.; Zhang, B.; Ueda, Y.; Li, E. Complete inactivation of DNMT1 leads to mitotic catastrophe in human cancer cells. *Nat. Genet.* **2007**, *39*, 391–396.
- <sup>35</sup> Gaudet, F.; Hodgson, J. G.; Eden, A.; Jackson-Grusby, L.; Dausman, J.; Gray, J. W.; Leonhardt, H.; Jaenisch, R. Induction of tumors in mice by genomic hypomethylation. *Science* **2003**, *300*, 489–492.
- <sup>36</sup> Eden, A.; Gaudet, F.; Waghmare, A.; Jaenisch, R. Chromosomal instability and tumors promoted by DNA hypomethylation. *Science* **2003**, *300*, 455.
- <sup>37</sup> Chik, F.; Szyf, M. Effects of specific DNMT gene depletion on cancer cell transformation and breast cancer cell invasion; toward selective DNMT inhibitors. *Carcinogenesis* **2011**, *32*, 224–232.
- <sup>38</sup> Sharif, J.; Koseki, H.; Recruitment of DNMT1 roles of the SRA protein Np95 (UHRF1) and other factors. *Prog. Mol. Biol. Transl. Sci.* **2011**, *101*, 289–310.
- <sup>39</sup> Iida, T.; Suetake, I.; Tajima, S.; Morioka, H.; Ohta, S.; Obuse, C.; Tsurimoto, T. PCNA clamp facilitates action of DNA cytosine methyltransferase 1 on hemimethylated DNA. *Genes Cells* **2002**, *7*, 997–1007.
- <sup>40</sup> Lan, J.; Hua, S.; He, X.; Zhang, Y. DNA methyltransferases and methyl-binding proteins of mammals. *Acta Biochim. Biophys. Sin. (Shanghai)* **2010**, *42*, 243–252.
- <sup>41</sup> Jones, P. A.; Liang, G. Rethinking how DNA methylation patterns are maintained. *Nat. Rev. Genet.* **2009**, *10*, 805–811.
- <sup>42</sup> Goll, M. G.; Bestor, T. H. Eukaryotic cytosine methyltransferases *Annu. Rev. Biochem.* **2005**, *74*, 481–514.
- <sup>43</sup> Schaefer, M.; Lyko, F. Solving the DNMT2 enigma. *Chromosoma* **2010**, *119*, 35–40.
- <sup>44</sup> Squires, J. E.; Patel, H. R.; Nousch, M.; Sibbritt, T.; Humphreys, D. T.; Parker, B. J.; Suter, C. M.; Preiss, T. Widespread occurrence of 5-methylcytosine in human coding and non-coding RNA. *Nucleic Acids Res.* **2012**, *40*, 5023–5033.

- 
- <sup>45</sup> Hermann, A.; Gowher, H.; Jeltsch, A. Biochemistry and biology of mammalian DNA methyltransferases. *Cell. Mol. Life Sci.* **2004**, *61*, 2571–2587.
- <sup>46</sup> Espada, J.; Esteller, M. DNA methylation and the functional organization of the nuclear compartment. *Semin. Cell Dev. Biol.* **2010**, *21*, 238–246.
- <sup>47</sup> Hansen, R. S.; Wijmenga, C.; Luo, P.; Stanek, A. M.; Canfield, T. K.; Weemaes, C. M.; Gartler, S. M. The DNMT3B DNA methyltransferase gene is mutated in the ICF immunodeficiency syndrome. *Proc. Natl. Acad. Sci. U. S. A.* **1999**, *96*, 14412–14417.
- <sup>48</sup> Deplus, R.; Brenner, C.; Burgers, W. A.; Putmans, P.; Kouzarides, T.; de Launoit, Y.; Fuks, F. DNMT3L is a transcriptional repressor that recruits histone deacetylase. *Nucleic Acids Res.* **2002**, *30*, 3831–3838.
- <sup>49</sup> Margot, J. B.; Ehrenhofer-Murray, A. E.; Leonhardt, H. Interactions within the mammalian DNA methyltransferase family. *BMC Mol. Biol.* **2003**, *4*, 7.
- <sup>50</sup> Jia, D.; Jurkowska, R. Z.; Zhang, X.; Jeltsch, A.; Cheng, X. Structure of DNMT3A bound to DNMT3L suggests a model for *de novo* DNA methylation. *Nature* **2007**, *449*, 248–251.
- <sup>51</sup> Jurkowska, R. Z.; Anspach, N.; Urbanke, C.; Jia, D.; Reinhardt, R.; Nellen, W.; Cheng, X.; Jeltsch, A. Formation of nucleoprotein filaments by mammalian DNA methyltransferase DNMT3A in complex with regulator DNMT3L. *Nucleic Acids Res.* **2008**, *36*, 6656–6663.
- <sup>52</sup> Ge, Y. Z.; Pu, M. T.; Gowher, H.; Wu, H. P.; Ding, J. P.; Jeltsch, A.; Xu, G. L. Chromatin targeting of *de novo* DNA methyltransferases by the PWWP domain. *J. Biol. Chem.* **2004**, *279*, 25447–25454.
- <sup>53</sup> Fatemi, M.; Hermann, A.; Gowher, H.; Jeltsch, A. DNMT3a and DNMT1 functionally cooperate during *de novo* methylation of DNA. *Eur. J. Biochem.* **2002**, *269*, 4981–4984.
- <sup>54</sup> Kim, G. D.; Ni, J.; Kelesoglu, N.; Roberts, R. J.; Pradhan, S. Co-operation and communication between the human maintenance and *de novo* DNA (cytosine-5) methyltransferases. *EMBO J.* **2002**, *21*, 4183–4195.
- <sup>55</sup> Xu, F.; Mao, C.; Ding, Y.; Rui, C.; Wu, L.; Shi, A.; Zhang, H.; Zhang, L.; Xu, Z. Molecular and enzymatic profiles of mammalian DNA methyltransferases: structures and targets for drugs. *Curr. Med. Chem.* **2010**, *17*, 4052–4071.
- <sup>56</sup> Goyal, R.; Reinhardt, R.; Jeltsch, A. Accuracy of DNA methylation pattern preservation by the DNMT1 methyltransferase. *Nucleic Acids Res.* **2006**, *34*, 1182–1188.
- <sup>57</sup> Rhee, I.; Bachman, K. E.; Park, B. H.; Jair, K. W.; Yen, R. W.; Schuebel, K. E.; Cui, H.; Feinberg, A. P.; Lengauer, C.; Kinzler, K. W.; Baylin, S. B.; Vogelstein, B. DNMT1 and DNMT3B cooperate to silence genes in human cancer cells. *Nature* **2002**, *416*, 552–556.

- 
- <sup>58</sup> Qureshi, I. A.; Mehler, M. F.; Advances in epigenetics and epigenomics for neurodegenerative diseases. *Curr. Neurol. Neurosci. Rep.* **2011**, *11*, 464–473.
- <sup>59</sup> Fuso, A.; Nicolia, V.; Cavallaro, R. A.; Scarpa, S. DNA methylase and demethylase activities are modulated by one-carbon metabolism in Alzheimer's disease models. *J. Nutr. Biochem.* **2011**, *22*, 242–251.
- <sup>60</sup> Higuchi, F.; Uchida, S.; Yamagata, H.; Otsuki, K.; Hobara, T.; Abe, N.; Shibata, T.; Watanabe, Y. State-dependent changes in the expression of DNA methyltransferases in mood disorder patients. *J. Psychiatr. Res.* **2011**, *45*, 1295–1300.
- <sup>61</sup> Lopez-Pedreria, C.; Perez-Sanchez, C.; Ramos-Casals, M.; Santos-Gonzalez, M.; Rodriguez-Ariza, A.; Cuadrado, M. J. Cardiovascular risk in systemic autoimmune diseases: epigenetic mechanisms of immune regulatory functions. *Clin. Dev. Immunol.* **2012**, *2012*, 1–10.
- <sup>62</sup> Sacconi, S.; Camano, P.; de Greef, J. C.; Lemmers, R. J.; Salviati, L.; Boileau, P.; Lopez de Munain, A. A.; van der Maarel, S. M.; Desnuelle, C. Patients with a phenotype consistent with facioscapulohumeral muscular dystrophy display genetic and epigenetic heterogeneity. *J. Med. Genet.* **2011**, *49*, 41–46.
- <sup>63</sup> Bressler, J.; Shimmin, L. C.; Boerwinkle, E.; Hixson, J. E. Global DNA methylation and risk of subclinical atherosclerosis in young adults: the pathobiological determinants of atherosclerosis in youth (PDAY) study. *Atherosclerosis* **2011**, *219*, 958–962.
- <sup>64</sup> Rodriguez, J.; Frigola, J.; Vendrell, E.; Risques, R. A.; Fraga, M. F.; Morales, C.; Moreno, V.; Esteller, M.; Capella, G.; Ribas, M.; Peinado, M. A. Chromosomal instability correlates with genome-wide DNA demethylation in human primary colorectal cancers. *Cancer Res.* **2006**, *66*, 8462–9468.
- <sup>65</sup> Farinha, N.J.; Shaker, S.; Lemaire, M.; Momparler, L.; Bernstein, M.; Momparler, R. L. Activation of expression of p15, p73 and E-cadherin in leukemic cells by different concentrations of 5-aza-20-deoxycytidine (decitabine). *Anticancer Res.* **2004**, *24*, 75–78.
- <sup>66</sup> Gore, S. D.; Baylin, S.; Sugar, E.; Carraway, H.; Miller, C. B.; Carducci, M.; Grever, M.; Galm, O.; Dausies, T.; Karp, J. E.; Rudek, M. A.; Zhao, M.; Smith, B. D.; Manning, J.; Jiemjit, A.; Dover, G.; Mays, A.; Zwiebel, J.; Murgo, A.; Weng, L. J.; Herman, J. G. Combined DNA methyltransferase and histone deacetylase inhibition in the treatment of myeloid neoplasms. *Cancer Res.* **2006**, *66*, 6361–6369.
- <sup>67</sup> Jung, Y.; Park, J.; Kim, T.; Park, J. H.; Jong, H. S.; Im, S. A.; Robertson, K.; Bang, Y. J.; Kim, T. Y. Potential advantages of DNA methyltransferase 1 (DNMT1)-targeted inhibition for cancer therapy. *J. Mol. Med.* **2007**, *85*, 1137–1148.
- <sup>68</sup> Suzuki, M.; Sunaga, N.; Shames, D. S.; Toyooka, S.; Gazdar, A. F.; Minna, J. D. RNA interference-mediated knockdown of DNA methyltransferase 1



---

leads to promoter demethylation and gene re-expression in human lung and breast cancer cells. *Cancer Res.* **2004**, *64*, 3137–3143.

<sup>69</sup> Mund, C.; Brueckner, B.; Lyko, F. Reactivation of epigenetically silenced genes by DNA methyltransferase inhibitors: basic concepts and clinical applications. *Epigenetics* **2006**, *1*, 7–13.

<sup>70</sup> Wijermans, P. W.; Lubbert, M.; Verhoef, G.; Klimek, V.; Bosly, A. An epigenetic approach to the treatment of advanced MDS; the experience with the DNA demethylating agent 5-aza-2'-deoxycytidine (decitabine) in 177 patients. *Ann. Hematol.* **2005**, *84*, 9–17.

<sup>71</sup> Lemaire, M.; Momparler, L. F.; Raynal, N. J.; Bernstein, M. L., Momparler, R. L. Inhibition of cytidine deaminase by zebularine enhances the antineoplastic action of 5-aza-2'-deoxycytidine. *Cancer Chemother. Pharmacol.* **2009**, *63*, 411–416.

<sup>72</sup> Yang, A. S.; Estecio, M. R.; Garcia-Manero, G.; Kantarjian, H. M.; Issa, J. P. Comment on “Chromosomal instability and tumors promoted by DNA hypomethylation” and “Induction of tumors in mice by genomic hypomethylation”. *Science* **2003**, *302*, 1153.

<sup>73</sup> Brueckner, B.; Rius, M.; Markelova, M. R.; Fichtner, I.; Hals, P. A.; Sandvold, M. L.; Lyko, F. Delivery of 5-azacytidine to human cancer cells by elaidic acid esterification increases therapeutic drug efficacy. *Mol. Cancer Ther.* **2010**, *9*, 1256–1264.

<sup>74</sup> Yoo, C.B.; Jeong, S.; Egger, G.; Liang, G.; Phiasivongsa, P.; Tang, C.; Redkar, S.; Jones, P. A. Delivery of 5-aza-2'-deoxycytidine to cells using oligodeoxynucleotides. *Cancer Res.* **2007**, *67*, 6400–6408.

<sup>75</sup> Yang, C. S.; Wang, X.; Lu, G.; Picinich, S. C. Cancer prevention by tea: animal studies, molecular mechanisms and human relevance. *Nat. Rev. Cancer* **2009**, *9*, 429–439.

<sup>76</sup> Walter, E. D. Genistein (an isoflavone glucoside) and its aglucone, genistein, from soybeans. *J. Am. Chem. Soc.* **1941**, *63*, 3273–3276.

<sup>77</sup> Fang, M. Z.; Chen, D.; Sun, Y.; Jin, Z.; Christman, J. K.; Yang, C. S. Reversal of hypermethylation and reactivation of p16INK4a, RARbeta, and MGMT genes by genistein and other isoflavones from soy. *Clin. Cancer Res.* **2005**, *11*, 7033–7041.

<sup>78</sup> Hoshino, O.; Murakata, M.; Yamada, K. A convenient synthesis of a bromotyrosine derived metabolite, psammaphin A, from psammaphysilla sp. *Bioorg. Med. Chem. Lett.* **1992**, *2*, 1561–1562.

<sup>79</sup> Pina, I. C.; Gautschi, J. T.; Wang, G. Y.; Sanders, M. L.; Schmitz, F. J.; France, D.; Cornell-Kennon, S.; Sambucetti, L. C.; Remiszewski, S. W.; Perez, L. B.; Bair, K. W.; Crews, P. Psammaphins from the sponge *Pseudoceratina purpurea*: inhibition of both histone deacetylase and DNA methyltransferase. *J. Org. Chem.* **2003**, *68*, 3866–3873.

- 
- <sup>80</sup> Godert, A. M.; Angelino, N.; Woloszynska-Read, A.; Morey, S. R.; James, S. R.; Karpf, A. R.; Sufrin, J. R. An improved synthesis of psammaplin A. *Bioorg. Med. Chem. Lett.* **2006**, *16*, 3330–3333.
- <sup>81</sup> Baud, M. G.; Leiser, T.; Haus, P.; Samlal, S.; Wong, A. C.; Wood, R. J.; Petrucci, V.; Gunaratnam, M.; Hughes, S. M.; Buluwela, L.; Turlais, F.; Neidle, S.; Meyer-Almes, F. J.; White, A. J.; Fuchter, M. J. Defining the mechanism of action and enzymatic selectivity of psammaplin A against its epigenetic targets. *J. Med. Chem.* **2012**, *55*, 1731–1750.
- <sup>82</sup> Liu, Z.; Xie, Z.; Jones, W.; Pavlovicz, R. E.; Liu, S.; Yu, J.; Li, P. K.; Lin, J.; Fuchs, J. R.; Marcucci, G.; Li, C.; Chan, K. K. Curcumin is a potent DNA hypomethylation agent. *Bioorg. Med. Chem. Lett.* **2009**, *19*, 706–709.
- <sup>83</sup> Kuck, D.; Singh, N.; Lyko, F.; Medina-Franco, J. L. Novel and selective DNA methyltransferase inhibitors: docking-based virtual screening and experimental evaluation. *Bioorg. Med. Chem.* **2010**, *18*, 822–829.
- <sup>84</sup> Kuck, D.; Caulfield, T.; Lyko, F.; Medina-Franco, J. L. Nanaomycin A selectively inhibits DNMT3B and reactivates silenced tumor suppressor genes in human cancer cells. *Mol. Cancer Ther.* **2010**, *9*, 3015–3023.
- <sup>85</sup> Brueckner, B.; Garcia, B. R.; Siedlecki, P.; Musch, T.; Kliem, H. C.; Zielenkiewicz, P.; Suhai, S.; Wiessler, M.; Lyko, F. Epigenetic reactivation of tumor suppressor genes by a novel small-molecule inhibitor of human DNA methyltransferases. *Cancer Res.* **2005**, *65*, 6305–6311.
- <sup>86</sup> Siedlecki, P.; Garcia, B. R.; Comagic, S.; Schirmacher, R.; Wiessler, M.; Zielenkiewicz, P.; Suhai, S.; Lyko, F. Establishment and functional validation of a structural homology model for human DNA methyltransferase 1. *Biochem. Biophys. Res. Commun.* **2003**, *306*, 558–563.
- <sup>87</sup> Mai, A.; Altucci, L. Epi-drugs to fight cancer: from chemistry to cancer treatment, the road ahead. *Int. J. Biochem. Cell Biol.* **2009**, *41*, 199–213.
- <sup>88</sup> Denny, W. A.; Atwell, G. J.; Baguley, B. C.; Cain, B. F. Potential antitumor agents. 29. Quantitative structure-activity relationships for the antileukemic bisquaternary ammonium heterocycles. *J. Med. Chem.* **1979**, *22*, 134–150.
- <sup>89</sup> Datta, J.; Ghoshal, K.; Denny, W. A.; Gamage, S. A.; Brooke, D. G.; Phiasivongsa, P.; Redkar, S.; Jacob, S. T. A new class of quinoline-based DNA hypomethylating agents reactivates tumor suppressor genes by blocking DNA methyltransferase 1 activity and inducing its degradation. *Cancer Res.* **2009**, *69*, 4277–4285.
- <sup>90</sup> Brueckner, B.; Kuck, D.; Lyko, F. DNA methyltransferase inhibitors for cancer therapy. *Cancer J.* **2007**, *13*, 17–22.
- <sup>91</sup> Villar-Garea, A.; Fraga, M. F.; Espada, J.; Esteller, M. Procaine is a DNA demethylating agent with growth-inhibitory effects in human cancer cells. *Cancer Res.* **2003**, *63*, 4984–4989.

- 
- <sup>92</sup> Singh, N.; Duenas-Gonzalez, A.; Lyko, F.; Medina-Franco, J. L. Molecular modeling and molecular dynamics studies of hydralazine with human DNA methyltransferase 1. *ChemMedChem* **2009**, *4*, 792–799.
- <sup>93</sup> Yoo, J.; Medina-Franco, J. L. Homology modeling, docking and structure-based pharmacophore of inhibitors of DNA methyltransferase, *J. Comput. Aided Mol. Des.* **2011**, *25*, 555–567.
- <sup>94</sup> Lee, B. H.; Yegnasubramanian, S.; Lin, X.; Nelson, W. G. Procainamide is a specific inhibitor of DNA methyltransferase 1. *J. Biol. Chem.* **2005**, *280*, 40749–40756.
- <sup>95</sup> Lin, Y. S.; Shaw, A.; Wang, S. G.; Hsu, C. C.; Teng, I. W.; Tseng, M. J.; Huang, T.; Chen, C. S.; Leu, Y. W.; Hsiao, S. H. Identification of novel DNA methylation inhibitors via a two-component reporter gene system. *J. Biomed. Sci.* **2011**, *18*, 3.
- <sup>96</sup> Lin, X.; Asgari, K.; Putzi, M. J.; Gage, W. R.; Yu, X.; Cornblatt, B. S.; Kumar, A.; Piantadosi, S.; De Weese, T. L.; De Marzo, A. M.; Nelson, W. G. Reversal of GSTP1 CpG Island hypermethylation and reactivation of  $\pi$ -class Glutathione S-Transferase (GSTP1) expression in human prostate cancer cells by treatment with procainamide. *Cancer Res.* **2001**, *61*, 8611–8616.
- <sup>97</sup> Segura-Pacheco, B.; Trejo-Becerril, C.; Perez-Cardenas, E.; Taja-Chayeb, L.; Mariscal, I.; Chavez, A.; Acuna, C.; Salazar, A. M.; Lizano, M.; Duenas-Gonzalez, A. Reactivation of tumor suppressor genes by the cardiovascular drugs hydralazine and procainamide and their potential use in cancer therapy. *Clin. Cancer Res.* **2003**, *9*, 1596–1603.
- <sup>98</sup> Castellano, S.; Kuck, D.; Sala, M.; Novellino, E.; Lyko, F.; Sbardella, G. Constrained analogues of procaine as novel small molecule inhibitors of DNA methyltransferase-1. *J. Med. Chem.* **2008**, *51*, 2321–2325.
- <sup>99</sup> Jorgensen, W. L. The many roles of computation in drug discovery. *Science* **2004**, *303*, 1813.
- <sup>100</sup> Caramella, P.; Grunanger, P. Nitrile oxides and imines. In 1,3-dipolar cycloaddition chemistry. *Padwa, A., Ed.; John Wiley & Sons Inc.: New York, 1984.*
- <sup>101</sup> Dubrovskiy, A. V.; Larock, R. C. Synthesis of benzisoxazoles by the [3 + 2] cycloaddition of in situ generated nitrile oxides and arynes. *Org. Lett.* **2010**, *12*, 1180–1183.
- <sup>102</sup> Vyas, D. M.; Chiang, Y.; Doyle, T. W. A short, efficient total synthesis of ( $\pm$ ) acivicin and ( $\pm$ ) bromo-acivicin. *Tetrahedron Lett.* **1984**, *25*, 487–490.
- <sup>103</sup> Tammana, R.; Shaik, A. A.; Erragunta, N.; Gutta, M.; Kagga, M. Practical one-pot and large-scale synthesis of *N*-(*tert*-butyloxycarbonyl)-3-pyrroline. *Org. Process Res. Dev.* **2009**, *13*, 638–640.
- <sup>104</sup> Conti, P.; De Amici, M.; Pinto, A.; Tamborini, L.; Grazioso, G.; Frølund, B.; Nielsen, B.; Thomsen, C.; Ebert, B.; De Micheli, C. Synthesis of 3-hydroxy- and 3-carboxy- $\Delta^2$ -isoxazoline amino acids and evaluation of their

---

interaction with GABA receptors and transporters. *Eur. J. Org. Chem.* **2006**, *24*, 5533–5542.

<sup>105</sup> Damm, M.; Glasnov, T. N.; Kappe, C. O. Translating high-temperature microwave chemistry to scalable continuous flow processes. *Org. Process Res. Dev.* **2010**, *14*, 215–224.

<sup>106</sup> Glasnov, T. N.; Findenig, S.; Kappe, C. O. Heterogeneous versus homogeneous palladium catalysts for ligandless Mizoroki–Heck reactions: a comparison of batch/microwave and continuous-flow processing. *Chem. Eur. J.* **2009**, *15*, 1001–1010.

<sup>107</sup> Castellano, S.; Tamborini, L.; Viviano, M.; Pinto, A.; Sbardella, G.; Conti, P. Synthesis of 3-aryl/benzyl-4,5,6,6a-tetrahydro-3aH-pyrrolo[3,4-d]isoxazole derivatives: a comparison between conventional, microwave-assisted and flow-based methodologies. *J. Org. Chem.* **2010**, *75*, 7439–7442.

<sup>108</sup> Baxendale, I. R.; Ley, S. V.; Smith, C. D.; Tamborini, L.; Voica, A. F. A bifurcated pathway to thiazoles and imidazoles using a modular flow microreactor. *J. Comb. Chem.* **2008**, *10*, 851–857.

<sup>109</sup> Robinson, B. *The Fischer indole synthesis*; Wiley: Chichester, **1982**.

<sup>110</sup> Bascop, S. I.; Laronze, J. Y.; Sapi, J. Synthesis of 2-(3-hydroxypropyl)indol-3-acetic acid and 3-(2-hydroxyethyl)indole-2-propanoic acid by selective functional group transformations. *Synthesis* **2002**, *12*, 1689–1694.

<sup>111</sup> Nakamura, T.; Noguchi, T.; Miyachi, H.; Hashimoto, Y. Hydrolyzed metabolites of thalidomide: synthesis and TNF- $\alpha$  production-inhibitory activity *Chem. Pharm. Bull.* **2007**, *55*, 651–654.

<sup>112</sup> Madhav, R.; Snyder, C. A.; Southwick, P. L. 2-amino-4-aryl-6-( $\omega$ -carboxyalkyl)-5H-pyrrolo[3,4-d]pyrimidin-7-(6H)ones. Preparation *via* a one-pot synthesis of 1-( $\omega$ -carboxyalkyl)-4-carbomethoxy-2,3-dioxopyrrolidines. *J. Heterocyclic Chem* **1980**, *17*, 1231–1235.

<sup>113</sup> Kappe, C. O.; Dallinger, D.; Murphree, S. S. *Practical microwave synthesis for organic chemists: strategies, instruments, and protocols*; Wiley-VCH: Weinheim, **2009**.

<sup>114</sup> Viviano, M.; Glasnov, T. N.; Reichart, B.; Tekautz, G.; Kappe, C. O. A scalable two-step continuous flow synthesis of nabumetone and related 4-aryl-2-butanones. *Org. Process Res. Dev.* **2011**, *15*, 858–870.

<sup>115</sup> Kappe, C. O. Controlled microwave heating in modern organic synthesis. *Angew. Chem., Int. Ed.* **2004**, *43*, 6250–6284.

<sup>116</sup> Raju, B. C.; Suman, P. New and facile approach for the synthesis of (E)- $\alpha,\beta$ -unsaturated esters and ketones. *Chem. Eur. J.* **2010**, *16*, 11840–11842.

<sup>117</sup> Li, X.; Li, L.; Tang, Y.; Zhong, L.; Cun, L.; Zhu, J.; Liao, J.; Deng, J. Chemoselective conjugate reduction of  $\alpha,\beta$ -unsaturated ketones catalyzed by rhodium amido complexes in aqueous media *J. Org. Chem.* **2010**, *75*, 2981–2988.

- 
- <sup>118</sup> Irfan, M.; Glasnov, T. N.; Kappe, C. O. Heterogeneous catalytic hydrogenation reactions in continuous-flow reactors. *ChemSusChem* **2011**, *4*, 300–316.
- <sup>119</sup> Lai, C. J.; Wu, J. C. A simple kinetic method for rapid mechanistic analysis of reversible enzyme inhibitors. *Assay Drug Dev. Technol.* **2003**, *1*, 527–535.
- <sup>120</sup> Hagemann, S.; Heil, O.; Lyko, F.; Brueckner, B. Azacytidine and decitabine induce gene-specific and non-random DNA demethylation in human cancer cell lines. *PLoS One* **2011**, *6*, 1–11.
- <sup>121</sup> Medina-Franco, J. L.; Caulfield, T. Advances in the computational development of DNA methyltransferase inhibitors. *Drug Discovery Today* **2011**, *16*, 418–425.
- <sup>122</sup> Song, J.; Rechkoblit, O.; Bestor, T. H.; Patel, D. J. Structure of DNMT1\_DNA complex reveals a role for autoinhibition in maintenance DNA methylation. *Science* **2011**, *331*, 1036–1040.
- <sup>123</sup> Friesner, R. A.; Murphy, R. B.; Repasky, M. P.; Frye, L. L.; Greenwood, J. R.; Halgren, T. A.; Sanschagrin, P. C.; Mainz, D. T. Extra precision glide: docking and scoring incorporating a model of hydrophobic enclosure for protein-ligand complexes. *J. Med. Chem.* **2006**, *49*, 6177–6196.
- <sup>124</sup> Jeltsch, A. Beyond Watson and Crick: DNA methylation and molecular enzymology of DNA Methyltransferases. *ChemBioChem* **2002**, *3*, 274–293.
- <sup>125</sup> Irwin, J. J.; Shoichet, B. K. J. ZINC – A free database of commercially available compounds for virtual screening. *Chem. Inf. Model.* **2005**, *45*, 177–182.
- <sup>126</sup> Charifson, P. S.; Walters, W. P. J. Filtering databases and chemical libraries. *Comput.-Aided Mol. Des.* **2002**, *16*, 311–323.
- <sup>127</sup> FILTER, version 2.0.1; Open Eye Scientific Software Inc.: Santa Fe, NM. <http://www.eyesopen.com> (accessed Sep 2009).
- <sup>128</sup> Siedlecki, P.; Garcia, B. R.; Musch, T.; Brueckner, B.; Suhai, S.; Lyko, F.; Zielenkiewicz, P. Discovery of two novel, small-molecule inhibitors of DNA methylation *J. Med. Chem.* **2006**, *49*, 678–683.
- <sup>129</sup> Ramon, R. S.; Bosson, J.; Diez-Gonzalez, S.; Marion, N.; Nolan, S. P. Au/Ag-Co catalyzed aldoximes to amides rearrangement under solvent- and acid-free Conditions. *J. Org. Chem.* **2010**, *75*, 1197–1202.
- <sup>130</sup> Jain, N.; Kumar, A.; Chauhan, S. M. S. Metalloporphyrin and heteropoly acid catalyzed oxidation of CNOH bonds in an ionic liquid: biomimetic models of nitric oxide synthase. *Tetrahedron Lett.* **2005**, *46*, 2599–2602.
- <sup>131</sup> Sanders, B. C.; Friscourt, F. d. r.; Ledin, P. A.; Mbua, N. E.; Arumugam, S.; Guo, J.; Boltje, T. J.; Popik, V. V.; Boons, G.-J. Metal-free sequential [3 + 2]-dipolar cycloadditions using cyclooctynes and 1,3-dipoles of different reactivity. *J. Am. Chem. Soc.* **2010**, *133*, 949–957.
- <sup>132</sup> Rapoport, H.; Nilsson, W. The reaction of aldoximes with alkali1. *J. Org. Chem.* **1962**, *27*, 629–631.

- 
- <sup>133</sup> Ritson, D. J.; Cox, R. J.; Berge, J. Indium mediated allylation of glyoxylate oxime ethers, esters and cyanofomates. *Organic & Biomolecular Chemistry* **2004**, *2*, 1921–1933.
- <sup>134</sup> Hishikawa, K.; Nakagawa, H.; Furuta, T.; Fukuhara, K.; Tsumoto, H.; Suzuki, T.; Miyata, N. Photo induced nitric oxide release from a hindered nitrobenzene derivative by two-photon excitation. *J. Am. Chem. Soc.* **2009**, *131*, 7488–7489.
- <sup>135</sup> Toth, M.; Kun, S.; Bokor, E.; Benlifa, M.; Tallec, G.; Vidal, S.; Docsa, T.; Gergely, P.; Somsak, L.; Praly, J.-P. Synthesis and structure-activity relationships of C-glycosylated oxadiazoles as inhibitors of glycogen phosphorylase. *Bioorg. Med. Chem.* **2009**, *17*, 4773–4785.
- <sup>136</sup> Di Nunno, L.; Vitale, P.; Scilimati, A.; Simone, L.; Capitelli, F. Stereoselective dimerization of 3- arylisoxazoles to cage-shaped bis-[beta]-lactams syn 2,6-diaryl-3,7-diazatricyclo[4.2.0.0<sup>2,5</sup>]octan-4,8-diones induced by hindered lithium amides. *Tetrahedron* **2007**, *63*, 12388–12395.
- <sup>137</sup> Kumaran, G.; Kulkarni, G. H. Synthesis of  $\alpha$ -functionalized and non-functionalized hydroximoyl chlorides from conjugated nitroalkenes and nitroalkanes. *J. Org. Chem.* **1997**, *62*, 1516–1520.
- <sup>138</sup> Velaparthy, S.; Brunsteiner, M.; Uddin, R.; Wan, B.; Franzblau, S. G.; Petukhov, P. A. 5-*tert*-butyl-*N*-pyrazol-4-yl-4,5,6,7-tetrahydrobenzo[*d*]isoxazole-3-carboxamide derivatives as novel potent inhibitors of mycobacterium tuberculosis pantothenate synthetase: initiating a quest for new antitubercular drugs. *J. Med. Chem.* **2008**, *51*, 1999–2002.